CHEMICAL REVIEWS

Review

Trinuclear Metallacycles: Metallatriangles and Much More

Ennio Zangrando, Massimo Casanova, and Enzo Alessio

Chem. Rev., **2008**, 108 (12), 4979-5013 • DOI: 10.1021/cr8002449 • Publication Date (Web): 10 December 2008

Trinuclear Metallacycles: Metallatriangles and Much More

Ennio Zangrando, Massimo Casanova, and Enzo Alessio*

Dipartimento di Scienze Chimiche, Università di Trieste, Via L. Giorgieri 1, 34127 Trieste, Italy

Received January 31, 2008

Contents

1. Introduction

In 1990, Fujita and co-workers described the first example of a rationally designed metallacycle, the molecular square $[\{Pd(en)(\mu-4,4'\text{-bipy})\}_4](NO_3)_8$, prepared by self-assembly of the *cis*-protected square-planar Pd(II) precursor with two adjacent labile ligands $[Pd(en)(ONO_2)_2]$ (en = ethylenediamine) with the linear linker 4,4′-bipyridine (4,4′-bipy).[1] Since then, supramolecular chemistry has produced an amazing number of fascinating 2D and 3D metal-mediated molecular architectures, including many macrocycles and cages. Several review articles have thoroughly covered this thriving field in recent years.[2−16] Beside their shared structural beauty, some of these assemblies are finding applications as receptors and molecular vessels for trapping reactive intermediates,[17,18] as well as for stoichiometric[19] and catalytic reactions.[20]

The smallest and simplest of the metal-mediated molecular polygons, the trinuclear metallacycles, are typically defined in the papers as *rare* or *seldom found*, but a search of the literature demonstrates that, indeed, they are not particularly rare. Instead, it is perhaps fair to say that very often their isolation was totally unexpected, or serendipitous at best, typically from reactions aimed at the preparation of larger metallacycles. In other words, the formation of trinuclear metallacycles is frequently in contrast with the paradigms of the *directional-bonding approach* as defined by Mirkin and Holliday (originally called the *molecular library model* by Stang and co-workers[7]), that rationalizes the metal-mediated construction of supramolecular architectures.[9] Thus, in their apparent simplicity, trinuclear metallacycles pose a number of questions, both practical and theoretical, to the chemists involved in metal-mediated supramolecular chemistry.

Despite their apparent rarity, trinuclear metallacycles are a somehow recurrent feature in our scientific career: one of us in previous years has determined the X-ray structures of several trinuclear metallacycles (see below) and very recently we isolated and structurally characterized two rare examples of molecular triangles with octahedral Ru(II) corners and pyrazine edges.[21,22] Thus, intrigued by our above-average familiarity with this so simple, and yet somehow elusive, metallacycle, we decided to perform a thorough search of the pertinent literature: this review article is intended to be a comprehensive, and yet critical, collection of the trinuclear metallacycles described to date. The main focus will be on the geometry of the metallacycles: the synthetic pathway leading to these species will not be used as a discriminating factor. In most cases, they were obtained (either on purpose or not) according to the principles of self-assembly, i.e., by the combination of metal fragments with two labile ligands (either with a *trans* or, more often, *cis* geometry) and ditopic linkers. However examples of trinuclear cyclic compounds obtained by different synthetic pathways (e.g., transformation of mononuclear metal complexes or metal-induced transformation of added reagents) will be equally considered. The demonstrated (or more often proposed) functions of these metallacycles (e.g., as receptors) will be mentioned occasionally, but not stressed.

* Corresponding author e-mail: alessi@units.it.

10.1021/cr8002449 CCC: $71.00
Published on Web 12/10/2008

Ennio Zangrando received his degree in Chemistry at the University of Trieste in 1974, and some years later he joined the Department of Chemical Sciences at the same University as an Associate Researcher, prior to become Associate Professor of Inorganic Chemistry. In 1987−1988 he spent some months at the Laboratorium für Chemisch-Mineralogische Kristallographie of the Universität Bern with Professor H.-B. Bürgi. His research interests deal with X-ray crystallography, using conventional sources as well as synchrotron radiation. His work was dedicated to the structure−properties relationships of bioinorganic complexes and has been extended in recent years to supramolecular chemistry.

Massimo Casanova was born in 1980 and studied chemistry at the University of Trieste, where he received his "Laurea" in 2004 and his Ph.D. degree in 2008. During the Ph.D., he did stages in the groups of Prof. J. Hupp at Northwestern University of Chicago (U.S.A.) and Prof. P. Ballester at ICIQ, Tarragona (Spain). In the near future, he will start a postdoctoral fellowship in the laboratories of Prof. Joost Reek at UVA, Amsterdam (The Netherlands), in the field of supramolecular catalysis.

Enzo Alessio was born in 1958 and studied chemistry at the University of Trieste, where he received his Ph.D. in 1989. After a NATO-CNR postdoctoral fellowship with Luigi G. Marzilli at Emory University (Atlanta), he became first Research Associate and then Associate Professor of Inorganic Chemistry at the University of Trieste, where he is now director of the Ph.D. School in Chemistry. He is coauthor of more than 140 publications and 10 patents in the fields of coordination chemistry, metal-based anticancer drugs, and metal-driven construction of supramolecular architectures, in particular multichromophore assemblies for photophysical applications.

2. Definitions

First of all, we believe that the field of trinuclear metallacycles needs a rationalization, and thus, we start by giving definitions. All definitions are questionable and might be perceived as relatively narrow. Nevertheless, we believe that they are rational, and this review will prove them useful and appropriate for the purpose of classification. We are, of course, far from being critical with respect to previous results that do not conform to our definitions: regardless of their allocation, many of them represent outstanding contributions in the field of metal-mediated supramolecular chemistry.

We define as a trinuclear metallacycle any metallacycle that contains three metal centers, or M−M bonded dimetal entities, *with structural functions* and three linkers (i.e., di- or polytopic bridging ligands).[23] The degree of metal−metal bonding interactions between the structural metal ions should be negligible, otherwise the compound would be more rightly defined as a cluster. The metallacycle may comprise additional metal atoms without structural functions, i.e., not involved in its construction, such as those inside metal-containing ligands. The three structural metal atoms are most often ca. equidistant and define the vertexes of a ca. equilateral triangle: nevertheless, not all the trinuclear metallacycles can be defined as molecular triangles (*metallatriangles*). According to the *directional-bonding approach*,[9] the design of a molecular triangular entity requires that six rigid ditopic components, three angular and three linear, are assembled in a cyclic manner. Strictly speaking, an ideal equilateral molecular triangle should be assembled by three equal linear linking units in combination with three equal 60° angular fragments (Scheme 1).

Since there are no appropriate metal complexes of common coordination numbers with 60° angles (Scheme 2a), the metal-mediated approach to *geometrically perfect* metallatriangles should rely on angular components featuring two functional donor moieties at 60° and linear metal fragments (Scheme 2b). However, less-than-ideal metallatriangles might derive from the combination of distorted angular components with angles wider than 60° (typically ca. 90°) and ca. linear linkers with angles narrower than 180° (Scheme 2c).

With the aim to give a systematic classification to the examples described in this paper, some general considerations about the linkers are appropriate. The two binding sites in the linkers need not be equal, even though they often are, and the typical linkers are symmetrical. When the linkers are unsymmetrical, their relative orientations within the metallacycle become relevant and stereoisomers are possible. The binding sites in the linkers can be either mono- or polydentate (which implies chelation unless dinuclear metal fragments are involved).

According to the definition by Caulder and Raymond,[6] each linker is characterized by two *coordinate vectors* that connect the binding sites X and Y to the metal centers M_1 and M_2 (Figure 1). In the case of a chelate, the coordinate vector goes from the center of the chelating fragment to the metal. The two coordinate vectors basically define the *shape* (or geometry) of the linker. The following ideal limiting cases can be defined: if the two vectors are collinear at 180°, the linker is *linear*, whereas it has a *sigmoidal-shape* if the two

Scheme 1

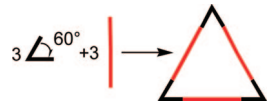

Scheme 2

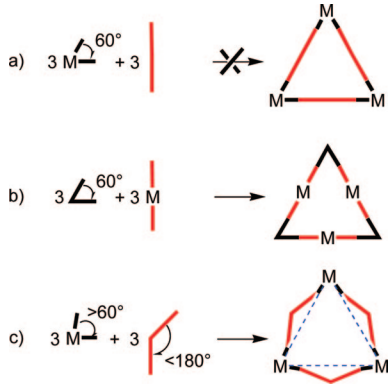

vectors lie at 180° on parallel lines (Figure 1 parts a and b). When the coordinate vectors are coplanar ($M_1-X\cdots Y-M_2$ torsion angle = 0) and their prolongations define an angle, the linker can be generically defined as *planar angular* (Figure 1c). Finally, when the torsion angle between the two coordinate vectors is ≠ 0, the linker will be generically defined as *angular*.

In principle, the directional-bonding approach should involve exclusively rigid linkers, which are supposed to undergo only minor deformations upon metal-coordination within the metallacycle. Thus, the orientations of their two coordinate vectors can be guessed quite precisely from a model structure. However, in some cases, even an educated guess may be difficult, for a number of reasons: (i) the linker might have more than two binding sites, and thus, its geometry (as defined above) depends on which sites are employed in the construction of the metallacycle. (ii) In general, a rigid linker is defined as a molecule that does not bend significantly, typically for the presence of extended conjugation. However, even rigid linkers can have one or more degrees of torsional freedom, i.e., free rotation about single bonds. A typical example is 2,2′-bipyrazine (2,2′-bpz, Figure 2): depending on the mutual orientation of the two six-membered rings and on which N atoms (1,1′ and/or 4,4′) are involved in the coordination, different combinations of coordinate vectors (and thus geometries) are possible. Finally, if the linker itself is not rigid, e.g., it comprises some aliphatic fragments between the two binding sites, then any guess about its geometry within the metallacycle will be very tentative at best.

On the basis of the shape of the trinuclear metallacycle, different subclasses can be identified considering the orientations of the coordinate vectors of each linker with respect to the plane defined by the three metal centers (M_3 plane): (i) When the coordinate vectors are coplanar with the three metal centers, the metallacycle is defined a *molecular triangle*. If the linkers define aromatic walls that are oriented ca. perpendicular to the plane of the metals, the metallacycle may also be called a *molecular triangular prism*. (ii) When both coordinate vectors of planar angular ligands are either above or below the M_3 plane, the metallacycle belongs to the category of *metalla-calix[3]arenes* (two conformers possible). (iii) When one vector is above and the other is below the plane of the metals, the metallacycle can be defined a *cyclic helicate*. All these families, and others, will be treated in detail below.

According to the rationalization sketched above, a trinuclear metallacycle can be defined as a molecular triangle only when it meets the appropriate combination of *nuclearity and shape*. Neither one of these properties *alone* is sufficient for identifying a molecular triangle.

These apparently trivial definitions nevertheless limit the number of compounds that will be treated in this review article. In particular, some metallacycles that are frequently cited as typical examples of molecular triangles, in our opinion, do not rightly belong to this group. One such example is the Pd_6-metallacycle (**1**) described by Loeb and co-workers,[24] obtained by self-assembly of linear organometallic dipalladium fragments and angular 4,7-phenathroline linkers (Scheme 3). Even though it has, indeed, a shape that recalls a triangle, it contains six structural Pd atoms and six (3 + 3) linkers. Thus, it should be better classified as a rare molecular hexagon (perhaps with a triangular shape) rather than a molecular triangle.

Similar considerations apply to elegant examples of cationic or neutral Pt_6-metallacycles described by the group of Stang.[25] They were obtained by self-assembly of diplatinum organometallic angular fragments and ca. linear linkers (either N or O donors). Two examples, one hexacationic with 4,4′-bipy linkers (**2a**, 4,4′-bipy = 4,4′-bipyridine) and one neutral with terephthalate linkers (**2b**), are reported in Scheme 4. More recently, the same group reported also novel Pt_6-metallacycles of triangular shape (**3**) that feature three linear Pt_2 fragments (e.g., [1,4-bis($(PEt_3)_2$Pt-benzene]$^{2+}$) connected by bispyridyl cavitand building blocks.[26]

On the other hand, metallacycles that feature only three structural metal atoms and three organic linkers such as **4** (Figure 3) that, because of their shape, were described as examples of molecular hexagons,[27] according to our classification, should be listed among the trinuclear metallacycles (see section 7.3).

3. Organization of the Work and Analytical Issues

In the following review, the trinuclear metallacycles are classified first according to the position of the metal fragments, either on the corners or on the edges. Each class is then divided into further subclasses or families, based on the general shape and the geometry of the linkers as defined above. However, some metallacycles fit perfectly only in one family, whereas others have a borderline nature and might be included in two (or more) subgroups. The many examples of trinuclear metallacycles with single-atom edges, i.e., of the type $[M_3X_3]$ (e.g., X = N, O, OH, Cl, Br,...), will not be included in this review, regardless if X is a single atom or belongs to a molecule, for two main reasons: (1) Often in these small metallacycles, the metal−metal bond component is not negligible (and they should be considered as metal clusters). (2) Typically, they were not prepared according to the metal-directed synthetic paradigm, i.e., with the specific purpose of making a metallacycle. Therefore, in the following examples, the shortest edge will comprise at least two atoms (e.g., CN^-). The linkers that have no specific abbreviation are labeled with a progressive L*n* (*n* = 1, 2,...).

The characterization of trinuclear metallacycles can be a complex problem, as is often the case in supramolecular chemistry for highly symmetrical assemblies made of identi-

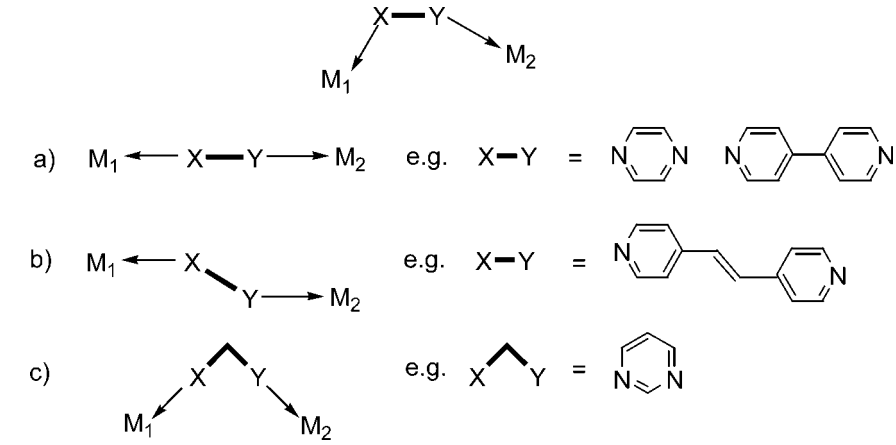

Figure 1. Schematic representations of a generic linker (top) with its coordinate vectors (gray arrows throughout the paper) and of some ideal cases of well-defined geometries with typical examples: (a) linear, (b) sigmoidal, and (c) planar angular.

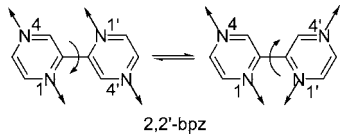

Figure 2. Conformational equilibrium for 2,2′-bpz. The arrows represent the potential coordinate vectors.

cal subunits. As a further complication, the trinuclear metallacycles are frequently obtained together with other symmetrical metallacycles of different nuclearity (e.g., molecular squares), that may or may not be in equilibrium. A powerful analytical tool, such as NMR spectroscopy, is typically insufficient in these cases: a single set of proton signals in the ^{1}H NMR spectrum, together with chemical shift considerations, indicate that a symmetrical metallacyclic species is present in solution but is insufficient for determining its nuclearity and geometry (e.g., for distinguishing between a molecular triangle and a square). In recent years, diffusion-ordered NMR spectroscopy (DOSY), based on pulse-gradient spin-echo (PGSE) NMR experiments, became a new powerful tool in supramolecular chemistry.[28] In principle, metallacycles of different nuclearity can be distinguished through DOSY NMR experiments that allow one to measure the diffusion coefficients of the compounds in solution that are, in turn, correlated with their size and shape. In the absence of an X-ray crystal structure determination, the only technique that can unambiguously establish the existence of a trinuclear metallacycle (provided that suitable single crystals can be grown and that the solid state reflects the solution system), molecular mass measurements become essential. Mass spectrometry can, in principle, provide accurate exact mass values and separate signals for components in mixtures. Nevertheless, ionization of the metallacycles as intact species (i.e., without complete fragmentation) is often a difficult task even with soft ionization techniques, such as electrospray ionization (ESI) and coldspray ionization (CSI).[29] Neutral species are even more difficult to analyze. Also gel-permeation chromatography (GPC) has been successfully used to discriminate metal-mediated molecular triangles and squares and related supramolecular complexes. Successful separation on a preparative scale of a mixture of molecular squares and triangles was also achieved.[30] However GPC, and also vapor-phase osmometry (VPO), are unsuitable for equilibrating systems since they give average values of molecular mass.

In the following pages, the X-ray structural characterization of the metallacycles, when available, are always mentioned explicitly and many have been redrawn.[31,32] The absence of a specific mention to an X-ray structure indicates that characterization of the compounds was supported by a number of complementary methods, most commonly multinuclear and DOSY NMR spectroscopy and mass spectrometry (but also IR and UV/vis spectroscopy and cyclic voltammetry), in some cases implemented by VPO and/or GPC measurements.

4. Metallatriangles with Angular Linkers and Metal-Containing Linear Edges

There is quite a large number of strain-free metallatriangles made by angular linkers with coordinate vectors at ca. 60° connected through linear metal fragments (see Introduction, Scheme 2). Basically, three different geometries for the metal connectors (edges) are possible, depending on the denticity of the binding sites on the angular linkers (Figure 4): thus, the geometry of the available coordination sites will be linear for monodentate linkers, square planar for bidentate linkers (or pairs of monodentate linkers), and octahedral for tridentate *mer* linkers.

4.1. Angular Linkers with Monodentate Binding Units

A family of metallatriangles of this type that has been known for many years is that in which the edges are made by d^{10} metal ions with a natural linear coordination, such as Au(I), Ag(I), and also Cu(I) (which, however, is typically three- or four-coordinate). The first example of a cyclic organogold molecular triangle with bridging 2-pyridyl linkers (**5**) was reported by Vaughan in 1970 (Figure 5a).[33]

Later, similar metallatriangles of general formula [{M(μ-pz)}$_3$] (M = Ag(I),[34−36] Au(I),[34,37] Cu(I)[36,38]) were obtained with a range of substituted pyrazolates (pz, Figure 5b): indeed, the binding vectors in the pentagonal ring of pz make an angle slightly wider than the ideal (ca. 72°). Also other 1,2-*C*,*N*-monoanionic 60° angular linkers, such as carbeniates (C(OR)═NR′, Figure 5c; C(NR$_2$)═NR′),[39] and imidazolates (Figure 5d),[40] were extensively employed for the preparation of trinuclear metallacycles with the same metal ions. Recently, examples with substituted 1,2,4-triazolates were also described.[41] Many of these molecular triangles were structurally characterized in the solid state by X-ray crystallography. In general, all Au metallacycles define a basically

Scheme 3

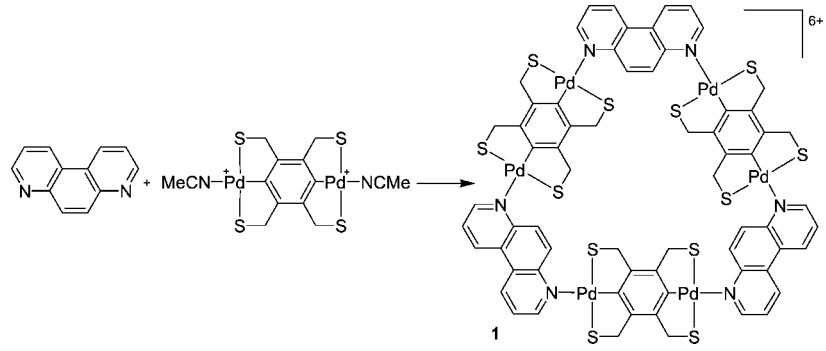

Scheme 4

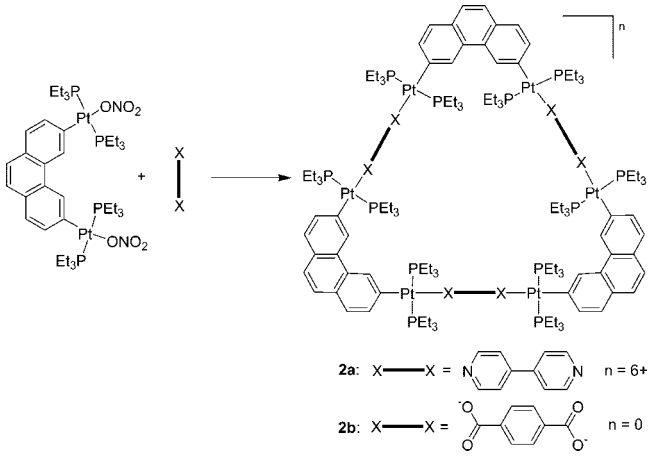

planar nine-membered Au_3N_6 or $Au_3N_3C_3$ ring, with Au···Au distances in the range 3.224(1)−3.368(1) Å.

Stepwise oxidative halogen additions to Au(I) metallatriangles to form mixed-valence Au(I)/Au(III) and even {Au(III)}$_3$ derivatives is wel-documented: the Au(III) fragments have a square-planar trans geometry.[42] Mixed-metal (Au(I) + Ag(I)) and mixed-ligand (pyrazolate + carbeniates)

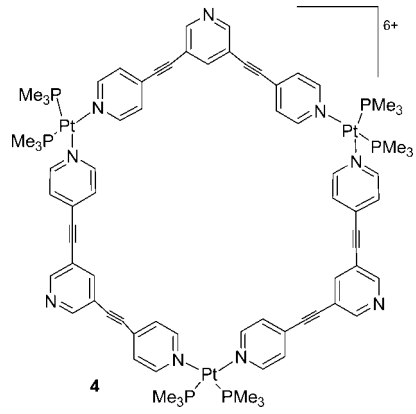

Figure 3. Metallacycle **4**, which features only three structural metal atoms and three organic linkers.

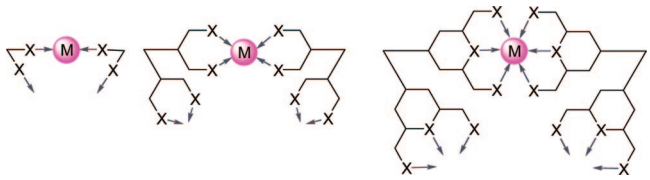

Figure 4. Three different geometries possible for the metal connectors.

metallacycles have also been described.[43] Triangular gold compounds were also investigated for their capability of sandwiching cations in the solid state[40b,44] and for their supramolecular aggregation through aurophilic attractions leading to luminescent assemblies.[42d,45] Gold(I) molecular triangles with pyrazolato corners featuring long alkyl side chains were found to organize into hexagonal columnar mesophases or luminescent superhelical fibers.[46]

The organometallic molecular triangles [{Hg(*o*-C_6H_4)}$_3$] (**6**),[47] [{Hg(*o*-C_6F_4)}$_3$] (**7**),[48] and [{Hg(1,2$C_2B_{10}H_{10}$)}$_3$] (**8**),[49] with linear Hg(II) edges and *o*-phenylene or *o*-carborane corners (Figure 6), were also prepared and structurally characterized by X-ray crystallography.

There are also a few more elaborate examples in which the metal centers along the edges of the triangles are coordination compounds bearing trans ancillary ligands rather than naked ions. An elegant example of this type, in which the corners of the molecular triangle are *metal-containing ligands*, was described by Lippert and co-workers in 1999.[50] First, reaction of $[Pd(en)(H_2O)_2]^{2+}$ with 2,2′-bpz yielded the mononuclear complex $[Pd(en)(2,2'\text{-bpz-}N^1,N^{1'})]^{2+}$ (**9**). In this compound, the coordinated 2,2′-bpz has two available binding sites, N^4 and $N^{4'}$, with coordinate vectors oriented at ca. 60° (Scheme 5). Treatment of **9** with the linear connecting unit *trans*-$[Pt(NH_3)_2]^{2+}$ afforded the cationic molecular triangle $[\{Pd(en)\}_3(2,2'\text{-bpz})_3\{Pt(NH_3)_2\}_3]^{12+}$ (**10**, crystallized as mixed ClO_4^- and NO_3^- salt) (Scheme 5). It is noteworthy that this molecular triangle contains six metal atoms, all essentially coplanar with the 2,2′-bpz ligands, but only the Pt atoms have a structural role, whereas the three Pd atoms have the function of locking the conformation of 2,2′-bpz. Interestingly, in the solid state, a ClO_4^- anion is encapsulated in the center of the triangular cations (Figure 7) that stack on top of each other in an antiprismatic fashion.

Later, Espinet and co-workers described the Pt(II) molecular triangle [{*trans*-Pt(C_6F_5)$_2$(μ-C_6H_4(CN)$_2$)}$_3$] (**11**) that features 1,2-phenylene diisocyanide corner linkers and *trans*-Pt(C_6F_5)$_2$ fragments as linear connectors (Scheme 6).[51] The X-ray molecular structure showed that the C_6F_5 planes are oriented perpendicularly to the Pt_3 plane.

A mixture of chiral organometallic molecular polygons of general formula [{*trans*-Pt(PEt_3)$_2$(μ-L1)}$_n$], n = 3−8, ranging from triangle to octagon, was obtained by reacting the atropoisomeric bridging ligand 2,2′-diacetyl-1,1′-binaphthyl-6,6′-bis(ethyne) (H_2L1, Chart 1) with 1 equiv of *trans*-$[PtCl_2(PEt_3)_2]$.[52] The analytically pure molecular triangle was obtained by silica gel column chromatography and characterized by mass spectrometry, NMR, and circular dichroism (CD) spectroscopy.

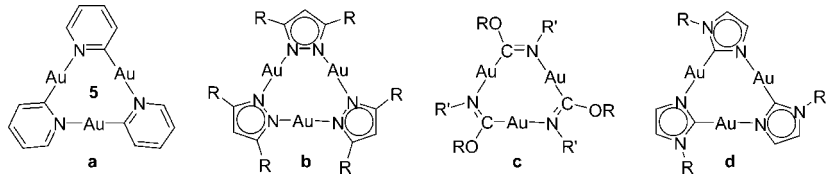

Figure 5. Examples of metallatriangles with linear Au(I) edges; R, R′ = alkyl or aryl groups.

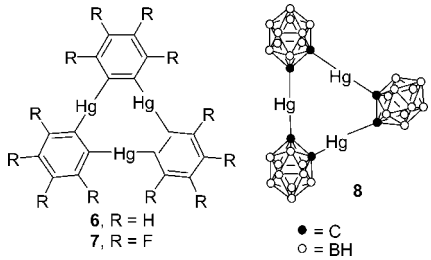

Figure 6. Organometallic molecular triangles **6**, **7**, and **8**.

Scheme 5

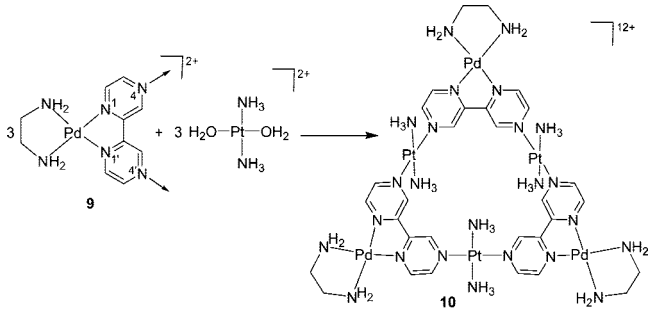

A similar homochiral molecular triangle of formula [{Cu(py)$_3$(μ-L2Cu)}$_3$] (**12**), in which chiral corner linkers (H_4L2, Figure 8) with two carboxylate binding groups at ca. 60° are linearly interconnected by square pyramidal Cu(py)$_3$ fragments (that coordinate in trans positions two carboxylate groups of two corner linkers), was recently reported by Mirkin and co-workers.[53] Each corner linker encloses an additional Cu(II) ion (without structural functions) chelated by the *N*,*N*,O^-,O^- set of donor atoms (Cu1, Figure 8). In this case, the molecular triangle was obtained selectively (no other polygon detected) and both the *S*,*S*,*S*- and the *R*,*R*,*R*-enantiomers were structurally characterized by X-ray crystallography. Interestingly, this species can be spontaneously and reversibly transformed into a homochiral helical polymer simply by addition of the appropriate solvent, and the chirality of the corner ligand dictates the helicity of the resulting polymer.

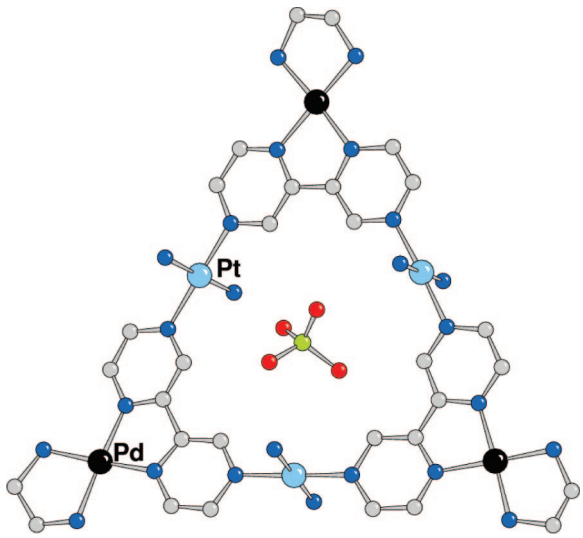

Figure 7. Molecular structure of [{Pd(en)}$_3$(2,2′-bpz)$_3${Pt(NH$_3$)$_2$}$_3$]$^{12+}$ (**10**) with the encapsulated ClO_4^- anion.

Scheme 6

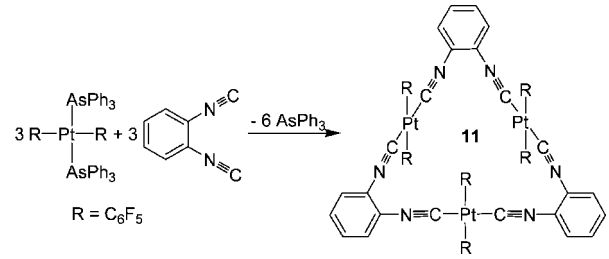

Chart 1

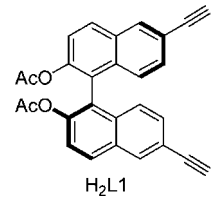

A heterodinuclear organometallic molecular triangle, (PPN)[{Au{Pt(PMe$_3$)$_2$}$_2$}{μ-*o*-C≡C(C$_6$Me$_4$)C≡C}$_3$] (**13**, PPN = (PPh$_3$)$_2$N$^+$), featuring two *trans*-[Pt(PMe$_3$)$_2$]$^{2+}$ edges and one Au(I) edge connected by *o*-C≡C(C$_6$Me$_4$)C≡C^{2-} dianionic fragments (Figure 9), was prepared and structurally characterized in the solid state by Vicente et al.[54] Interest-

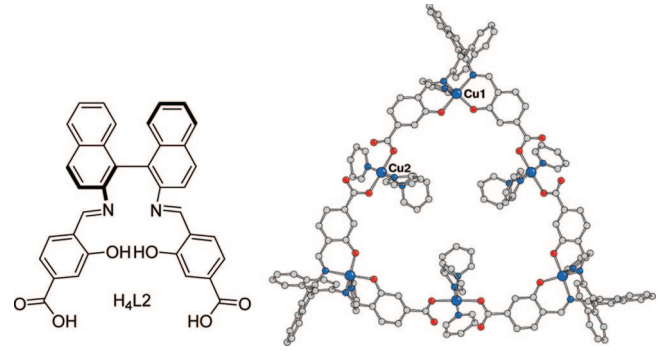

Figure 8. Linker H_4L2 (left) and molecular structure of [{Cu(py)$_3$(μ-L2Cu)}$_3$] (**12**) (right) located on a crystallographic 3-fold axis.

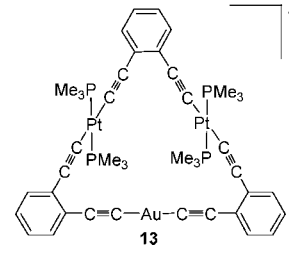

Figure 9. Heterodinuclear organometallic molecular triangle **13**.

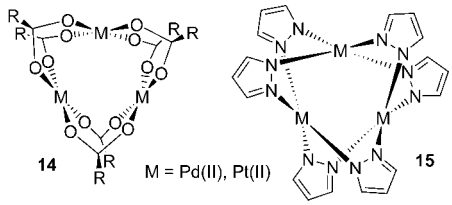

Figure 10. Double-walled carboxylate and pyrazolato trinuclear metallacycles **14** and **15**.

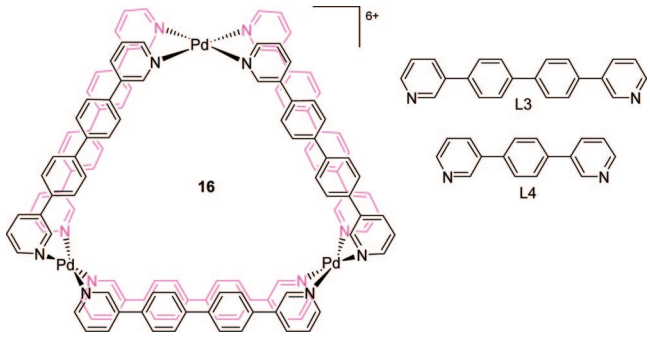

Figure 11. L3 and L4 linkers.

ingly, Takahashi and co-workers previously reported that treatment of *o*-diethynylbenzene with an equimolar amount of $[PdCl_2(PEt_3)_2]$ in the presence of a CuCl catalyst affords the organometallic molecular square $[\{trans\text{-}Pd(PEt_3)_2(\mu\text{-}o\text{-}C{\equiv}C(C_6H_4)C{\equiv}C)\}_4]$ rather than the corresponding triangle.[55]

When the metal center offers a square planar, rather than linear, coordination motif, homoleptic trinuclear metallacycles can be obtained in which each corner is composed by *a pair* of angular linkers with monodentate binding units and coordinate vectors at ca. 60°. Typical examples are the structurally similar *double-walled* carboxylate and pyrazolato (or substituted pyrazolato) metallacycles of d^8 metal ions of general formula $[\{M(\mu\text{-}O_2CR)_2\}_3]$ (**14**)[56] and $[\{M(\mu\text{-}pz)_2\}_3]$ (**15**)[57] (M = Pd(II), Pt(II), R = alkyl or aryl group), respectively (Figure 10).

Fujita and co-workers, based mainly on NMR and MS evidence, reported that the reaction of the 4,4′-bis(3-pyridyl)biphenyl linker (L3, Figure 11) with $Pd(CF_3SO_3)_2$ afforded mainly the double-walled trinuclear metallacycle $[\{Pd(L3)_2\}_3]^{6+}$ (**16**), in which each Pd atom is supposed to bind in a square-planar geometry four pyridyl rings from four different *cis*-L3 strands (Figure 11).[58] Similar results were obtained with the shorter 1,4-bis(3-pyridyl)benzene linker (L4, Figure 11). Unfortunately, no structural characterization of these metallacycles was available. In contrast, when treated with Pd(*p*-tosylate)$_2$, L3 afforded a partially double-walled tetrahedral $[Pd_4(L3)_8](p\text{-tosylate})_8$ assembly, which was structurally characterized by X-ray crystallography.[58]

In 2007, the same group reported that treatment of $Pd(NO_3)_2$ with 2 equiv of 1,2-bis[2-(pyridin-4-yl)ethynyl-]benzene (L5, Scheme 7) yields a mixture of the double-walled molecular square $[\{Pd(L5)_2\}_4]^{8+}$ (**17**) and triangle $[\{Pd(L5)_2\}_3]^{6+}$ (**18**), whose ratio is almost completely controlled by the nature of the solvent.[59] Thus, the square **17** prevailed in dmso, whereas the triangle **18** prevailed in acetonitrile (Scheme 7). Both metallacycles were crystallized independently, and their X-ray molecular structures determined. Solution studies indicated that, beside the solvent, the nature of the anion also affects significantly the equilibrium between **17** and **18**, presumably through a combined templating effect.

Scheme 7

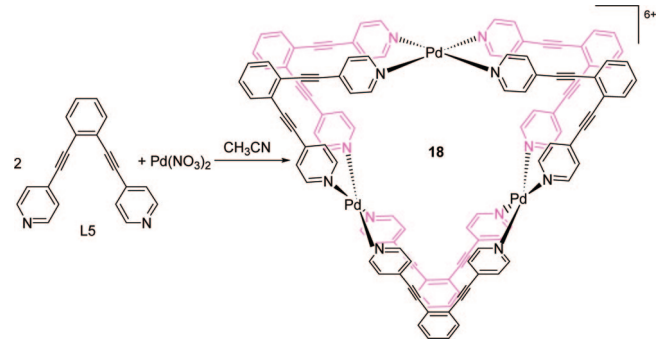

Chart 2

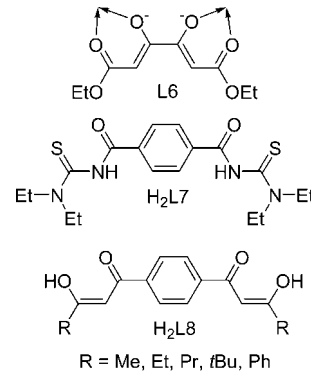

If the metal centers have square-pyramidal or octahedral, rather than square-planar, geometry, additional axial ligands are needed: when at least one of these has a μ_3 coordination, "filled" (e.g., oxo-centered) or "capped" trinuclear metallacycles are obtained (see below).

4.2. Angular Linkers with Bidentate Binding Units

When the corner linkers have bis-chelating binding moieties, the metal ions along the edges must offer a square-planar coordination (Figure 4). Thus, their geometry can be square planar, square pyramidal, or octahedral. A number of molecular triangles of this type were obtained using bis-1,3-dicarbonyl compounds or structurally similar molecules (H_2L6, Chart 2) as corner linkers: after double deprotonation, in the cis conformation, they provide two coplanar bidentate chelating groups oriented at ca. 60°.

Actually, the first trinuclear metallacycles of this kind were described in 1986 by Hoyer and co-workers using bis-bidentate S,O corner linkers, such as the 3,3′-terephthaloyl-bis-*N*-acylthiourea H_2L7 (Chart 2), and square planar Ni^{2+} or Cu^{2+} ions as connecting metal centers.[60] The X-ray molecular structure of the nickel molecular triangle was also determined.

In 1998, Saalfrank and co-workers showed that reaction of the diethyl ketipinate H_2L6 (Chart 2) with Cu(II) ions in the presence of NaOH and $NaBF_4$ afforded the corresponding neutral molecular triangle.[61] The isolated product contained an encapsulated sodium ion: $[Na{\subset}Cu(\mu\text{-}L6)\}_3](BF_4)$ (**19**). The three Cu(II) atoms in the 15-membered macrocycle have a square-pyramidal geometry and bind the bis-bidentate dianions in the basal coordination plane; the apical position is occupied by a water or a tetrahydrofuran (thf) molecule. Similar equilateral copper triangles were obtained by reaction of Cu(II) with a series of 1,4-phenylene linked bis-β-diketones H_2L8 (Chart 2), upon double deprotonation.[62] The

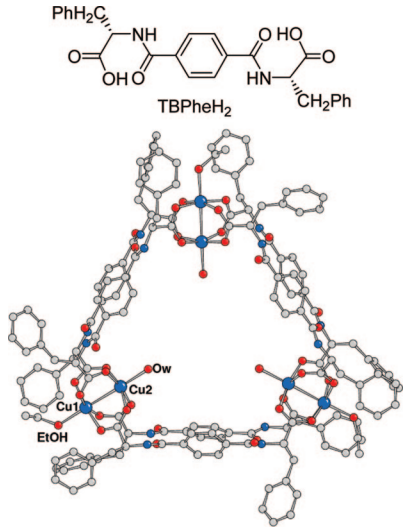

Figure 12. Schematic drawing of $TBPheH_2$ and molecular structure of $[\{Cu_2(\mu_4\text{-}TBPhe)_2(H_2O)(EtOH)\}_3]$ (**20**).

coordination geometry of the connecting Cu(II) ions is either square planar or square pyramidal with a solvent molecule occupying the axial position.

A chiral double-walled double-decker metallatriangle, $[\{Cu_2(\mu_4\text{-}TBPhe)_2(H_2O)(EtOH)\}_3]$ (**20**) ($TBPheH_2$ = *N*,*N*′-terephthaloyl-bis(*L*-phenylalanine), Figure 12), was very recently prepared and structurally characterized by Janiak and co-workers.[63] The X-ray structure (Figure 12) showed that the C_3-symmetric metallacycle is formed by three dinuclear paddlewheel units: each pair of Cu(II) atoms is bound to four carboxylate groups from four different $TBPhe^{2-}$ linkers. The square-pyramidal coordination geometry of the Cu atoms is completed, in each pair, by a terminal ethanol and a water molecule.

Neutral molecular triangles of the type $[\{M(\mu\text{-}L8)(py)_2\}_3]$ with octahedral metal connectors on the edges were obtained by treatment of H_2L8 linkers (Chart 2, R = Ph or *t*-Bu), with Co(II), Ni(II), and Zn(II) salts.[64] The coordination environment of each metal ion is distorted octahedral, with two chelate rings in the equatorial plane and two axially coordinated pyridines (from the solvent). On the other hand, it is well-known that the treatment of bis-β-diketones such as H_2L8 with naked octahedral metal ions M^{n+} (n = 2 or 3) affords, upon double deprotonation, tetrahedral assemblies of general formula $[M_4(L8)_6]^{4(3-n)-}$.[64,65]

4.2.1. μ_3-X-Centered Trinuclear Metallacycles

A large class of compounds closely related to those described above is that of X-centered trinuclear metallacycles: in these compounds, the three metal ions on the edges of the molecular triangle are connected, as in the previous examples, by three angular linkers that define the corners and, in addition, by one (or two) μ_3-X ligand(s) located in the center (X = O) or above (and eventually below) the center of the metallacycle (typically X = OH, Cl). In some cases, there are also additional μ (e.g., Cl) or μ_3 (e.g., SO_4) linkers between the metal ions. Strictly speaking, these compounds do not fit in our initial definition of trinuclear metallacycles, despite having three metal atoms that occupy the vertexes of an equilateral triangle, because of the additional bridging ligand(s), and are, therefore, not exhaustively covered here. They might be defined as *filled* or *capped* (or double-capped) molecular triangles.

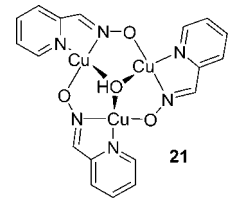

Figure 13. Schematic structure of **21**. The (μ_3-SO_4) below the Cu_3 plane is not shown.

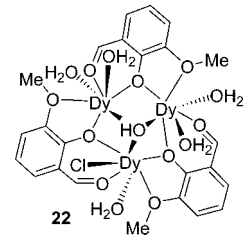

Figure 14. Schematic structure of **22**. The (μ_3-OH) below the Dy_3 plane is not shown.

Many examples concern Cu(II) metallacycles. The first, $[Cu_3(\mu_3\text{-}OH)(\mu_3\text{-}SO_4)(\mu\text{-}L9)_3]$ (**21**, where HL9 is pyridine-2-aldehyde oxime), was described in 1969 by Beckett et al. (Figure 13).[66] The Cu(II) ions, with a distorted square-pyramidal geometry, define an equilateral triangle of sides 3.22 Å. In this case, beside the hydroxide, also the sulfato anion acts as a tripodal bridge between the three Cu(II) atoms (on the opposite side of the Cu_3 plane with respect to OH).

Similar systems containing oxime ligands,[67] or other tridentate N_2O ligands,[68] were later reported. More recently, the Dy(III) trinuclear metallacycle $[Dy_3(\mu_3\text{-}OH)_2(\mu\text{-}L10)_3Cl(H_2O)_5]Cl_3$ (**22**, Figure 14; HL10 = *o*-vanillin) was structurally characterized by X-ray crystallography and investigated for its magnetic properties.[69]

In 1983, Reedijk and co-workers prepared and structurally characterized the OH-capped Cu(II) trinuclear metallacycle with pyrazolato corners $[Cu_3(\mu_3\text{-}OH)(\mu\text{-}pz)_3(Hpz)_2(NO_3)_2]$ (**23**).[70] Structurally similar compounds with μ_3-OH, μ_3-O, $(\mu_3\text{-}Cl)_2$, or $(\mu_3\text{-}Br)_2$ cores were later described by other groups and extensively investigated for their magnetic properties.[71] A mixed-valence Co(II)/Co(III)/Co(III) trinuclear metallacycle, of formula $[Co_3(\mu_3\text{-}OH)(\mu\text{-}pz)_4(DBM)_3]$ (**24**, DBM = dibenzoylmethanato), featuring four bridging pyrazolato ligands, was also described and structurally characterized by X-ray crystallography.[72]

4.2.2. Oxo-centered Trinuclear Metal Carboxylates and Pyrazolates

Another large group of structurally similar trinuclear metallacycles that, despite having three metal ions at the vertexes of an equilateral triangle, cannot be strictly defined as molecular triangles for the same reason as above, is that of oxo-centered trinuclear metal carboxylates, also known as *basic carboxylates*. The general formula, $[M_3(\mu_3\text{-}O)(\mu\text{-}O_2CR)_6(L)_3]^n$ (Figure 15, n = from −2 to +1), comprises a divalent or trivalent octahedral transition metal ion (e.g., M = Cr, Mn, Ru, Rh, Fe, Co; also mixed-valence and mixed-metal examples are known), an organic carboxylate anion RCO_2^-, and a neutral monodentate (or bis-monodentate) ligand L (e.g., L = H_2O, CO, or pyridine).[73]

The long metal−metal distances within the $M_3(\mu_3\text{-}O)$ unit preclude substantial direct metal−metal bonding. The bridging carboxylates can be formally replaced by pyrazolate

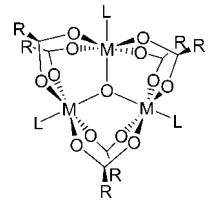

Figure 15. Example of a generic oxo-centered trinuclear metal carboxylate.

Chart 3

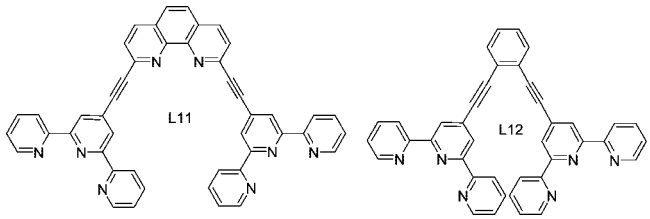

linkers, yielding a parallel series of structurally similar trinuclear compounds. The metallacycle $[Fe_3(\mu_3\text{-}O)(\mu\text{-}4\text{-}NO_2\text{-}pz)_6Cl_3]^{2-}$ (**25**) was recently reported, together with a series of similar Fe(III) compounds in which the metal-core motif remains mostly unperturbed.[74] A description of the many examples of compounds belonging to these groups, which have been mainly investigated with regard to the magnetic and electronic interactions occurring among the metal centers (e.g., as multielectron redox systems and single-molecule magnets), is beyond the scope of this review.

4.3. Angular Linkers with Tridentate Binding Units

Finally, there are a few examples of molecular metallatriangles in which the angular linkers possess two *mer* tridentate binding units (Figure 4). Usually the terpy−M(II)−terpy (terpy = 2,2′:6′,2″-terpyridine) connectivity was exploited, i.e., the corner linkers feature two terpyridine binding sites rigidly held at 60° from one another and are linearly connected by M(II) ions (typically Fe(II) or Ru(II)) that seat in the middle of each side of the molecular triangle. Each terpy unit occupies three *mer* coordination positions of the octahedral cation. In the corner ligand L11 (Chart 3), the terpy units are connected via a 2,9-phen spacer (phen = 1,10-phenanthroline),[75] whereas in L12 (Chart 3) they are connected via a 1,2-bis(ethynyl)benzene fragment.[76]

According to NMR and MS evidence, treatment of L11 with $FeSO_4$ yielded a ca. 75/25 equilibrium mixture of molecular triangle $[\{Fe(\mu\text{-}L11)\}_3]^{6+}$ (**26**) and molecular square $[\{Fe(\mu\text{-}L11)\}_4]^{8+}$,[75] whereas the reaction of L12 with $FeCl_2$ or with $RuCl_2(dmso)_4$ afforded exclusively the molecular triangles $[\{Fe(\mu\text{-}L12)\}_3]^{6+}$ (**27a**) and $[\{Ru(\mu\text{-}L12)\}_3]^{6+}$ (**27b**), respectively.[76]

5. Trinuclear Metallacycles with Metal Corners

5.1. Generic Trinuclear Metallacycles (Miscellaneous)

There are several examples of trinuclear metallacycles, most often obtained serendipitously, whose shape does not recall any abstract geometrical figure, even though the three metal atoms roughly define an equilateral triangle. Typically, in these cases, the linkers are not rigid or show hardly predictable coordination modes and geometries, they do not

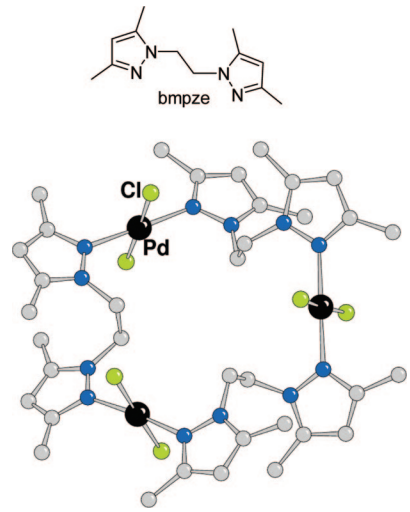

Figure 16. Schematic drawing of bmpze (top) and molecular structure of $[\{trans\text{-}PdCl_2(\mu\text{-bmpze})\}_3]$ (**28**).

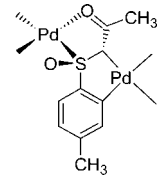

Figure 17. Repeating unit in the Pd_3 metallacycle **29**.

define aromatic walls, and their coordinate vectors do not lay in the plane of the three metals. Aside from being trinuclear, these macrocycles share no common features and are, thus, collected all together in this section.

In 1995, Baker et al. described the trinuclear metallacycle $[\{trans\text{-}PdCl_2(\mu\text{-bmpze})\}_3]$ (**28**), defined a "molecular tricorn", obtained by coordination of 1,2-bis(3,5-dimethylpyrazol-1-yl)ethane (bmpze, Figure 16) units to *trans*-$PdCl_2$ fragments.[77] The X-ray structure showed that, in the solid state, the flexible bmpze linkers assume a conformation in which the two coordinate vectors make a ca. 60° angle (torsion angle about CH_2-CH_2 bond of ca. 70°), thus representing the vertexes of the metallacyle connected through the linear *trans*-$PdCl_2$ edges (Figure 16).

In the same year, Garcia-Ruano et al. prepared and structurally characterized by X-ray diffraction an enantiomerically pure Pd_3 metallacycle (**29**) in which the square-planar Pd(II) ions are connected by C-metalated β-ketosulfoxide (*R*)-3-*p*-tolylsulfinyl-2-propanone units (Figure 17).[78] Each linker binds to one Pd atom through the sulfoxide and the carbonyl moieties, and to the other through the methyne carbon and the *ortho*-carbon of the *p*-tolyl fragment, forming two five-membered rings (Figure 17). The core of the trimer is a nine-membered ring with alternating Pd, S, and C(H) atoms, which defines a cavity of ca. 4.0 Å in diameter. The methyne groups lay above, and the S atoms below, the plane of the Pd atoms. The angle between the coordination planes of two adjacent palladium atoms is 62.3°.

A homochiral trinuclear *cis*-dioxomolybdenum(VI) macrocycle of formula Δ,Δ,Δ-$[\{cis\text{-}MoO_2((1R,2R)\text{-dachcam})\}_3]^{6-}$ (**30**) was obtained by treatment of sodium or potassium molybdate with H_4-(1*R*,2*R*)-dachcam (Chart 4), a chiral analogue of the azotochelin siderophore.[79] Each Mo atom binds two catecholamide units from two different ligands. The X-ray structure showed that the catecholamide units have the *cis,cis,cis*-orientation in two Mo corners and

Chart 4

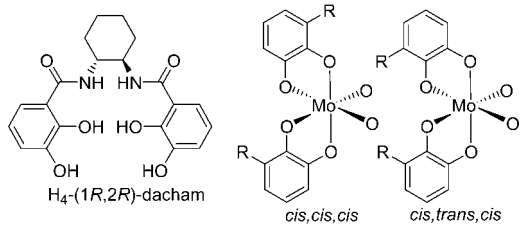

the *cis,trans,cis*-orientation in the third one (Chart 4). The Mo atoms form an approximately equilateral triangle with Mo···Mo distances in the range 11.104(4)−11.236(4) Å.

Latos-Grazyński and co-workers described several cyclic porphyrin trimers obtained by self-coordination of M(III)-2-hydroxy-5,10,15,20-tetraphenylporphyrin (M·2−OH−TPP, M = Fe(III), Mn(III), Ga(III)).[80] Each metalloporphyrin has two coordinate vectors available at an angle of ca. 60°: one from the peripheral oxygen atom and the other corresponding to an axial position of M(III) inside the porphyrin core (Figure 18). In the case of the Fe(III)-porphyrin, the structure of [{Fe·(2-O-TPP)}$_3$] (**31**) was confirmed by X-ray crystallography.[80d] Head-to-tail self-coordination yields an approximately equilateral molecular triangle at a distance of ca. 7 Å, in which the porphyrin planes are ca. perpendicular to the plane of the three iron atoms.

Two similar trinuclear metallacycles of metalloporphyrins were later described by other groups: one (**32**) obtained by self-coordination from an Al(III)-porphyrin bearing a *para*-benzoate in one *meso*-position,[81] and the other (**33**) from a Zn(II)-porphyrin with a *meso*-cinchomeronimide moiety.[82] The X-ray structure of **33** was also determined (Figure 19).[82]

In 2002, Dreos and co-workers prepared and structurally characterized another unusual trinuclear metallacycle (**34**), obtained by the reaction of Co(III)-methylaquabis(dimethylglyoximate) with 3-aminophenylboronic acid in water (Scheme 8).[83] In this cyclic trimer, each linker binds through the amino group to one cobalt atom and through the boron atom to the oxime oxygens (i.e., with the ligand) of the other cobalt atom.

A chiral trinuclear metallacycle [{Cu(DMF)(μ-(*S*,*S*)L13)}$_3$] (**35**) was obtained by Jeong and co-workers by self-assembly

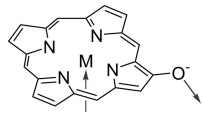

Figure 18. Deprotonated M·2−OH−TPP (M = Fe(III), Mn(III), Ga(III)) with coordinate vectors.

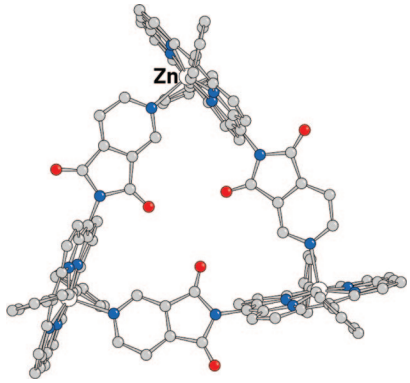

Figure 19. X-ray structure (top view) of **33** (*t*-butyl groups at peripheral phenyl rings omitted for clarity).

Scheme 8

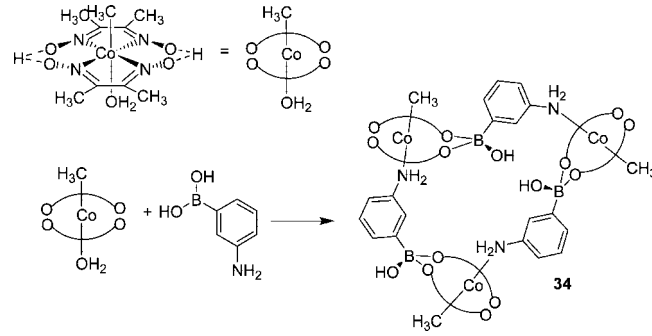

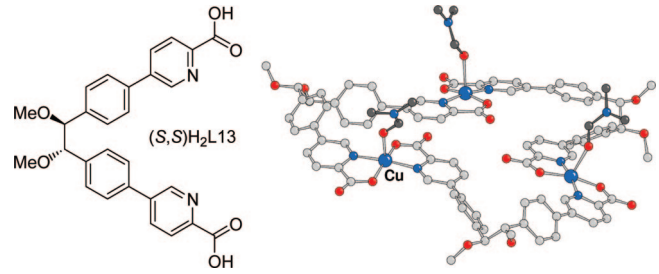

Figure 20. Schematic drawing of (*S*,*S*)H_2L13 (left) and X-ray structure of [{Cu(DMF)(μ-(*S*,*S*)L13)}$_3$] (**35**).

Scheme 9

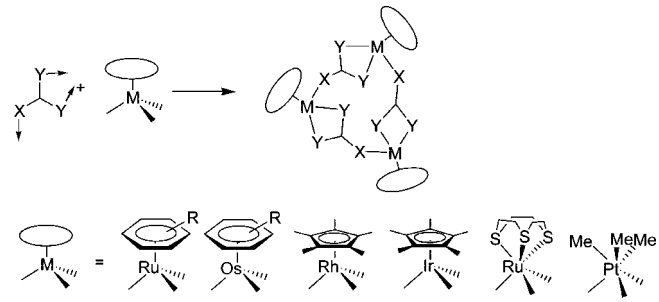

of the chiral flexible linker (*S*,*S*)-1,2-dimethoxy-di-4-(2′-carboxyl-5′-pyridyl)phenyl ethane, (*S*,*S*)H_2L13 (Figure 20), with Cu(II) ions.[84] The X-ray structure (Figure 20) showed that each copper ion has a square-pyramidal geometry, with the basal plane defined by two chelating 2′-carboxylic pyridine moieties and a dimethylformamide (DMF) molecule in apical position. With the exception of DMF ligands, the metallacycle (side length = 11.069 Å) has an almost coplanar arrangement.

5.2. Half-Sandwich Metal Corners and Tridentate Linkers

There is a quite large class of bowl-shaped trinuclear metallacycles that share common structural features (Scheme 9): (i) the linkers are tridentate O,O′,N or O,N,N′ neutral or anionic molecules, most commonly planar aromatics, that bind one metal in a bidentate chelating fashion and the other in a monodentate fashion (Chart 5). (ii) The metal corners are half-sandwich complexes with three facial coordination sites available for complexation. Most commonly, the ancillary ligand that firmly holds the other three coordination positions is an organometallic fragment, i.e., an arene, Cp or Cp* (Cp* = η^5-pentamethylcyclopentadienyl), but in some cases the face-capping macrocycle 1,4,7-trithiacyclononane ([9]aneS3) has also been used. In addition to their appealing structures, some of these trinuclear metallacycles were proved

Chart 5. Commonly used linkers for the trinuclear metallacycles described in this section. They all share one common feature: the coordinate vectors (arrows) of the two binding sites (one chelating and the other monodentate) are oriented ca. orthogonal to one another.

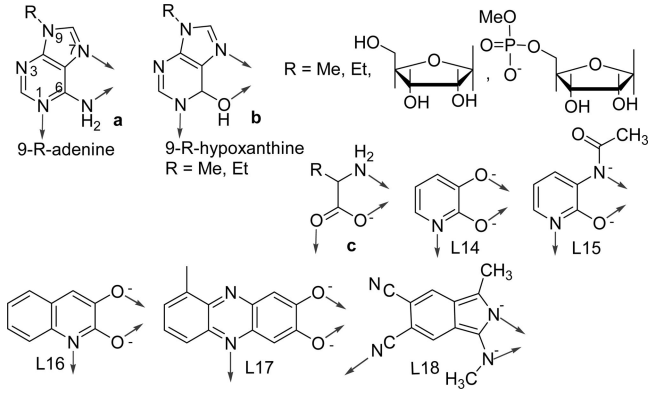

to act as highly specific hosts and sensors for neutral molecules, cations, and anions.

This field was pioneered by Fish and co-workers, who prepared a series of cationic trinuclear metallacycles using deprotonated 9-substituted adenine or hypoxanthine derivatives as linkers (Chart 5 parts a and b) and cationic Cp*Rh(III) fragments as metal corners.[85] The X-ray structure of [{Cp*Rh(μ−9-EtHpx)}$_3$](CF$_3$SO$_3$)$_3$ (**36**, 9-EtHpxH = 9-ethylhypoxanthine) is reported in Figure 21.

These cationic metallacycles, which define a 12-membered ring, were found to be effective hosts for molecular recognition of aromatic amino acid guests, e.g., L-Phe and L-Trp, in aqueous solution. Structurally related cationic metallacycles with the same linkers and (arene)Ru(II), ([9]aneS3)Ru(II), Cp*Ir(III), or Cp*Rh(III) corners were subsequently reported by the groups of Sheldrick,[86] Yamanary,[87] and Thomas.[88] A neutral Pt(IV) metallacycle with bridging 9-methyladeninate, [{*fac*-Pt(Me)$_3$(μ−9-MeAd)}$_3$] (**37**, 9-MeAdH = 9-methyladenine), in which the three facial positions of the angular metal fragments are occupied by three methyl groups rather than by an aromatic fragment, was prepared and structurally characterized by Steinborn and co-workers (Figure 22).[89]

Similar metallacyclic trimers were obtained by the groups of Beck[90] and Carmona,[91] using as linkers deprotonated

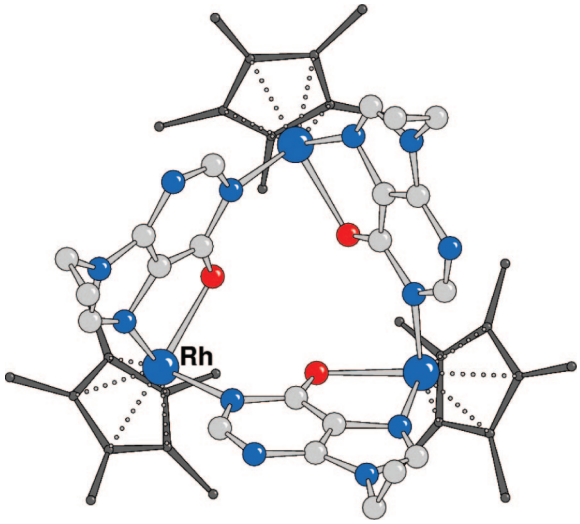

Figure 21. Molecular structure of the cation [{Cp*Rh(μ−9-EtHpx)}$_3$]$^{3+}$ (**36**) evidencing the 12-membered ring.

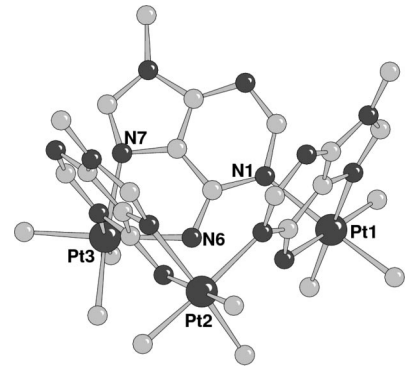

Figure 22. Molecular structure of [{*fac*-Pt(Me)$_3$(μ−9-MeAd)}$_3$] (**37**).

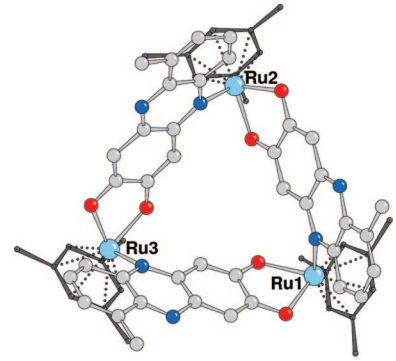

Figure 23. X-ray structure of [{(cymene)Ru(μ-L17)}$_3$] (**38**) evidencing the 18-membered ring.

amino acids that act both as (N,O)-chelating and as carboxylate bridging ligands (Chart 5c).

Severin and co-workers instead prepared and structurally characterized a series of neutral cyclic trimers of general formula [{(π-ligand)M(μ-L14)}$_3$] (π-ligand = arene, Cp*; M = Ru, Rh, Ir) using deprotonated 2,3-dihydroxypyridine (L14, Chart 5) as linker.[92] The 12-membered rings of these macrocycles contain three oxygen atoms in close proximity to each other and were thus defined as organometallic analogues of the [12]crown-3 ethers. M···M distances are between 5.27 and 7.24 Å, depending on the orientation of the ligands with respect to the plane of the three metals (see below). Similar metallacycles, defining 12- or larger 18-membered rings (M···M distance = 7.46 ± 0.02 Å), were also obtained using deprotonated 3-acetamido-2-pyridone (L15, Chart 5),[92] 2,3-dihydroxyquinoline (L16, Chart 5), or 6-methyl-2,3-phenazinediol (L17, Chart 5) as linkers.[93] The X-ray structure of a representative 18-membered ring metallacycle, [{(cymene)Ru(μ-L17)}$_3$] (**38**), is shown in Figure 23.

The cationic trinuclear metallacycles described above are basically soluble only in water, whereas these neutral compounds display a good solubility in a wide range of organic solvents. As a consequence, they have also an interesting host−guest chemistry: in organic solvents (e.g., chloroform), they proved to be excellent receptors for lithium and sodium salts, which are bound as ion pairs, with selectivity depending on the nature of the (π-ligand)M fragment. They have potential application as chemosensors for such cations through electrochemical detection. In addition, it was suggested that the Li$^+$ containing metallamacrocycles might behave as specific receptors for fluoride.[92,93]

In general, the trinuclear metallacycles belonging to this class were comprehensively studied by single-crystal X-ray

Scheme 10. 9-Substituted Adeninate Yields Trinuclear Metallacycles (Top), Whereas Adeninate Yields Molecular Squares (Bottom); Red-Dotted Lines Represent the Prolongations of the Coordinate Vectors

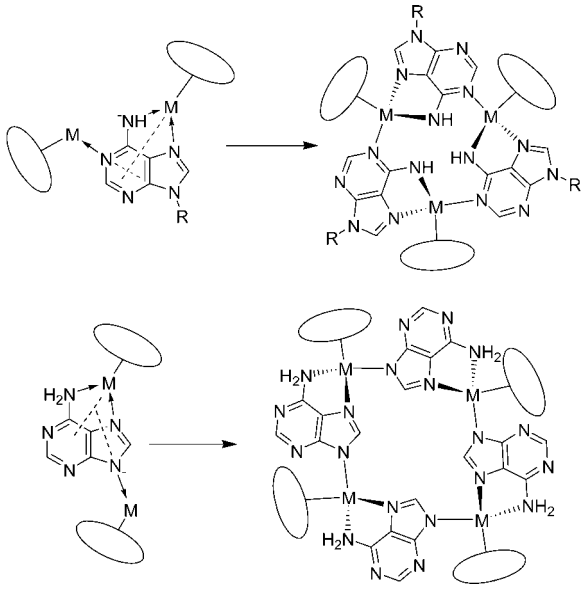

analysis. They all have a (pseudo-)C_3 symmetry. The size and shape of the resulting metallacycle were shown to depend on the orientation of the coordinate vectors and on the nature of the donor atoms in the linkers.[6] When the linkers are planar aromatic molecules, in most cases the cyclic trimers have a domelike (or bowl-shaped) structure, with the three metal atoms forming a ca. equilateral triangle at the top of the dome, the three face-capping ligands (e.g., Cp*) stretching out from the top of the dome, and the planes of the three aromatic linkers forming the walls of the cavity. The cavity opening at the bottom of the dome is ca. 7.5 Å, while its depth is ca. 4 Å. In some cases, however, the planes defined by the heterocyclic ligands are almost perpendicular to the M_3 plane, resulting in an expanded macrocycle. All these systems assemble from mixtures of organometallic precursors and linkers in specific conditions (e.g., in the presence of base) under thermodynamic control and are generally obtained in good yield. Only the 9-methyladenine metallacycle $[\{([9]aneS_3)Ru(\mu-9\text{-MeAd})\}_3]^{3+}$ (**39**) was described as kinetically locked and can be reversibly oxidized into mixed-valence states.[88]

The wealth of structural information gained for these trinuclear metallacycles led Severin and co-workers to a rationalization of the field with the establishment of some guidelines:[93] suitable tridentate linkers must be relatively rigid (to avoid formation of entropically favored dinuclear species), and above all, their two coordinate vectors must be approximately orthogonal to each other (as evidenced in Scheme 9 and Chart 5). The case of adenine is explicative (Scheme 10): while 9-substituted adeninate derivatives afford trinuclear metallacycles (the ligand adopts a $\mu-1\kappa N^1:2\kappa^2N^6,N^7$ binding mode, i.e., it binds to one metal ion in a bidentate fashion via the NH^6 and N^7 donors, forming a five-membered chelate ring, and bridges to another metal ion through the N^1 moiety, Chart 5a), free adeninate forms molecular squares (the ligand adopts a $\mu-1\kappa N^9:2\kappa^2N^6,N^7$ binding mode).[86b] The coordinate vectors are ca. orthogonal in the first case and form a much wider angle in the second (Scheme 10).

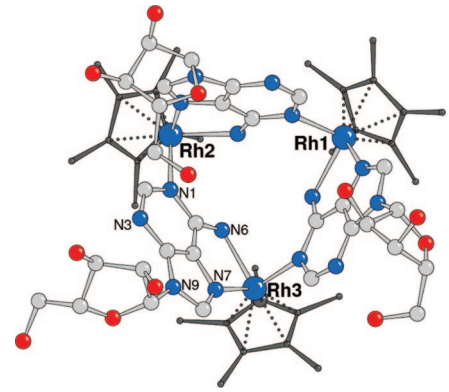

Figure 24. X-ray structure of the cation $[\{(Cp^*)Rh(Ado)\}_3]^{3+}$ (**40**).

Upon trimerization, the (π-ligand)M fragments become stereogenic centers. Interestingly, both in solution and in the solid state, only the two diastereomers with the same configuration at the three chiral metal centers, $M_RM_RM_R$ and $M_SM_SM_S$, were found, i.e., trimerization occurs with strong chiral self-recognition between the metal fragments (i.e., the self-assembly process is completely diastereoselective). The metallacycles with achiral bridging ligands, such as 9-MeAd or 2,3-dihydroxypyridine, form as racemic mixtures, while those with chiral linkers (e.g., adenosinato or aminoacids) form as mixtures of two diastereomers. The original cyclic trimer first prepared by Fish and co-workers, $[\{(Cp^*)Rh(Ado)\}_3](CF_3SO_3)_3$ (**40**, AdoH = adenosine), was a mixture of two diastereomers due to the chirality of the ribose group, but the mixture was not resolved.[85] One of the two diastereomers of **40** in pure form was later obtained by fractional crystallization by Yamanari and co-workers, who also determined the X-ray crystal structure (Figure 24).[87]

More recently, Amouri and co-workers described the resolution of the enantiomers of $[\{(Cp^*)Rh(5\text{-chloro-2,3-dioxopyridine})\}_3]$ (**41**).[94] Conversion of the racemate to a mixture of diastereomeric salts exploited the encapsulation of Li^+ followed by anion metathesis using an optically pure Δ-Trisphat salt. The pair of diastereomers *R*,*R*,*R* and *S*,*S*,*S* [Li⊂**41**][Δ-Trisphat] were separated by fractional crystallization.

The unusual neutral trinuclear metallacycles $[\{(Cp^*)_2M(\mu\text{-L18})\}_3]$ (**42**, M = U; **43**, M = Th), which fit into this class even though the metal corners bear two rather than one face-capping ligands, were obtained by reaction of 1,2,4,5-tetracyanobenzene with the actinide precursor $[(Cp^*)_2M(CH_3)_2]$ (M = U, Th) (Scheme 11).[95] The three planar 5,6-dicyano-1-methyl-3-(*N*-methylamino)isoindolyl linkers (L18, derived by an unprecedented actinide-mediated cyclization of 1,2,4,5-tetracyanobenzene, Chart 5) bind one metal in a bidentate-chelating fashion (through the *N*-methylamide moiety and the isoindole ring nitrogen) and the other in a monodentate fashion (through one of the two nitrile groups), and the two coordinate vectors form approximately a 90° angle (Chart 5). The X-ray structure of the U(IV) derivative **42** was also determined: in the solid state, the metallacycle has C_{3h} symmetry and each uranium is 9-coordinate, with a U···U distance of 10.92 Å.

Finally, there are trinuclear metallacycles that might fit within this class, even though the metal corners are square planar Pd(II) or Pt(II) complexes rather than half-sandwich fragments. Williams and co-workers obtained the trinuclear metallacycle $[\{Pd(OAc)(\mu\text{-mbzimp})\}_3]$ (**44**) in high yield by reaction of 1,3-bis(1-methyl-benzimidazol-2-yl)benzene (mb-

Scheme 11. Preparation of the Actinide Metallacycles 42 (M = U) and 43 (M = Th); Methyls Omitted on Cp* Ligands

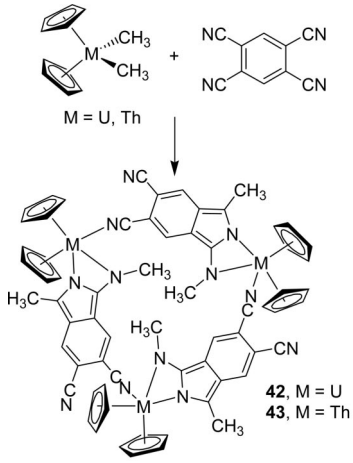

zimpH) with palladium acetate.[96] In **44**, characterized also by X-ray crystallography (Figure 25), the deprotonated ligands are cyclometalated at the phenyl 6-position. Thus, in each linker, one benzimidazole group forms a five-membered N−C chelate ring with one Pd ion and the other benzimidazole group binds via the N atom to the second Pd ion (trans to the nitrogen of the chelate ring) (Figure 26). A monodentate acetato ligand occupies the last coordination site on each Pd ion. The two binding fragments in each ligand form a dihedral angle of 50°, and as a consequence, also in this case the two coordinate vectors are ca. orthogonal to one another.

A similar cyclic trimer was very recently described by Connick and co-workers.[97] Treatment of K_2PtCl_4 with 1,3-bis(N-pyrazolyl)benzene (bpzphH) yields, under appropriate

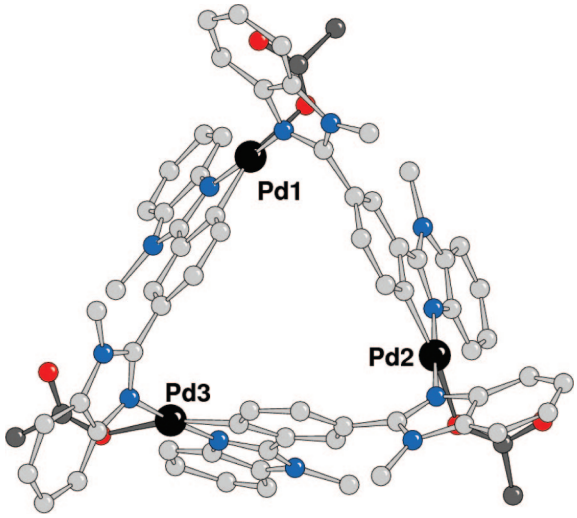

Figure 25. Molecular structure of [{Pd(OAc)(μ-mbzimp)}$_3$] (**44**).

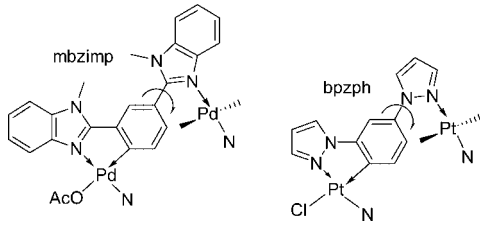

Figure 26. Repeating units in the similar trinuclear metallacycles **44** (left) and **45** (right).

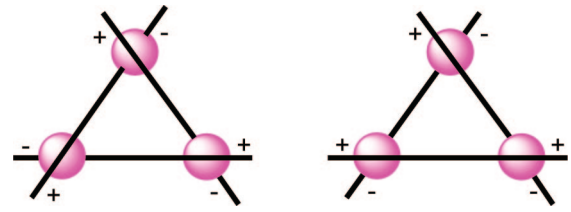

Figure 27. Trinuclear double-stranded cyclic helicate with three trans strands (left) and pseudo 3 × 3 grid with one trans and two cis strands.

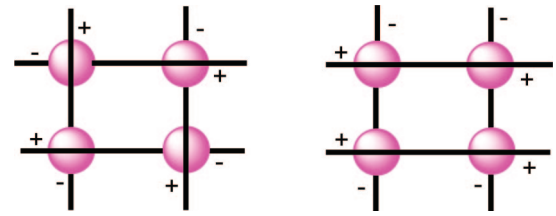

Figure 28. When combined with appropriate metal centers, trans strands generate tetranuclear cyclic helicates (left), whereas cis strands generate 4 × 4 grids (right).

conditions, the trinuclear compound [{Pt(μ-bpzph)Cl}$_3$] (**45**), whose X-ray structure was determined. The binding mode of the bpzph$^-$ unit is similar to that described above for mbzimp$^-$ (Figure 26). Thus, each Pt atom binds two pyrazolyl groups in trans geometry and a chloride in the last coordination position. The Pt(II) coordination planes are almost perpendicular to the Pt_3 plane, thus defining a ca. 8 Å deep cavity. As a concluding remark, we note that most of the trinuclear metallacycles described above might fit well also in section 6, dedicated to metallacalix[3]arenes (see below).

5.3. Cyclohelicates

A small number of trinuclear metallacycles might be better defined as cyclic double-stranded helicates. Most of them share a common structural feature: the connecting metal atoms are *naked* tetrahedral ions, either Cu(I) or Zn(II), and the linkers, which in this case can be better defined as *strands*, have two antiparallel bidentate-chelating binding units (i.e., each strand has a trans conformation). Thus, for each strand, one coordinate vector is above (+) and the other is below (−) the plane of the three metal ions (Figure 27).

Very often, however, the antiparallel geometry of the two binding sites on each strand is not rigidly enforced, and the two coordinate vectors may, in principle, assume either a trans or a cis arrangement. Whereas in a tetranuclear metallacycle with tetrahedral metal corners the cis strands can generate the 4 × 4 grid-type geometry in which, for each linker, both coordination vectors are either above or below the average plane of the four metals (Figure 28), this arrangement is not allowed in a trinuclear metallacycle, where at least one of the three strands *must* bind in an antiparallel fashion to two metal centers: thus, in principle, only pseudo (or imperfect) 3 × 3 grids are possible (Figure 27).

The majority of trinuclear cyclohelicates are based on tetrahedral Cu(I) ions. In 1997, Lehn and co-workers reported that the linker L19 (Chart 6) self-assembles with Cu(I) ions (1:1 ratio) in nitromethane solution to generate (according to mass spectrometry and NMR measurements) an equilibrium mixture of a dinuclear complex (a double helicate), a trinuclear cyclic helicate, and a 4 × 4 grid.[98] Only the double

Chart 6

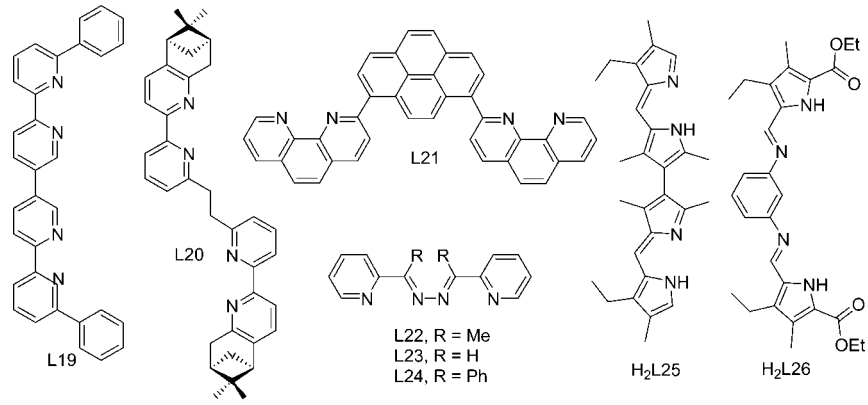

helicate could be crystallized from the mixture and was structurally characterized.

Similarly, the group of Constable reported that treatment of the chiral linker L20 (Chart 6) with $[Cu(MeCN)_4][PF_6]$ gives a library of $[\{Cu(L20)\}_n][PF_6]_n$ species ($n = 2-5$).[99] From this equilibrium mixture, the double helicate ($n = 2$) and the trinuclear cyclic helicate ($n = 3$) were separately crystallized under different conditions and structurally characterized by X-ray crystallography. The trinuclear compound $[\{Cu(L20)\}_3][PF_6]_3$ (**46**, Cu(I)···Cu(I) distance in the range 6.905−6.983 Å) crystallized as a pair of diastereomeric *P* and *M* cyclic helicates.

Another similar cyclohelicate with Cu(I) corners, $[\{Cu(L21)\}_3][ClO_4]_3$ (**47**) was selectively obtained by Thummel and co-workers by treatment of the 1,8-di(1,10-phenanthrolin-2-yl)pyrene ligand (L21, Chart 6) with $[Cu(MeCN)_4][ClO_4]$.[100] The nature of the adduct was confirmed by a low-quality X-ray structural characterization. All three linkers have the same helical twist about the phen−pyrene−phen bonds (57.8−59.7°).

More recently, Hannon and co-workers reported that reaction of the bis-pyridylimine linker L22 (Chart 6, R = Me) with an equivalent amount of $[Cu(MeCN)_4][PF_6]$ yielded the trinuclear cyclohelicate $[\{Cu(L22)\}_3][PF_6]_3$ (**48**), whose X-ray structure was determined (Figure 29).[101] In the metallacycle, each tetrahedral Cu(I) atom is chelated by the pyridylimine groups of two distinct linkers in trans conformation (induced by a substantial twist about the central N−N bonds). The Cu(I)···Cu(I) distance is in the range 4.45−4.53 Å. The same reaction with L23 (R = H) yielded a polymer, whereas it afforded a dinuclear double helicate with L24 (R = Ph). Similarly, it had been previously reported that reaction of L23 with $Ni(SCN)_2$ yields the trinuclear cyclic helicate $[\{Ni(L23)(SCN)_2\}_3]$ (**49**).[102] The X-ray structure showed that the coordination sphere of each distorted octahedral Ni(II) atom (average Ni(II)···Ni(II) distance = 4.95 Å) is completed by two adjacent thiocyanates (Figure 30).

Other examples of trinuclear cyclohelicates were obtained with tetrahedral Zn(II) ions. Dolphin and co-workers reported that linker H_2L25, comprising two dipyrromethene units linked at the β-position (Chart 6), after double deprotonation self-assembles with Zn(II) ions to give selectively and in high yield the neutral trinuclear cyclohelicate $[\{Zn(L25)\}_3]$ (**50**), which was also characterized by X-ray crystallography (Zn(II)···Zn(II) distance is in the range 9.27−9.36 Å).[103] A similar trimer (not structurally characterized) was selectively obtained also with Co(II). These trimers were believed to be both the kinetic and the thermodynamic products of the above-described reactions, since they formed in high yields under several different conditions. Similarly, the self-assembly of the benzene-bridged bis(pyrrol-2-ylmethyleneamine) linker H_2L26 with Zn(II) ions selectively yielded (after double deprotonation) the corresponding neutral trinuclear cyclohelicate $[\{Zn(L26)\}_3]$ (**51**), which was also characterized by X-ray crystallography (average Zn(II)···Zn(II) distance = 7.5 Å).[104] Other Zn(II) metallacycles, namely, a molecular square and double helicates, could be obtained by changing the geometry of the spacer between the two binding units in the linker.

To our knowledge, no pseudo 3 × 3 grid (Figure 27) was explicitly mentioned until very recently, when Schmittel and Mahata described the preparation of heteropletic trinuclear cyclic helicates.[105] The compounds were assembled in a stepwise manner (Figure 31): first, the kinetically locked $[Cu(L27)_2](PF_6)$ complex was prepared, in which both ligands have a free phen coordination site. Treatment of this

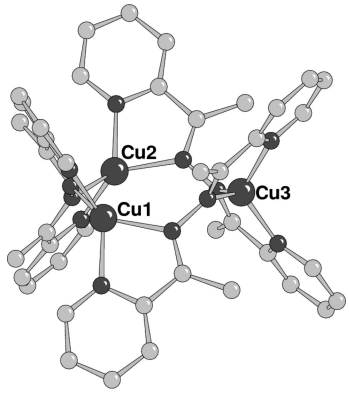

Figure 29. X-ray structure of the cation of $[\{Cu(L22)\}_3][PF_6]_3$ (**48**).

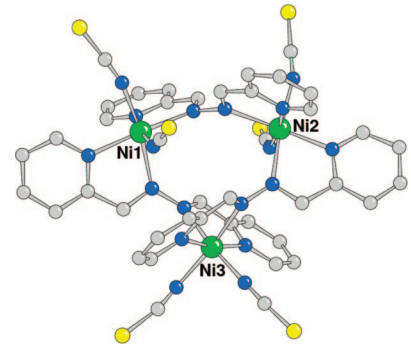

Figure 30. Molecular structure of the cation of $[\{Ni(L23)(SCN)_2\}_3]$ (**49**).

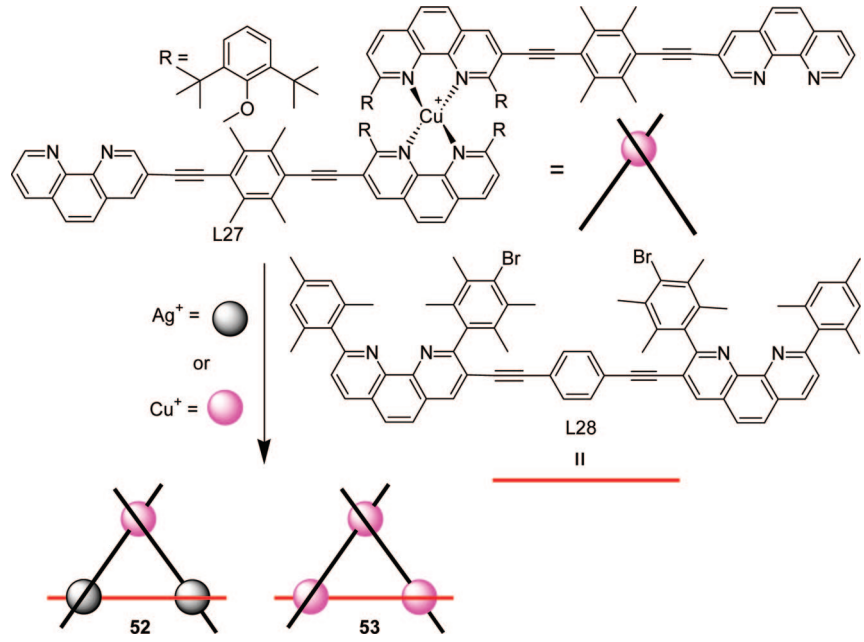

Figure 31. Compounds **52** and **53**.

flexible hinge with another, very similar, strand (L28) in the presence of Ag(I) or Cu(I) ions afforded (according to spectroscopic and ESI-MS evidence) the trinuclear metallacycles $[CuAg_2(L27)_2(L28)](PF_6)_3$ (**52**, heterometallic and heteroleptic) and $[Cu_3(L27)_2(L28)](PF_6)_3$ (**53**, homometallic and heteroleptic), respectively. The strands L27 and L28 can assume either a trans- or a cis-conformation. On the basis of ^{1}H NMR evidence, the authors suggested that in solution **53** is an equilibrium mixture of the symmetrical cyclic helicate and two pseudo 3 × 3 grids.[106]

A particular case of trinuclear cyclic compound, which closely recalls the cyclohelicates with tetrahedral metal ions described above (even though it is not chiral), was recently reported by Sauvage and co-workers.[107] An equilibrium mixture of trinuclear $[\{Cu(L29)\}_3]^{3+}$ (**54**) and tetranuclear $[\{Cu(L29)\}_4]^{4+}$ (**55**) cyclic pseudorotaxanes was obtained by Cu(I)-mediated assembly of linker L29, in which a phen-containing macrocycle is rigidly attached to a filament bearing a second phen unit. The two bidentate chelates are disposed in the linker in such a way that their coordinate vectors are (ideally) orthogonal to each other (rather than at 180° as in the trans strands, Figure 32). Owing to the presence of the macrocycle, the linkers are forced to assemble in a head-to-tail fashion. Unfortunately, no X-ray structure was available, but the tetrahedral geometry of the connecting Cu(I) atoms, together with orthogonal orientation of the two coordinate vectors of each linker, implies a helical structure.

More recently, the same group reported that the highly rigid phen−terpy linker L30, with two orthogonal coordinate vectors, yields a mixture of dinuclear $[\{Cu(L30)\}_2]^{4+}$ and trinuclear $[\{Cu(L30)\}_3]^{6+}$ (**56**) cyclic species (Figure 33) in which the Cu(II) corners are five-coordinate and bound to one terpy and one phen unit from two different linkers.[108]

With the exception of this last example, the two binding units in linkers described so far in this section were invariably bidentate N−N chelates. However, trinuclear cyclic helicates were obtained also from the combination of strands with binding sites of denticity other than two and appropriate metal ions with geometries other than tetrahedral. Williams and co-workers reported that treatment of the two similar chiral oxazoline linkers (L31 and L32, Chart 7) with Ag(I)

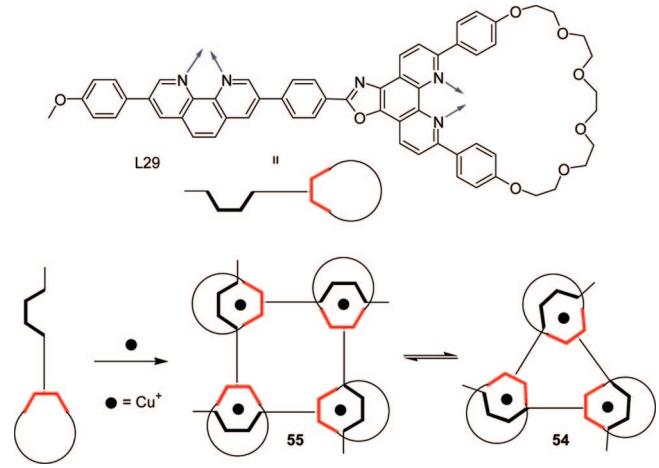

Figure 32. Equilibrium mixture of **54** and **55** obtained by Cu(I)-mediated assembly of linker L29.

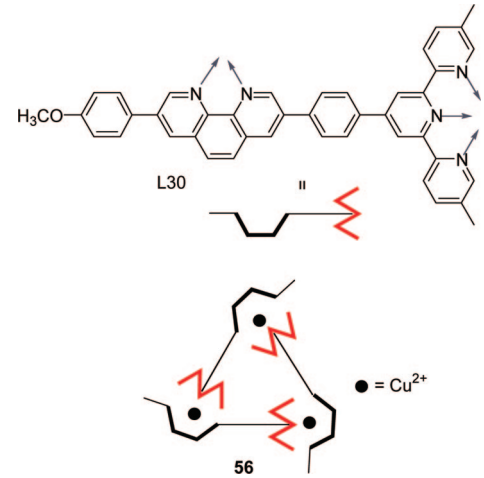

Figure 33. Mixture of dinuclear $[\{Cu(L30)\}_2]^{4+}$ and trinuclear $[\{Cu(L30)\}_3]^{6+}$ (**56**) cyclic species.

afforded different products.[109] In fact, while (*S*,*S*)-2,6-bis(4′-benzyl-ox-azolin-2′-yl)pyridine (L31) specifically yielded the *P* (or Δ) double helicate $[Ag_2(L31)_2]^{2+}$, the similar (*R*,*R*)-

Chart 7

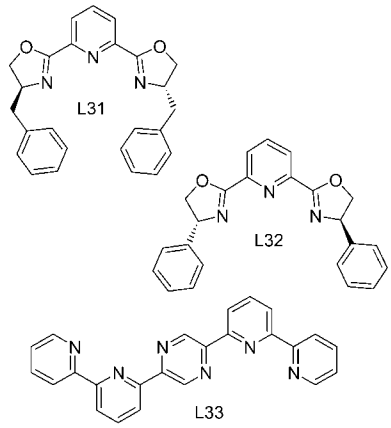

2,6-bis(4′-phenyloxazolin-2′-yl)pyridine (L32), instead of the expected *M* double helicate, selectively afforded the *P* trinuclear cyclohelicate $[\{Ag(L32)\}_3]^{3+}$ (**57**). A reasonable explanation of this preference for L32 is the existence of $\pi-\pi$ stacking interactions in the trinuclear complex (Figure 34). The X-ray structures of both compounds (as BF_4 salts) showed that only the oxazoline N atoms are involved in the coordination and that, in the metallacycle **57**, unlike in the double helicate, the coordination of the silver ions is not strictly linear (angle N−Ag−N = 153.3(6)°). Thus, each linker binds to one metal from below and to the other from above the plane of the three Ag atoms, which defines an equilateral triangle with Ag···Ag distance of 3.001(2) Å.

The group of von Zelewsky reported that the rigid strand L33 (Chart 7), with two antiparallel terpyridine-like binding sites, self-assembles with Zn^{2+} ions to yield, according to NMR and mass-spectrometry evidence, an equilibrium mixture of trinuclear, $[\{Zn(L33)\}_3]^{6+}$ (**58**), and tetranuclear, $[\{Zn(L33)\}_4]^{8+}$ (**59**), cyclic helicates (Figure 35).[110] In this case, the Zn(II) ions, as confirmed by the X-ray structure of the 4 × 4 grid obtained with a very similar chiral strand, have an octahedral coordination geometry. The trinuclear metallacycle **58** is the minor species within the concentration range investigated. The thermodynamic data for this equilibrium, obtained by NMR spectroscopy, unexpectedly indicated that, for the 3□ → 4Δ reaction, both $\Delta H°$ and $\Delta S°$ are negative, i.e., have signs opposite to those expected for the equilibrium between metallacycles of different nuclearity

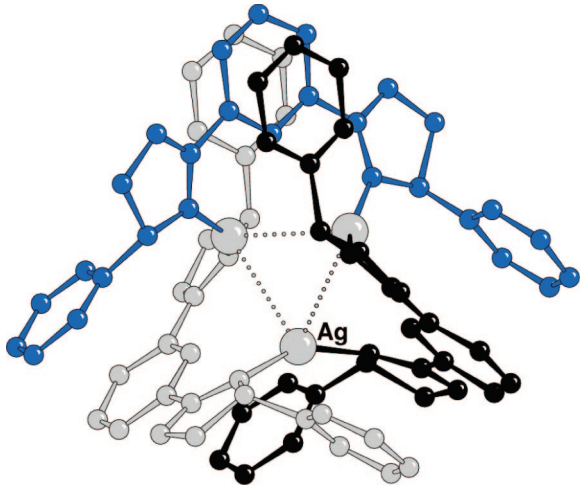

Figure 34. X-ray structure of $[\{Ag(L32)\}_3]^{3+}$ (**57**), with the three L32 strands in different colors.

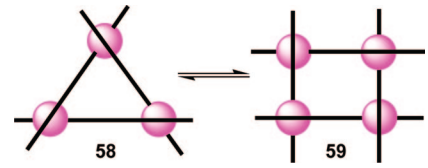

Figure 35. Schematic drawings of the equilibrating compounds **58** and **59**.

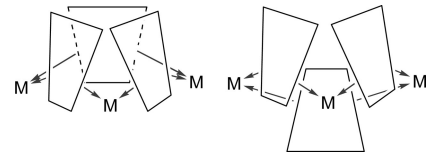

Figure 36. Schematic drawing of a metallacalix[3]arene with coordinate vectors. The two possible conformers are shown: cone (left) and partial cone (right).

(see section 7.1). The exothermicity ($\Delta H° = -74.5 \pm 10.0$ kJ mol^{-1}) was interpreted as the result of a better solvation of the trimer compared to the tetramer: probably in this case the higher strain expected for the smaller metallacycle, due to deviations from the ideal octahedral coordination geometry at the metal centers, can be neglected because Zn^{2+} ions have no ligand-field stabilization. Perhaps even more unexpected was the negative $\Delta S°$ for the 3□ → 4Δ transformation: this counterintuitive behavior could not be explained by the authors.

6. Metallacalix[3]arenes

Quite a large number of trinuclear metallacycles can be defined as metallacalix[3]arenes, by structural analogy with the organic calix[*n*]arenes. Metallacycles belonging to this group must have edges with relatively large aromatic planar fragments that define the walls of the calix[3]arene. Two conformations are possible, depending on the relative orientations of the three linkers: cone (*syn*,*syn*,*syn*-orientation) and partial cone (*syn*,*syn*,*anti*-orientation). In the cone conformer, all the coordinate vectors lay on the same side with respect to the M_3 plane, while in the partial cone conformer, four consecutive coordinate vectors are above and two are below the M_3 plane (Figure 36). When the aromatic walls are almost perpendicular to the M_3 plane, the metallacycle might resemble a *trigonal prism* rather than a calix[3]arene.

The first trinuclear metallacycle defined as metallacalix[3]arene, $[\{Pt(thpy)(\mu\text{-bzim})\}_3]$ (**60**) (thpyH = 2-(2′-thienyl)pyridine), was obtained in high yield by Che and co-workers in 1999: it featured *cis*-protected Pt corners and benzimidazolate (bzim) edges.[111] According to models, the coplanar coordinate vectors of bzim make an angle of ca. 150° (Chart 8). The molecular structure evidenced that, in the solid state, **60** has a partial cone conformation, with an average Pt···Pt distance of 6.1 Å (Figure 37). The almost ideal N−Pt−N coordination angles (range 87.8(3)−89.0(3)°) suggested minimal strain for the metallacycle.

Two structurally similar metallacycles, featuring either triazolate (tz) or imidazolate (im) linkers, had been reported previously (but not defined as metallacalix[3]arenes): in 1986, Oro and co-workers prepared and structurally characterized the organometallic metallacycle $[\{Rh(\eta^3\text{-}C_3H_5)_2(\mu\text{-tz})\}_3]$ (**61**) (that remains, to our knowledge, the first example of a compound that might be listed in this class).[112] The Rh(III) corners have a distorted octahedral geometry and are bridged

Chart 8

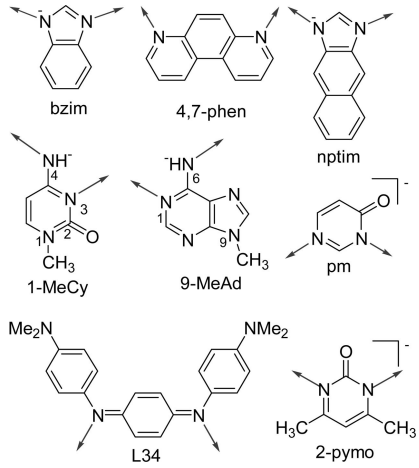

by the triazolate ligands through the nonadjacent N atoms (which, thus, are similar to the benzimidazolate linkers described above). In 1992, Chaudhuri and co-workers prepared and structurally characterized [{Cu(Me_3tacn)(μ-im)}$_3$](ClO_4)$_3$ (**62**) (Me_3tacn = 1,4,7-trimethyl-1,4,7-triazacyclononane), in which the Cu(II) metal corners have a distorted square-pyramidal geometry with two adjacent coordination sites bound to the imidazolate linkers (Cu···Cu distance = 5.92 Å).[113] Both metallacycles have the partial-cone conformation in the solid state. However, we note that, despite the formal analogy with the case described by Che (see above), owing to the small size of the aromatic walls, it might seem inappropriate to consider these metallacycles as examples of metallacalix[3]arenes (and they might be listed among the metallatriangles with angular linkers in section 7.3).

Several metallacalix[3]arenes utilize nucleobases or nucleosides as aromatic linkers and *cis*-Pt fragments as metal corners. The detailed investigation of the interaction of DNA fragments with Pt compounds was stimulated by the anticancer properties of cisplatin and related compounds, whose activity relies on in vivo coordination to DNA.[114] The first such example was described in 1994 by Longato and co-workers, who reported the quantitative formation and structural characterization of [{*cis*-Pt(PMe_3)$_2$(μ−1-MeCy)}$_3$](ClO_4)$_3$ (**63**) (1-MeCyH = 1-methylcytosine).[115] The 1-methylcytosinato linkers bind to adjacent positions of the square-planar Pt fragments through the endocyclic N(3) and the deprotonated exocyclic N(4) atoms (Chart 8). In the metallacycle, the pyrimidinic rings have a *syn*,*syn*,*syn*-orientation and their mean planes form dihedral angles in the range 56.2−68.1° with respect to the Pt_3 plane. Each Pt atom has a square-planar coordination with an average

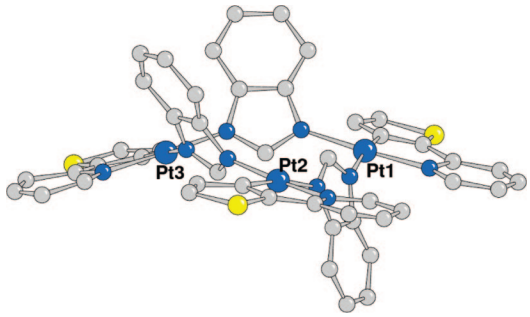

Figure 37. Molecular structure of [{Pt(thpy)(μ-bzim)}$_3$] (**60**) evidencing the *syn*,*syn*,*anti*-orientation of the bzim linkers.

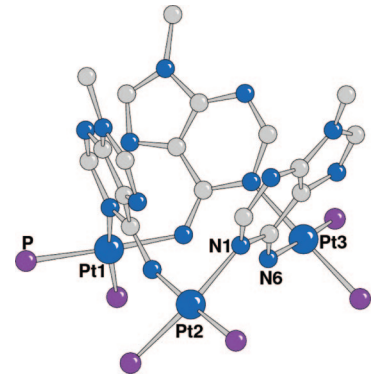

Figure 38. X-ray structure of the cation [{*cis*-Pt($PMePh_2$)$_2$(μ−9-MeAd)}$_3$]$^{3+}$ (**64**) evidencing the *syn*,*syn*,*syn*-orientation of the 9-MeAd linkers (substituents on P atoms omitted).

Pt···Pt distance of 5.2 Å. The same group later prepared and structurally characterized the similar tris-Pt metallacycles, [{*cis*-Pt($PMePh_2$)$_2$(μ−9-MeAd)}$_3$](NO_3)$_3$ (**64**), in which the deprotonated 9-methyladenosine linker binds through the N(1) and N(6) atoms (Chart 8, Figure 38), and [{*cis*-Pt(PMe_2Ph)$_2$(μ−1-MeCy)}$_3$](NO_3)$_3$ (**65**).[116] Also in **64**, the metallacalix[3]arene (average Pt···Pt distance of 5.36 Å) has a cone conformation in the solid state, with the nucleobases forming dihedral angles of 55−76° with respect to the Pt_3 plane. The similar [{*cis*-Pt(PMe_2Ph)$_2$(μ−9-MeAd)}$_3$](NO_3)$_3$ (**66**), in which the Pt atoms bear a slightly different phosphine ligand, had been reported previously by the same group and characterized by multinuclear NMR spectroscopy and mass spectrometry, but the X-ray was not determined.[117]

Relevant contributions to the field of metallacycles with *N*-heterocyclic linkers, including nucleobases, have been published in the past decade by Lippert and co-workers.[118] In 2005, they described the trinuclear Pd metallacycle [{Pd(tmeda)(μ−1-MeCy)}$_3$](ClO_4)$_3$ (**67**, tmeda = *N*,*N*,*N*′,*N*′-tetramethylethylenediamine), whose geometrical parameters in the solid state are similar to those found for the Pt trimers **63** and **65** described by Longato and co-workers (see above):[115,116b] average Pd···Pd distance close to 5.2 Å and dihedral angles of the nucleobases with respect to the Pd_3 plane in the range 67.1(3)−74.7(3)°.[119]

The same group had previously described other metallacalix[3]arenes with 2,2′-bipyrazine edges. This ligand, when combined with *cis*-protected metal fragments, generates different trinuclear metallacycles depending on whether the two pyrazine rings adopt a *trans* or *cis* arrangement about the C2−C2′ bond (see Figure 2 in Introduction). Depending on the nature of the counterions, two isomers of formula [{Pt(en)(μ-bpz-*N*4,*N*4′)}$_3$]$^{6+}$ were isolated from a mixture of [Pt(en)(H_2O)$_2$]$^{2+}$ and bpz and structurally characterized:[120] in the former, crystallized as [{Pt(en)(μ-bpz-*N*4,*N*4′)}$_3$](NO_3)$_6$ (**68**) (it will be also described in section 7.4), all three bpz ligands displayed trans conformation,[121] while in the second, crystallized as [{Pt(en)(μ-bpz-*N*4,*N*4′)}$_3$](NO_3)$_2$(ClO_4)$_4$ (**69**), all three bpz ligands had cis conformation.[120] The overall shape of the two metallacyclic conformers and their dimensions are remarkably different: the all-trans conformer **68** has a relatively flat shape more reminiscent of a triangle (or of a trigonal prism, since the bpz ligands are almost perpendicular to the Pt_3 plane), whereas the all-cis isomer **69** (Figure 39) has a cone shape, with the bpz ligands inclined at 130−135° with respect to the Pt_3 plane (and, thus, is listed here among the metallacalix[3]arenes), and hosts both a

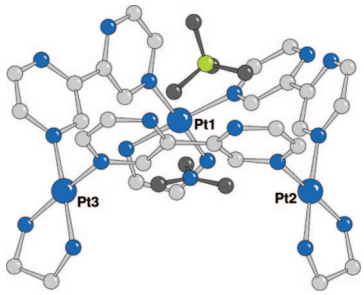

Figure 39. X-ray structure of the cation $[\{Pt(en)(\mu\text{-bpz-}N4,N4')\}_3]^{6+}$ (**69**), with all bpz linkers in cis conformation and hosting a NO_3^- and a ClO_4^- within the cavity.

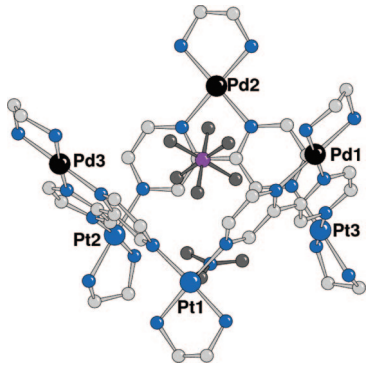

Figure 40. X-ray structure of the cation $[\{(en)Pt(N4,N4'\text{-bpz-}N1,N1')Pd(en)\}_3]^{12+}$ (**70**) with all bpz linkers in cis conformation and hosting a NO_3^- and a PF_6^- within the cavity.

NO_3^- and a ClO_4^- within the cavity, one on top of the other. As a consequence of the relative orientations of the coordinate vectors at the N4 and N4′ atoms in the two conformers, the Pt···Pt distances are significantly longer in **68** (ca. 9.4 Å) compared to **69** (ca. 7.7−8.0 Å).

The same group also showed that the all-cis structure of the Pt_3 metallacycle can be locked by binding three cis-protected metal fragments to the convergent N1 and N1′ atoms on the three edges. Thus, treatment of the all-trans isomer **68** with $Pd(en)^{2+}$ caused the conformational rearrangement of the bpz linkers and formation of all-*cis*-$[\{(en)Pt(N4,N4'\text{-bpz-}N1,N1')Pd(en)\}_3]^{12+}$ (**70**) (Figure 40).[122] It should be noted that, in this hexanuclear metallacycle, the three Pd atoms have no structural role: the $[(en)Pd(N1,N1'\text{-bpz})]^{2+}$ edges can be considered as *metal-containing ligands*. The molecular structure shows that the three Pd atoms describe a nearly isosceles triangle considerably larger than that, almost equilateral, defined by the three Pt atoms.

Also, the corresponding Pd_3/Pt_3 (in which the role of Pd and Pt ions is inverted compared to the example above) and the homonuclear Pt_3/Pt_3 and Pd_3/Pd_3 metallacycles were prepared and structurally characterized.[120] All four compounds crystallized as mixed NO_3^-/PF_6^- salts, and, in the solid state, two different anions are embedded in the +12 cationic cavity.

The coordination motif developed by the group of Lippert was subsequently exploited for the preparation of other metallacalix[3]arenes in which the corners are cis-protected square-planar $Pd/Pt(chel)^{2+}$ fragments and the edges are planar aromatic linkers with divergent coordinate vectors. Actually, these metallacycles, which preferentially crystallize in the cone conformation, define two opposite cone-shaped cavities, above and below the M_3 plane: one is formed by the three aromatic edges, and the second is formed by the three square-planar M(chel) fragments. Both the planar

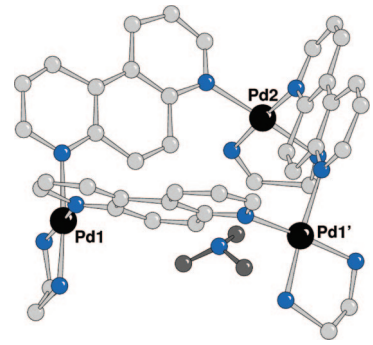

Figure 41. X-ray structure of the cation $[\{Pd(en)(\mu\text{−}4,7\text{-phen})\}_3]^{6+}$ (**73**). One nitrate anion is hosted in the bottom cone, making weak interactions with the Lewis acidic Pd atoms.

linkers and the square-planar M(chel) fragments exhibit *syn,syn,syn*-orientations.

Thus, treatment of $[Pd(en)(ONO_2)_2]$ with the π-conjugated linker *N*,*N*′-bis(4-dimethylaminophenyl)-1,4-benzoquinonediimine (L34, Chart 8) afforded quantitatively the Pd calix[3]arene $[\{Pd(en)(\mu\text{-L34})\}_3](NO_3)_6$ (**71**) (average Pd···Pd distance = 7.68 Å),[123] whereas treatment of $[Pd(bu_2bipy)(thf)_2](X)_2$ (bu_2bipy = 4,4′-di-*tert*-butyl-2,2′-bipyridine, X = BF_4, ClO_4, CF_3SO_3, NO_3) with 4(3*H*)-pyrimidone (pmH, Chart 8) in basic conditions yielded the cyclic trimers $[\{Pd(bu_2bipy)(\mu\text{-pm})\}_3](X)_3$ (**72**) (average Pd···Pd distance = 5.88 Å for X = BF_4).[124] According to X-ray structural determinations, these latter metallacalix[3]arenes host an anion in the larger cone-shaped cavity defined by the three $Pd(bu_2bipy)$ units.

Yu and co-workers described a number of structurally similar metallacalix[3]arenes of general formula $[\{M(chel)(\mu\text{−}4,7\text{-phen})\}_3](NO_3)_6$ obtained by combination of cis-protected $[M(chel)(ONO_2)_2]$ metal precursors (M = Pd(II) or Pt(II), chel = en, bipy, phen, phen-crown-6) with the planar linker 4,7-phenanthroline (4,7-phen, Chart 8).[125] The cone conformation was maintained also in solution. The X-ray structure of $[\{Pd(en)(\mu\text{−}4,7\text{-phen})\}_3](NO_3)_6$ (**73**) (Figure 41) showed that the three Pd atoms define an almost equilateral triangle, with Pd···Pd distances in the very narrow range 7.64(1)−7.69(1) Å, dihedral angles between the 4,7-phen linkers and the Pd_3 plane in the range 45.9(1)−52.0(2)° (upper rim opening of ca. 8.5 Å). In the structurally similar $[\{Pd(phen\text{-}crown\text{-}6)(\mu\text{−}4,7\text{-phen})\}_3](NO_3)_6$ (**74**) metallacycle, the two opposite cavities have different properties:[125b] the one defined by the 4,7-phen linkers is hydrophobic, whereas the other, which is larger and deeper, is hydrophilic due to the crown-ether modified rim and, in the solid state, encapsulates two nitrate anions. More recently, the same group prepared and structurally characterized the naphtoimidazolate-bridged metallacalix[3]arene $[\{Pd(phen\text{-}crown\text{-}5)(\mu\text{-nptim})\}_3](NO_3)_6$ (**75**) (nptimH = naphtoimidazole, Chart 8), which in the solid state and in solution has the cone conformation.[126]

Similar homochiral Pd calix[3]arenes, $[\{Pd(dach)(\mu\text{−}4,7\text{-phen})\}_3](NO_3)_6$ (**76**), were more recently obtained using $[Pd(dach)(ONO_2)_2]$ as metal precursor (dach = (*R*,*R*)- or (*S*,*S*)-1,2-diaminocyclohexane).[127] In aqueous solution, the macrocycles showed some binding affinity for mononucleotides, which are believed to be hosted inside the 4,7-phen cone by synergistic electrostatic, anion−π, and π−π interactions. The same group described also tri- and tetranuclear Pd(II) metallacycles containing two different linkers, 4,7-phen and 4,6-dimethyl-2-pyrimidinolato (2-pymo, Chart

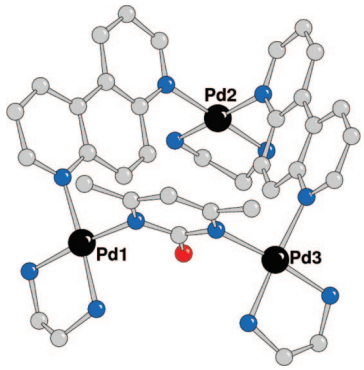

Figure 42. X-ray structure of the cation $[Pd_3(en)_3(\mu-2\text{-pymo})(\mu-4,7\text{-phen})_2]^{5+}$ (**77**).

Scheme 12

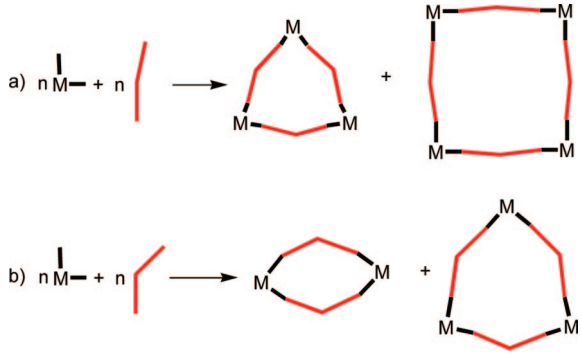

8).[128] The heterotopic metallacalix[3]arene $[Pd_3(en)_3(\mu-2\text{-pymo})(\mu-4,7\text{-phen})_2]^{5+}$ (**77**) in the solid state contains almost isosceles triangles with edges of 7.56, 7.60, and 5.71 Å and a pinched-cone conformation (Figure 42).

7. Molecular Triangles with ca. 90° Metal Corners

7.1. General Considerations

The following sections contain examples of molecular triangles featuring ca. 90° cis-protected metal corners, which occasionally consist of M−M bonded dimetallic units. The classification is done according to the geometry of the rigid organic linkers: one section is devoted to angular linkers and the others are devoted to approximately linear (or sigmoidal) linkers of variable length and rigidity. Flexible linkers will be treated separately, since the nature of the metallacycle obtained by their combination with 90° metal corners is hardly predictable.

In principle, according to the directional-bonding approach, the self-assembly of rigid linear linkers and 90° metal fragments is expected to yield a molecular square.[9] Very often, however, the combination of fragments that are not completely rigid yields mixtures of molecular squares and triangles that may or may not be in equilibrium (Scheme 12a). Similarly, the combination of ca. 90° metal corners with angular linkers (e.g., having an angle of ca. 120° between the two coordinate vectors) is likely to produce a mixture of the trinuclear and dinuclear metallacycles, also called rhomboids (Scheme 12b).[26]

It is generally accepted that, in the self-assembly reaction of linear linkers and 90°-angular metal fragments, the molecular square is enthalpically favored (less strain in the cycle), whereas the molecular triangle is entropically preferred (combination of less fragments). Closure of the smaller

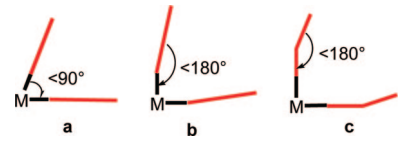

Figure 43. Schematic representation of the three main geometrical distortions that may occur in the formation of a molecular triangle: (a) coordination angles smaller than the ideal 90°, (b) nonlinear coordination geometries (inward tilt), and (c) bending of the linkers.

Scheme 13

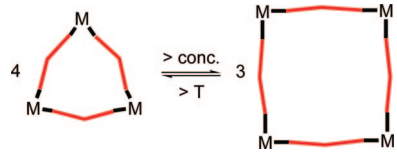

metallacycle *must* obviously involve the occurrence of some distortions, leading to strain. The three main geometrical distortions that may take place are schematically depicted in Figure 43.

Thus, if the two metallacycles are in equilibrium, according to Le Châtelier's principle, the relative amount of molecular triangle is expected to increase upon reducing the total concentration and upon raising the temperature (Scheme 13). The effect of temperature contains both enthalpic and entropic contributions. The transformation $3\square \rightarrow 4\Delta$ is expected to be endothermal and, therefore, favored at higher temperatures. In addition, $\Delta S > 0$, and thus, the $-T\Delta S$ term in the expression of Gibbs free energy becomes more relevant upon increasing the temperature. In other words, when, in a self-assembly process, an enthalpically favored supramolecule (e.g., a □) is in equilibrium with an entropically favored species (e.g., a Δ), raising the reaction temperature can make the entropy effects more relevant than the enthalpy effects.

In addition, it is also accepted that the molecular triangle should become more favorable upon decreasing the rigidity (i.e., upon increasing the length) of the edges. Longer linkers, even though rigid in principle, may allow coordination angles very close to 90° and distribute the strain of the trinuclear metallacycle in several small deformations in their backbone.

The equilibrium can be also influenced by the addition of appropriate templating molecules that stabilize one metallacycle better than the other. In some cases, the counterions and the solvent itself may have a templating effect and, thus, affect the equilibrium ratio.[59]

The solvent entropy, even though of difficult assessment, is another factor that is believed to affect significantly the equilibrium between metallacycles of different nuclearities. The larger metallacycles can trap a higher number of solvent molecules inside their cavity. Finally, it must be stressed (as already pointed out in the Introduction) that the characterization of such systems can be a complex problem, as is often the case in supramolecular chemistry for highly symmetrical assemblies made of identical subunits.

7.2. Flexible Linkers

In 1990, Süss-Fink and co-workers obtained, upon treatment of $Ru_3(CO)_{12}$ with tartaric acid (*R*,*R*, *S*,*S*, and *R*,*S*), the molecular triangles with diruthenium corner units $[\{Ru_2(CO)_4(CH_3CN)_2(\mu,\eta^4\text{-tartrato})\}_3]$ (**78**) (all-(*R*,*R*), all(*S*,*S*), and all-(*R*,*S*)) (Figure 44).[129] According to the X-ray structure, the angle defined by two adjacent edges on each $Ru_2(CO)_4$ corner

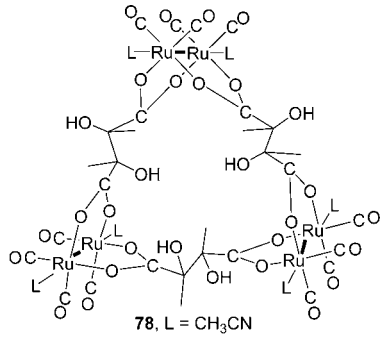

Figure 44. Molecular triangles with diruthenium corner units $[\{Ru_2(CO)_4(CH_3CN)_2(\mu,\eta^4\text{-tartrato})\}_3]$ (**78**).

Scheme 14. Preparation of the *molecular necklace* 80

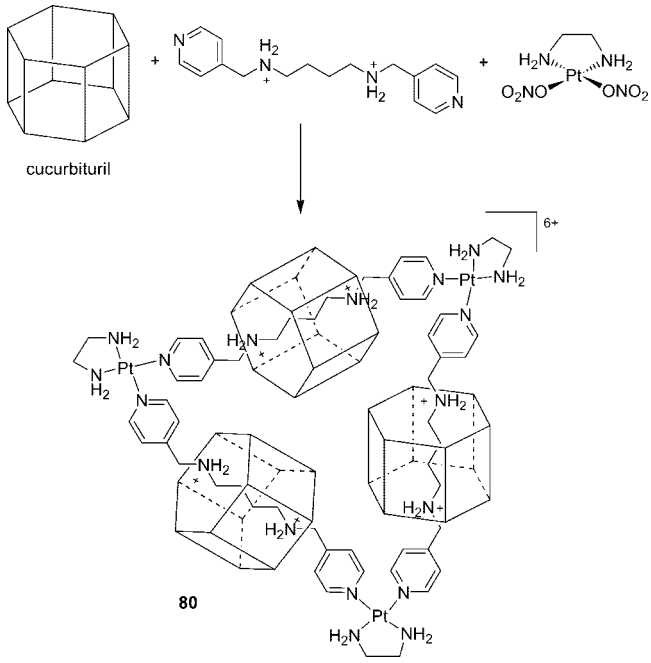

unit is ca. 80° and, in all the three independent complexes, the flexible tartrato edges present the six OH groups on the same side of the trinuclear entity. A similar trinuclear metallacycle featuring the more rigid 4,4′-biphenyldicarboxylate linker, $[\{Ru_2(CO)_4(PPh_3)_2(\mu,\eta^4\text{-}4,4'\text{-}O_2CC_6H_4C_6H_4CO_2)\}_3]$ (**79**), was more recently prapared and structurally characterized by Shiu and co-workers.[130]

An unusual type of molecular triangle, a trinuclear cyclic oligorotaxane defined as a *molecular necklace* (MN), was prepared by Kim and co-workers by a one-pot quantitative self-assembly procedure that can be schematically described as follows:[131] 1,4-diaminobutane (or 1,5-diaminopentane), functionalized at both ends with 4-pyridylmethyl groups to produce a short ditopic flexible string, was threaded through cucurbituril "beads" to form a stable pseudorotaxane that finally self-assembled with the cis-protected metal precursor $[Pt(en)(ONO_2)_2]$ to yield the trinuclear molecular necklace (**80**) (Scheme 14). The cucurbituril confers some rigidity to the otherwise flexible linker.

Compound **80**, which features three small rings threaded on the large ring, is labeled [4]MN and is a topological stereoisomer of a classical [4]catenane. The X-ray structure of **80** (Figure 45) showed that each corner of the equilateral triangle (which has C_3 symmetry) is occupied by a Pt(en) fragment (Pt···Pt distance = 19.45 Å) and each edge is occupied by a sigmoidal-shaped pseudorotaxane that binds

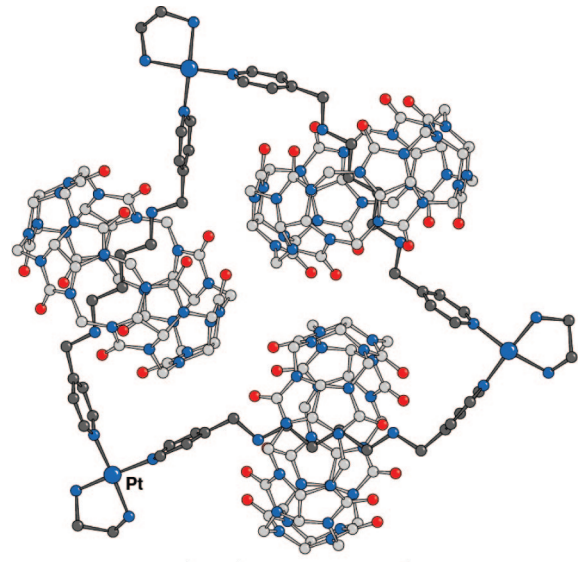

Figure 45. Molecular structure of **80**.

to the two Pt moieties by coordination of the terminal pyridyl groups. No unusual bond parameters were observed, including $Pt-N_{py}$ distances and $N_{py}-Pt-N_{py}$ angles, indicating that the metallacycle suffers no obvious strain. It is worth noting that, in the corresponding metallacycle with 1,5-diaminopentane edges (**81**), the average Pt···Pt distance (18.38 Å) is shorter than in **80** (19.45 Å), indicating that **81** is smaller and sterically more congested.

It was found that the nature of the reaction product is very sensitive to the reaction conditions and the nature of the pseudorotaxane linkers. Thus, under reflux conditions, the above-described reaction yields exclusively the trinuclear metallacycle, while affords mixtures of the tri- and tetranuclear ([5]MN) metallacycles when performed at lower temperatures. In addition, under reflux conditions, the similar linkers functionalized with 3-pyridylmethyl (rather than 4-pyridylmethyl) moieties yielded the tetranuclear metallacycles exclusively.[131]

The group of Cotton has described a large number of neutral metallacycles built from corner pieces containing dimetal paddlewheel units linked by divalent anions such as dicarboxylates, including several molecular triangles of formula $[\{cis\text{-}M_2(DAniF)_2(\mu,\eta^4\text{-}O_2C\text{-}R\text{-}CO_2)\}]_3$ (M = Mo, Rh; DAniF = *N*,*N*′-di-*p*-anisylformamidinate, Figure 46).[132] The length and flexibility of the linker depends on the nature of R. In particular, treatment of the paddle-wheel dinuclear corner precursor $[cis\text{-}Mo_2(DAniF)_2(CH_3CN)_4](BF_4)_2$ with the flexible 1,4-cyclohexanedicarboxylate linker yielded the molecular triangle $[\{cis\text{-}Mo_2(DAniF)_2(\mu,\eta^4\text{-}1,4\text{-}O_2CC_6H_{10}CO_2)\}]_3$ (**82**, Figure 46) quantitatively.[133] The X-ray structure showed that, in the molecule, the three $Mo_2(DAniF)_2$ units define a ca. equilateral triangle with an average distance between the vertexes of 11.16 Å, and the conformation of each 1,4-cyclohexanedicarboxylate dianion is such that both carboxylate groups are equatorial (*eq*,*eq*). Each corner consists of a quadruply bonded dimolybdenum unit, with two *cisoid* formamidinate paddles and two carboxylate paddles from the linkers. The molecular triangle is apparently strain-free: each paddle in the paddlewheel corners is nearly 90° from its neighbors. Since with more rigid linkers such as oxalate, fumarate, and tetrafluorophthalate the same synthetic protocol had previously afforded the expected molecular squares, it was believed that the flex-

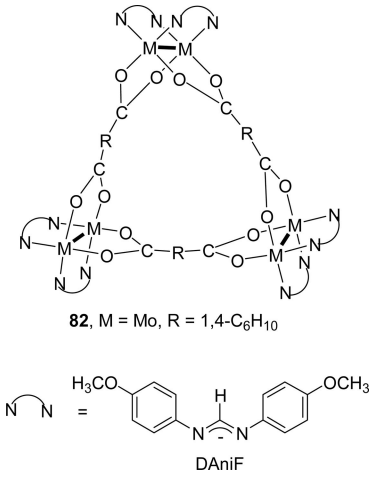

Figure 46. Neutral metallacycles built from corner pieces containing dimetal paddlewheel units linked by divalent anions such as dicarboxylates.

Scheme 15

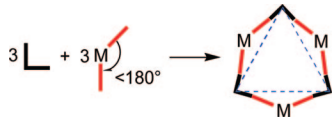

Chart 9

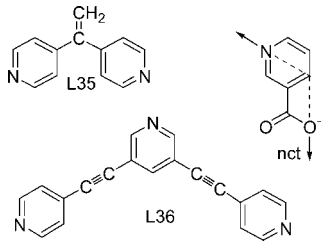

ibility of 1,4-cyclohexanedicarboxylate allowed for the formation of a molecular triangle instead.[132]

7.3. Angular Linkers

There is quite a number of trinuclear metallacycles in which ditopic linkers with angles much narrower than 180° between the coordinate vectors are connected by ca. 90° angular metal fragments (Scheme 15). The shape of the metallacycles (if the coordinate vectors of the linkers are ca. coplanar with the three metal atoms) might resemble that of a hexagon rather than a triangle. Most often, these trinuclear metallacycles are in equilibrium with other cyclic, typically dinuclear, species and feature square-planar metal corners.

The first example was described by Fujita and co-workers in 1996: treatment of 1,1-bis(4-pyridyl)ethylene (L35, Chart 9), a ditopic linker with two coordinate vectors at 120°, with the cis-protected [Pd(en)(ONO_2)$_2$] metal precursor yielded an equilibrium mixture of dinuclear [{Pd(en)(μ-L35)}$_2$]$^{4+}$ (**83**) and trinuclear [{Pd(en)(μ-L35)}$_3$]$^{6+}$ (**84**) symmetrical metallacycles (Figure 47).[134] NMR spectroscopy showed that, as expected, the equilibrium shifts toward the trinuclear species upon increasing the concentration and in the opposite direction upon raising the temperature. More recently, the same group, relaying mainly upon NMR and MS evidence, reported that the reaction of the 1,4-bis(3-pyridyl)benzene linker (L4, Figure 11) with the cis-protected metal fragment [Pd(en)]$^{2+}$ in dmso affords a dynamic equilibrium mixture of the dinuclear, the trinuclear, and, at higher concentrations, also the tetranuclear macrocycles [{Pd(en)(μ-L4)}$_n$]$^{2n+}$ (n = 2−4).[58] Similar results were obtained also with the longer 4,4′-bis(3-pyridyl)biphenyl linker (L3, Figure 11). Unfortunately, no structural characterization was available. The reaction of the same linkers with naked Pd(II) ions (from Pd(CF_3SO_3)$_2$) was described in section 4.1.[58]

More recently, Stang and co-workers investigated the dynamic equilibrium between a dinuclear and a trinuclear metallacycle, similar to that described above for L35.[26] The two equilibrating species were obtained by self-assembly of the 120° linker 3,5-bis(4-pyridylethynyl)pyridine (L36, Chart 9) and *cis*-[Pt(PMe_3)$_2$(O_3SCF_3)$_2$], precursor of the 90° angular fragment. The shapes of the dinuclear and trinuclear metallacycles, [{Pt(PMe_3)$_2$(μ-L36)}$_2$]$^{4+}$ and [{Pt(PMe_3)$_2$(μ-L36)}$_3$]$^{6+}$ (**4**, Figure 3), were described as rhomboidal and hexagonal, respectively. The rhomboid was selectively crystallized out of the equilibrium mixture, and its structure was determined by X-ray diffraction. The equilibrium had the expected concentration- and temperature-dependence and was shown to follow Le Châtelier's principle. In addition, in this case, the standard enthalpy and entropy changes were determined for the equilibrium: $\Delta H° = -18 \pm 1$ kJ mol^{-1} and $\Delta S° = -43 \pm 4$ J mol^{-1} K^{-1} for the forward reaction from dinuclear to trinuclear species.

The cationic metallacycle [{Pd(dppf)(μ-nct)}$_3$](CF_3SO_3)$_3$ (**85**) (dppf = 1,1′-bis-(diphenylphosphino)ferrocene, nct = nicotinate, Chart 9) was selectively obtained by self-assembly of the ca. 100° angular nicotinate linker with the cis-protected palladium precursor [Pd(dppf)(O_3SCF_3)$_2$].[135] Formation of the expected rhomboid (2 + 2)-metallacycle was not observed. The X-ray structure of **85** (Figure 48), in agreement with NMR data, showed that only one of the two possible linkage isomers formed, the most symmetrical one in which all the ambidentate ligands are iso-oriented (i.e., each Pd atom is bound to a pyridyl nitrogen and to a carboxylate oxygen atom). All the Pd ions are square planar, with relatively small distortions from ideal coordination geometry: N−Pd−O angles fall in the range from 88.2(9)° to 84.8(8)°.

Also recently, an example involving six-coordinate metal fragments was reported: reaction of di-*n*-butyltin(IV) oxide with isophthalic acid ($iptH_2$) afforded, according to multinuclear NMR spectroscopy and mass spectrometry evidence, a mixture of discrete cyclo-oligomeric species that in solution are in fast equilibrium.[136] Crystallization, however, yielded selectively the trinuclear metallacycle [{Sn(nBu)$_2$(μ-ipt)}$_3$] (**86**) (Figure 49). According to the X-ray solid-state structure, the 24-membered macrocycle with six *endo*-oxygen atoms is almost completely planar. The six *n*-butyl groups are ca. perpendicular to the Sn_3 plane. Each tin(IV) ion has a distorted octahedral coordination environment, better described as bicapped tetrahedral. The six Sn−O distances involving the *endo*-oxygen atoms have a covalent character, 2.095(5)−2.137(5) Å, whereas those external to the triangle are much longer, 2.515(6)−2.568(6) Å.

7.4. Trans Strands

Ditopic linkers such as the bisphosphines L37 and L38 (Chart 10), even though they are basically linear molecules, should be considered as angular linkers when the two coordinate vectors have a cis orientation or as trans strands when the coordinate vectors have opposite orientations.

The trinuclear metallacycles obtained by the coordination of trans strands to square-planar cis-protected metal frag-

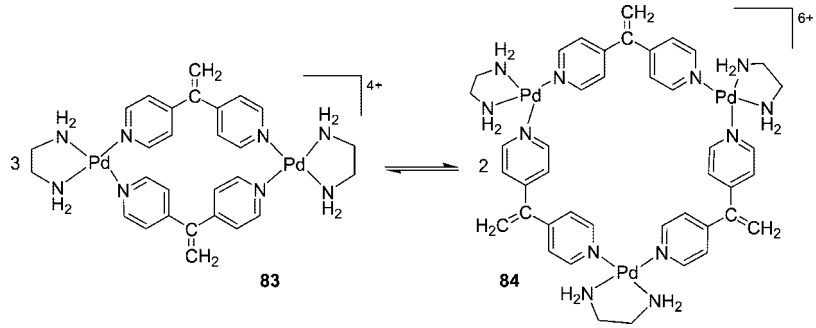

Figure 47. Equilibrium mixture of dinuclear $[\{Pd(en)(\mu\text{-L35})\}_2]^{4+}$ (**83**) and trinuclear $[\{Pd(en)(\mu\text{-L35})\}_3]^{6+}$ (**84**) symmetrical metallacycles.

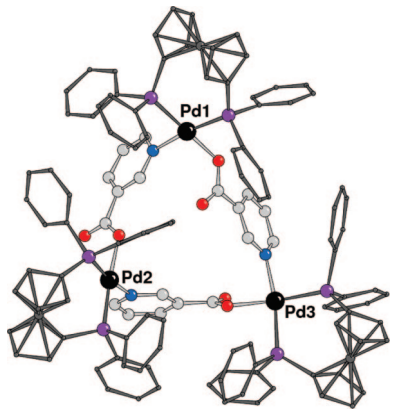

Figure 48. X-ray structure of the cation $[\{Pd(dppf)(\mu\text{-nct})\}_3]^{3+}$ (**85**).

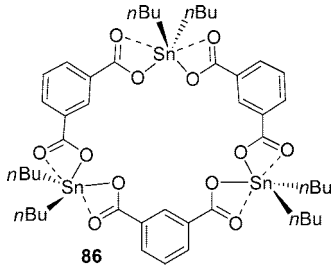

Figure 49. Trinuclear metallacycle $[\{Sn(n\text{Bu})_2(\mu\text{-ipt})\}_3]$ (**86**).

Chart 10

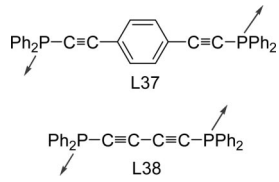

ments might also be defined as cyclic helicates. It is noteworthy that the combination of antiparallel (or trans) strands with naked ions capable of providing trans coordination can afford only cyclic helicates (see section 5.3), whereas with cis-protected metal fragments, "imperfect" helicates also become possible, depending on the orientation of the coordination planes of the corner fragments with respect to the M_3 plane.[120] In the symmetrical trinuclear cyclic helicate, each corner metal atom binds one linker from above and the other from below the M_3 plane, whereas in the less symmetrical isomer (an *imperfect* helicate), one metal binds both linkers above and another binds both linkers below the M_3 plane (Figure 50).

Manners and co-workers reported the unexpected quantitative formation of the neutral trinuclear metallacycle $[\{cis\text{-}PtCl_2(\mu\text{-L37})\}_3]$ (**87**) by reaction of the rigid bisphosphine linker L37 (Chart 10) with K_2PtCl_4.[137] A similar metallacycle, $[\{cis\text{-}Pt(CH_3)_2(\mu\text{-L38})\}_3]$ (**88**), was obtained a few years later by reaction of $[Pt(CH_3)_2(COD)]$ with bis(diphenylphosphino)butadiyne ($Ph_2PC_4PPh_2$, L38, Chart 10).[138] The trinuclear species **88** was obtained as a minor product in a mixture with the corresponding dinuclear compound $[\{cis\text{-}Pt(CH_3)_2(\mu\text{-L38})\}_2]$. The X-ray structures showed that both trinuclear Pt/diphosphine metallacycles **87** and **88** are symmetrical helicates, with the coordinate vectors of each linker alternatively above and below the plane of the Pt atoms (Figure 51). Each square-planar corner is almost perpendicular to the ring plane in order to accommodate the ca. 90° angles at platinum and the ca. tetrahedral angles at phosphorus.[137,138]

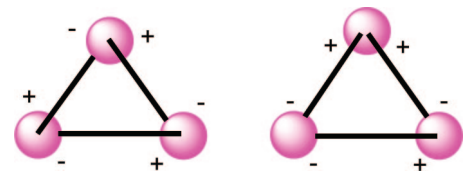

Figure 50. Schematic representation of the two isomeric trinuclear metallacycles that can be obtained from cis-protected metal corners and trans strands with monodentate binding sites: cyclic helicate (left) and *imperfect* cyclic helicate (right).

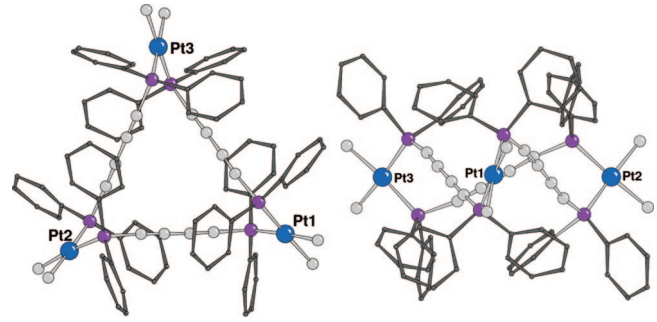

Figure 51. X-ray structure of $[\{cis\text{-}Pt(CH_3)_2(\mu\text{-L38})\}_3]$ (**88**). The side view (right) evidences the symmetrical cyclic helicate geometry.

An example of an "imperfect" trinuclear cyclic helicate was described by Lippert and co-workers: treatment of the cis-protected metal fragment $[Pt(en)(H_2O)_2]^{2+}$ with 2,2′-bipyrazine afforded the trinuclear metallacycle $[\{Pt(en)(\mu\text{-bpz-}N4,N4')\}_3]^{6+}$ (**68**; see also section 6). The molecular structure of the NO_3^- salt showed that the least symmetrical (C_2 symmetry) of the two possible isomers crystallized (Figure 52).[121] All three bpz linkers have a trans conformation (and, thus, can be described as trans strands), bind to the Pt atoms through N4 and N4′, and are nearly orthogonal to the Pt_3 plane.

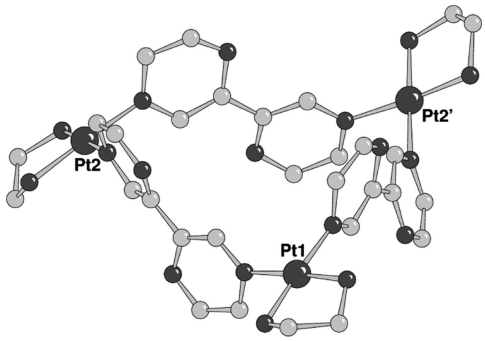

Figure 52. X-ray structure of the "imperfect" cyclic helicate cation $[\{Pt(en)(\mu\text{-bpz-}N4,N4')\}_3]^{6+}$ (**68**); Pt2 and Pt2′ are referred by a 2-fold axis.

Scheme 16

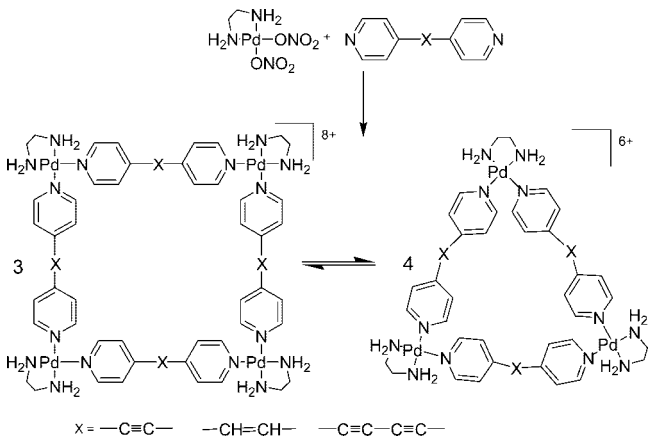

7.5. Linear Linkers

In the following sections, the equilibria between molecular triangles and squares will be treated first, followed by the cases in which the two metallacycles are obtained as nonequilibrating mixtures and then by those in which *either* molecular triangles *or* squares (or other polynuclear species) are obtained *selectively*, depending on relatively small variations in the reaction conditions or in the nature of the reactants. Finally, the examples in which molecular triangles are formed exclusively will be treated: short and rigid linear linkers, and pyrazine in particular, will be described and commented on in more detail. The last section is dedicated to very short linkers such as CN^-.

7.5.1. Triangles and Squares in Equilibrium

As mentioned above, very often the self-assembly of ca. 90° metal fragments with ca. linear and relatively rigid linkers affords equilibrium mixtures of molecular squares and triangles. The first report came from the group of Fujita in 1996.[139] They found that, whereas the self-assembly of $[Pd(en)(ONO_2)_2]$ with 4,4′-bipy yields the molecular square $[\{Pd(en)(\mu\text{-}4,4'\text{-bipy})\}_4](NO_3)_8$ exclusively,[1] longer and more flexible py−X−py ligands (py = 4-pyridyl, X = CH=CH, C≡C, *p*-C_6H_4) afford equilibrium mixtures of molecular squares and triangles (Scheme 16). The trinuclear metallacycles were found to be favored at lower concentrations, as expected from Le Châtelier's principle.

In the same work, it was found that even the shorter and stiffer 4,4′-bipy afforded a mixture of molecular squares, $[\{Pd(2,2'\text{-bipy})(\mu\text{-}4,4'\text{-bipy})\}_4]^{8+}$ (**89**), and triangles, $[\{Pd(2,2'\text{-bipy})(\mu\text{-}4,4'\text{-bipy})\}_3]^{6+}$ (**90**), when the ethylenediamine protective group was replaced by the larger 2,2′-bipy (Scheme 17).[139]

Scheme 17

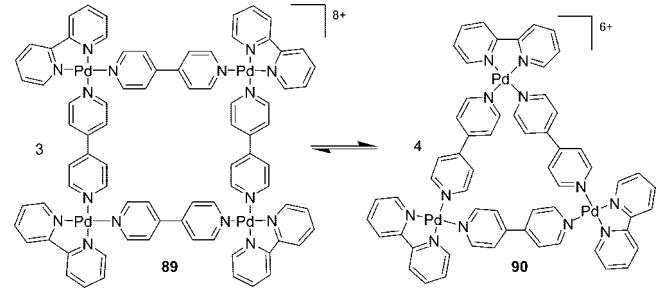

Chart 11

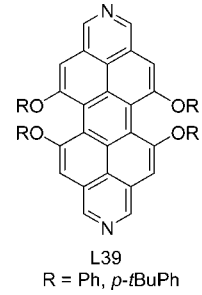

In 1998, Hong and co-workers described a similar triangle/square equilibrium from the combination of $[Pd(en)(ONO_2)_2]$ with the sigmoidal linker 1,2-bis(4-pyridyl)ethylene (BPE).[140] Beside being concentration-dependent, the equilibrium was also influenced by hydrophobic interactions with guests in aqueous solution. Thus, the molecular triangle $[\{Pd(en)(\mu\text{-BPE})\}_3]^{6+}$ (**91**) prevailed either at low concentration or in the presence of guests, such as *p*-dimethoxybenzene, that have a better complementarity to the triangular than to the square cavity.

Equilibrating molecular triangles and squares were also obtained by Würthner and co-workers by self-assembly of cis-protected square-planar precursors $[M(dppp)(O_3SCF_3)_2]$ (M = Pd, Pt; dppp = diphenylphosphinopropane) with phenoxy-substituted diazadibenzoperylene linear linkers L39 (Chart 11).[141] The equilibria were investigated exclusively in solution state by a number of techniques (multinuclear NMR spectroscopy, mass spectrometry, VPO).

A remarkable contribution to the understanding of these systems was reported in 2002 by Stang and co-workers, when they investigated the equilibrium mixture of triangular and square supramolecular species obtained by reaction of $[cis\text{-}Pt(PMe_3)_2(O_3SCF_3)_2]$ with BPE.[142] Besides characterizing the products in solution by multinuclear NMR spectroscopy, for the first time they succeeded in the selective crystallization and structural characterization of both cationic species by the appropriate choice of the counterions (Figure 53). Thus, the molecular square was crystallized as triflate salt, $[\{cis\text{-}Pt(PMe_3)_2(\mu\text{-BPE})\}_4](CF_3SO_3)_8$ (**92**), whereas the molecular triangle was crystallized as a mixed triflate/cobalticarborane ($CoB_{18}C_4H_{22}^-$) salt, $[\{cis\text{-}Pt(PMe_3)_2(\mu\text{-BPE})\}_3](CF_3SO_3)_4(CoB_{18}C_4H_{22})_2$ (**93**).

Interestingly, the prevalent species in the solid state did not always correspond to that prevailing in solution. The N−Pt−N bond angles of the molecular triangle **93** (range 82−83°) are only slightly smaller than those of the square **92** (range 84−87°). According to the authors, most likely any strain in the smaller metallacycle is delocalized through-

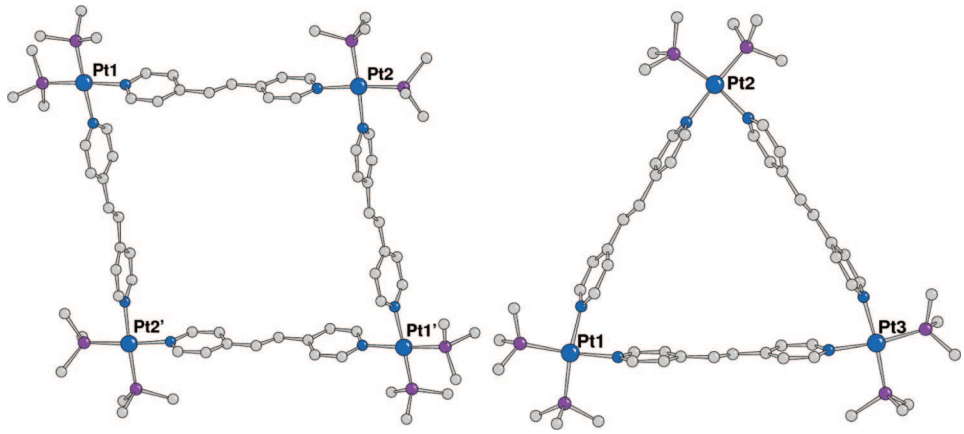

Figure 53. X-ray structures of the cations $[\{cis\text{-}Pt(PMe_3)_2(\mu\text{-BPE})\}_4]^{8+}$ (**92**) (left) and $[\{cis\text{-}Pt(PMe_3)_2(\mu\text{-BPE})\}_3]^{6+}$ (**93**) (right).

out the relatively flexible linkers, which are considerably more bowed in the triangle than in the square.

Very recently, Mizuno and co-workers also crystallized separately (from different solvents) both components of the equilibrium mixture of the molecular triangle $[\{Pd(tmeda)(\mu\text{-}4,4'\text{-bipy})\}_3](NO_3)_6$ (**94**) and square $[\{Pd(tmeda)(\mu\text{-}4,4'\text{-bipy})\}_4](NO_3)_8$ (**95**).[143] The X-ray structural determination of both compounds showed that, in the molecular triangle **94** (Pd···Pd distance ca. 11.0 Å), the $N_{py}-Pd-N_{py}$ angles (82.4(4)−86.0(4)°) are only slightly narrower than in the square (86.8(2)−87.3(2)°). Probably the strain of the smaller metallacycle is reflected in the torsion angles between the pyridyl rings, which are considerably wider in the square (21.89−32.02°) than in the triangle (16.36−20.89°).

The group of Cotton investigated the dynamic equilibrium in chloroform between a neutral molecular triangle and a square made by quadruply bonded dimolybdenum corners and perfluoroterephthalate linkers, $[\{cis\text{-}Mo_2(DAniF)_2(\mu,\eta^4\text{-}O_2CC_6F_4CO_2)\}_3]$ (**96**) and $[\{cis\text{-}Mo_2(DAniF)_2(\mu,\eta^4\text{-}O_2CC_6F_4CO_2)\}_4]$ (**97**), respectively, and accomplished a full spectroscopic (in solution) and solid-state crystallographic characterization of both species.[144] Crystals of the two compounds were obtained together (with the triangle as a minor species). The molecular structures showed that the perfluoroterephthalate linkers are bowed in **96**, whereas they are relatively linear in **97**, suggesting that the triangle is strained. Also, the angles between two adjacent carboxylate paddles at each dimolybdenum corner are slightly smaller in the triangle (83.7(2)−85.1(2)°) than in the square (86.4(3)−87.7(3)°). Interestingly, in the crystals, the neutral triangles pack on top of each other in a parallel fashion. In solution, at 23.7 °C, the conversion of 3 mol of molecular square to 4 mol of molecular triangle, as expected, was found to be enthalpically disfavored ($\Delta H° = 23.5$ kJ mol^{-1}) but entropically favored ($\Delta S° = 8.2$ J K^{-1} mol^{-1}). These values indicate that the strain energy in the triangle is very small (ca. 1.8 kJ/edge) compared to that in the square.

Several investigations were performed with cis-protected square-planar metal precursors with the aim of establishing how the nature, and in particular the steric bulk, of the ancillary chelating ligand affects the square/triangle equilibrium. The group of Ferrer investigated the self-assembly of a number of $[M(P-P)(O_3SCF_3)_2]$ precursors (M = Pt, Pd; P−P = dppp, dppf, depe (1,2-bis(diethylphosphino)ethane), dppbz (1,2-bis(diphenylphosphino)benzene)) with the linear linkers 1,4-bis(4-pyridyl)butadiyne (L40) and 1,4-bis(4-pyridyl)tetrafluorobenzene (L41) (Chart 12).[145]

Chart 12

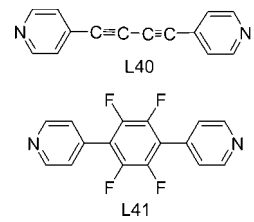

Chart 13

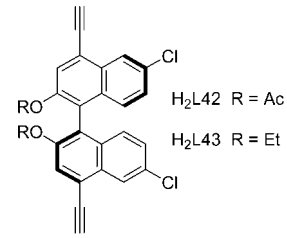

Equilibria between the molecular squares and triangles were found in all cases and investigated in solution by multinuclear NMR spectroscopy in combination with mass spectrometry. The square/triangle ratio was seen to depend on the nature of the metal corners, the concentration, and the solvent. The same group very recently investigated the self-assembly reactions between L41 and Pt(II) and Pd(II) complexes with cis-protecting nitrogen-chelating ligands: $[M(N-N)(O_3SCF_3)_2]$ (N−N = en; 4,4′-R_2bipy, R = H, Me, *t*-Bu).[146] As previously observed by Fujita,[139] the nature of the ancillary ligand on the metal corners was found to play a decisive role in determining the outcome of the reaction. According to combined multinuclear NMR spectroscopy and mass spectrometry measurements, molecular squares were found to form as unique products when the less sterically demanding and more flexible ethylenediamine was used as an end-capping ligand in the metal corners, whereas dynamic equilibria between molecular triangles and squares were observed when the ancillary ligand was 4,4′-R_2bipy. Similar conclusions were reported very recently by Besenyei and coworkes in a systematic study focused on the reaction of 4,4′-bipy with a series of square-planar Pd(II) precursors, $[Pd(N-N)(ONO_2)_2]$, that differ in the bulkiness on the diamine-chelating ligand: N−N = en, tmeda, *N*,*N*,*N*′,*N*′-tetraethylethylenediamine (teeda), 1,3-diaminopropane (dap), *N*,*N*′-dimethylpiperazine (dmpip), and homopiperazine (hpip).[147] The investigation was performed in aqueous solution exclusively by NMR and DOSY spectroscopy and wide-angle X-ray diffraction. For every chelating diamine,

Scheme 18

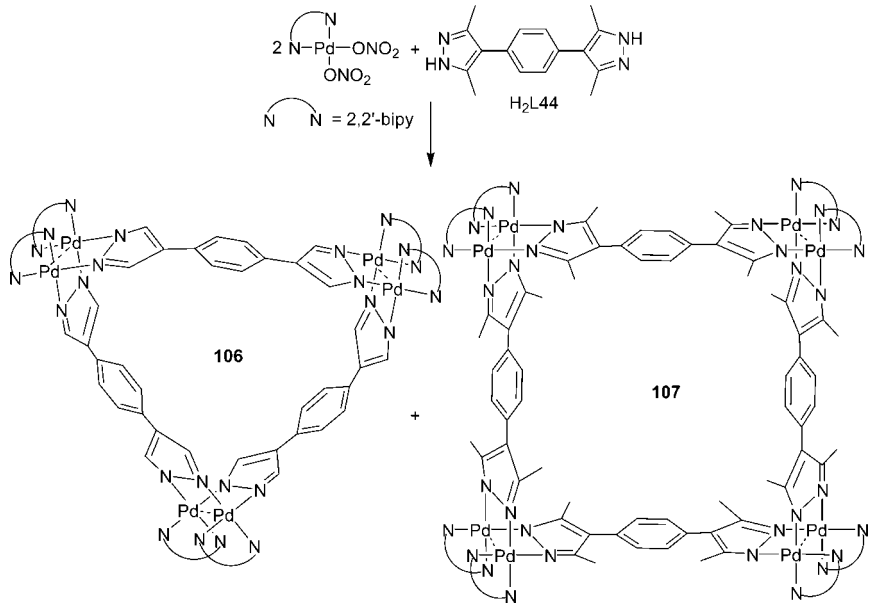

an equilibrium between molecular triangles and squares was observed; the dependence of the equilibrium on temperature and concentration was as expected. Trinuclear metallacycles prevailed with the bulkier chelating ligands (e.g., teeda), whereas tetramers were preferred for diamines of decreasing steric demand. Nevertheless, and in contrast with a previous report,[139] the molecular triangle was observed in measurable amounts also with the least sterically demanding en ligand. It is worth noting that the molecular triangle $[\{Pd(en)(\mu-4,4'\text{-bipy})\}_3]^{6+}$ (**98**) had never been observed before.

7.5.2. Triangles Plus Squares (Nonequilibrating Mixtures)

In 1990, Diederich and co-workers reported that oxidative cyclization of $[Co_2(CO)_4(\mu\text{-dppm})(C{-}C{\equiv}CH)_2]$ (dppm = diphenylphosphinomethane) yielded a nonequilibrium mixture of a cyclic trimer and tetramer, $[\{Co_2(CO)_4(dppm)(C{-}C{\equiv}C{-}C{\equiv}C{-}C)\}]_n$ (n = 3, 4), in which the dicobalt $Co_2(CO)_4(\mu$-dppm) units are linked by diacetylide groups.[148] The two metallacycles were separated by thin-layer chromatography (TLC), and the molecular triangle (**99**, major species) was structurally characterized in the solid state. The ring is nearly planar, and the diyne units show considerable deviations from linearity as a result of C≡C–C bending.

In the late 1990s, Jones and co-workers reported that the reaction of $[M(NO)(Tp)I_2]$ (M = Mo, W; Tp^- = hydrotris(3,5-dimethylpyrazol-1-yl)borate) with 1,4-dihydroxybenzene leads to mixtures of molecular triangles $[\{M(NO)(Tp)(\mu-1,4\text{-}O_2C_6H_4)\}_3]$ and squares $[\{M(NO)(Tp)(\mu-1,4\text{-}O_2C_6H_4)\}_4]$.[149] Two isomers of the cyclic trimer are possible, depending on the orientations of the NO groups relative to the M_3 plane: *syn*,*syn*,*syn* and *syn*,*syn*,*anti*. Similarly, four isomers are possible for the molecular square. Repeated column chromatography afforded pure single isomers of *syn*,*syn*,*anti*-$[\{M(NO)(Tp)(\mu-1,4\text{-}O_2C_6H_4)\}_3]$ (M = Mo, W) and of *syn*,*syn*,*syn*-$[\{Mo(NO)(Tp)(\mu-1,4\text{-}O_2C_6H_4)\}_3]$. The X-ray structures of *syn*,*syn*,*anti*-$[\{W(NO)(Tp)(\mu-1,4\text{-}O_2C_6H_4)\}_3]$ (**100**) and *syn*,*syn*,*syn*-$[\{Mo(NO)(Tp)(\mu-1,4\text{-}O_2C_6H_4)\}_3]$ (**101**) were determined. In both cases, the three metal atoms, which have a slightly distorted octahedral geometry, are located at the vertexes of a triangle, ca. equilateral for W (W···W distance in the range 8.40(1)−8.48(1) Å) and ca. isosceles for Mo (Mo···Mo distance in the range 7.886(3)−8.703(3) Å). Both triangles **100** and **101** define an almost planar 12-membered ring, containing the three metal atoms, the six O atoms, and the six adjacent C atoms of the 1,4-dihydroxybenzene edges. The phenyl rings make dihedral angles with respect to this plane in the wide range 12.2(6)−58.9(3)°. Similar results were also obtained by reaction of $[Mo(NO)(Tp)I_2]$ with 1,3-dihydroxybenzene (resorcinol). In this case, also a small amount of a cyclic dimer was obtained. Chromatographic separation of the reaction products afforded a single isomer of the cyclic trimer, *syn*,*syn*,*anti*-$[\{Mo(NO)(Tp)(\mu-1,3\text{-}O_2C_6H_4)\}_3]$ (**102**). The same group had previously described the preparation of larger molecular triangles and squares featuring Mo(NO)(Tp) corner fragments and 4,4′-biphenol edges, which were obtained in pure form by column chromatography.[150]

In 2005, Lin and co-workers reported that the chiral organometallic molecular triangle $[\{Pt(4,4'\text{-}tBu_2bipy)(\mu\text{-}L42)\}_3]$ (**103**) and square $[\{Pt(4,4'\text{-}tBu_2bipy)(\mu\text{-}L42)\}_4]$ (**104**) were obtained in moderate yields (as a mixture) by reaction of $[Pt(4,4'\text{-}tBu_2bipy)Cl_2]$ with the BINOL-derived 4,4′-bis(alkynyl) linear linker H_2L42 ((Chart 13), BINOL = 1,1′-bi-2-naphthol).[151] Interestingly, although both metallacyles were isolated from the reaction mixture, a 4 mM CD_2Cl_2 solution of the molecular triangle **103** was found to convert cleanly to the square **104** with a half-life of 2 days. The similar linker H_2L43 (Chart 13) afforded the molecular square exclusively when reacted with the metal corner under the same conditions, i.e., the formation of either metallacycle is apparently very sensitive to the dihedral angle of the two naphthyl units in the bis(alkynyl) linkers.[151] In contrast, the same group had previously reported the exclusive formation of the chiral organometallic triangle $[\{cis\text{-}Pt(PEt_3)_2(\mu\text{-}L43)\}_3]$ (**105**) upon reaction of H_2L43 (and of similar linkers with R = Me or bis(*t*-butyldimethylsilyl)) with $[cis\text{-}Pt(PEt_3)_2Cl_2]$.[152]

Yu and co-workers reported that treatment of $[Pd(bipy)(ONO_2)_2]$ with the immiscible bipyrazole ligand H_2L44 (H_2L44 = 1,4-bis-4′-(3′,5′-dimethyl)-pyrazolylbenzene) in a 2:1 molar ratio in a water/acetone solution afforded a mixture of molecular triangle $[\{Pd_2(bipy)_2(\mu\text{-}L44)\}_3](NO_3)_6$ (**106**, ca.

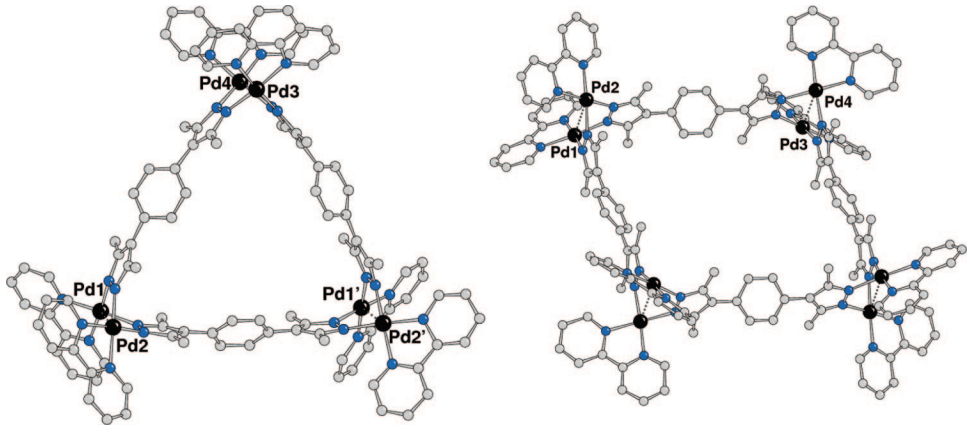

Figure 54. X-ray structures of the cations $[\{Pd_2(bipy)_2(\mu\text{-L44})\}_3]^{6+}$ (**106**, left) and $[\{Pd_2(bipy)_2(\mu\text{-L44})\}_4]^{8+}$ (**107**, right).

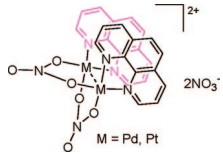

Figure 55. Dipalladium(II,II) and diplatinum(II,II) corner precursors, $[Pd_2(phen)_2(NO_3)_2](NO_3)_2$ and $[Pt_2(phen)_2(NO_3)_2](NO_3)_2$.

20%) and square $[\{Pd_2(bipy)_2(\mu\text{-L44})\}_4](NO_3)_8$ (**107**, ca. 80%) in quantitative total yield (Scheme 18).[153] The two products were found to be stable in solution (no interconversion between them could be detected by ^{1}H NMR spectroscopy) and were separated by repeated crystallization. The X-ray structural analysis (on the PF_6 salts) showed that both metallacycles feature either three (**106**) or four (**107**) (μ-pyrazolato-*N*,*N*′)$_2$ doubly bridged [(bipy)Pd]$_2$ dimetal corners (Figure 54). The Pd···Pd separation in each corner is slightly shorter than the sum of the van der Waals radii of palladium, suggesting weak Pd···Pd interactions. The average distance between the vertexes was found to be 13.3 Å in the triangle and 13.5 Å in the square. The dihedral angle between two pyrazolate paddles on a dipalladium corner is remarkably narrower in **106** (71.5−79.4°) than in **107** (82.8−92.9°). However, the coordination geometry of the pyrazolate moieties is not perfectly linear. In the crystals, the neutral molecular triangles have an antiprismatic stacking (i.e., stack with alternating orientations differing by about 60°).

Interestingly, while a similar mixture of molecular triangle and square was obtained by reaction of $[Pd(bipy)(ONO_2)_2]$ with the longer 1,4-bis-4′-(3′,5′-dimethyl)pyrazolylbiphenyl linker (H_2L45), the shorter 3,3′,5,5′-tetramethyl-4,4′-bipyrazolyl linker (H_2L46) afforded the molecular square exclusively, and the angular linkers 1,3-bis-4′-(3′,5′-dimethyl) pyrazolylbenzene (H_2L47) and 1,2-bis-4′-(3′,5′-dimethyl)pyrazolylbenzene (H_2L48) yielded the smaller [2 + 2]-molecular rhomboids selectively (Chart 14).

Very recently, the same group investigated also the formation of similar double-decker metallacycles, both tri- and tetranuclear, obtained by reaction of 4,4′-bipyrazole (H_2L49, Chart 14) with a series of dipalladium(II,II) and diplatinum(II,II) corner precursors, such as $[Pd_2(bipy)_2(NO_3)_2](NO_3)_2$ and $[Pt_2(phen)_2(NO_3)_2](NO_3)_2$ (Figure 55).[154] In general, it was found that, when treated with H_2L49, the dipalladium(II,II) clips tend to form double-decker molecular squares, whereas the diplatinum(II, II) clips afford mixtures of squares and triangles. The X-ray structure of the molecular triangle $[\{Pt_2(bipy)_2(\mu\text{-L49})\}_3](NO_3)_6$ (**108**) was also determined (average side length = 9.0 Å); the internal angles are close to 75° and are much smaller than in the corresponding molecular square with $Pd_2(bipy)_2$ metal corners.

Chart 14

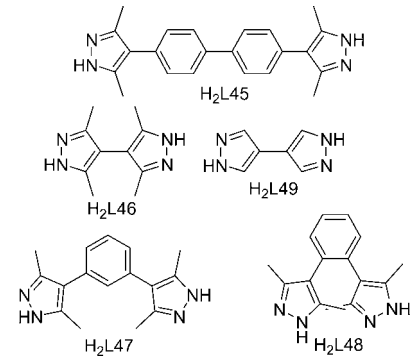

7.5.3. Triangles or Squares

In several cases, it was found that the combination of ca. 90° metal corners with linear rigid linkers led selectively *either* to molecular triangles *or* squares (or other polynuclear species) depending on relatively small variations on the reaction conditions or on the nature of the reactants. Several examples of this kind were described by the group of Cotton. In 1999, they reported that treatment of the paddlewheel, metal−metal linked dinuclear precursor $[Rh_2(DArF)_2(CH_3CN)_4][BF_4]_2$ (DArF = *N*,*N*′-diarylformamidinate, see Figure 46) with an equimolar amount of $[Bu_4N]_2[C_2O_4]$ afforded quantitatively the molecular triangle with oxalato edges $[\{Rh_2(DArF)_2(\mu,\eta^4\text{-}C_2O_4)\}_3]$ (**109**).[155] This result was unexpected since the corresponding molybdenum precursor, under the same reaction conditions, yielded the molecular square $[\{Mo_2(DArF)_2(\mu,\eta^4\text{-}C_2O_4)\}_4]$ selectively.[155] In addition, with the rhodium precursor, it was found that, by a suitable choice of the reaction conditions (i.e., by using a 10-fold excess of the oxalate salt), the corresponding molecular square $[\{Rh_2(DArF)_2(\mu,\eta^4\text{-}C_2O_4)\}_4]$ (**110**) could also be obtained selectively.[155,156] The molecular structure showed that, in the triangle, the oxalate linkers are bowed and their coordination is not linear. As a comment to this unexpected result, Cotton wrote: "*we simply do not know why this strained triangular structure, cf., the bowed oxalate bridge, is ever adopted rather than the expected square one.*"

The same group later reported that reaction of the dirhenium(II) precursor $[cis\text{-}Re_2(\mu\text{-}O_2CCH_3)_2Cl_2(\mu\text{-dppm})_2]$, which contains two labile adjacent acetato ligands and two

Chart 15

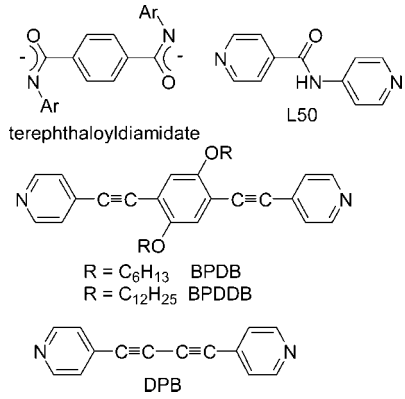

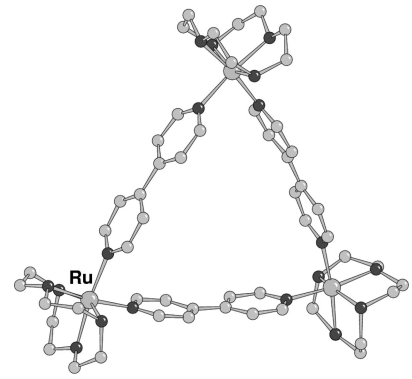

Figure 56. X-ray structure of the cation $[\{Ru(cyclen)(\mu-4,4'\text{-bipy})\}_3]^{6+}$ (**116**).

inert bridging dppm ligands that stabilize the quadruply bonded $[Re_2]^{4+}$ fragment, with an excess of terephthalic acid afforded in high yield the molecular triangle $[\{cis\text{-}Re_2Cl_2(\mu\text{-dppm})_2(\mu,\eta^4\text{-}O_2CC_6H_4CO_2)\}_3]$ (**111**), whose X-ray structure was determined.[157] The corresponding molecular square was not observed. In contrast, the use of an excess of *trans*-1,4-cyclohexanedicarboxylic acid in place of terephthalic acid under the same reaction conditions led to the isolation of the dinuclear compound $[\{cis\text{-}Re_2Cl_2(\mu\text{-dppm})_2(\mu\text{-}O_2CC_6H_{10}CO_2)\}_2(\mu,\eta^4\text{-}O_2CC_6H_{10}CO_2)]$, in which on each dirhenium unit there is one molecule of *trans*-1,4-cyclohexanedicarboxylic acid with an unbound carboxylic acid group.

The combination of the dimetal $cis\text{-}[Mo_2(DAniF)_2]^{2+}$ corner (see Figure 46) with terephthaloyldiamidate linkers $(ArNOC)_2C_6H_4$ (Chart 15) provided yet another example in which small variations can change the nature of the metallacyclic product.[158]In each case, only one neutral metallacyclic product of general formula $cis\text{-}[\{Mo_2(DAniF)_2(\mu\text{-}(ArNOC)_2C_6H_4)_2\}_n]$ was selectively obtained, either a molecular triangle (**112**, $n = 3$) or a square (**113**, $n = 4$) depending on small variations in the Ar substituents on the linkers. Thus, with *N*,*N*-diphenylterephthaloydiamidate, the only product was the molecular triangle **112**. In contrast, only the molecular square **113** was obtained when the ligand has a trifluoromethyl substituent on the phenyl groups. No evidence for equilibration between metallacycles of different nuclearity was found.[158]

Sun and Lees described a series of neutral tri- and tetranuclear macrocycles featuring $fac\text{-}Re(CO)_3X$ (X = Cl, Br) corners and linear extended 4,4′-bipyridyne linkers (Chart 15).[159] The compounds were characterized by NMR spectroscopy and mass spectrometry, but no X-ray structure was determined. The molecular triangle $[\{fac\text{-}Re(CO)_3Br(\mu\text{-BPDB})\}_3]$ (**114**) was obtained in almost quantitative yield by refluxing $ReBr(CO)_5$ and 1,4-bis(4-pyridylethynyl)-2,5-dihexyloxybenzene (BPDB) (or its 2,5-didodecyloxybenzene analogue, BPDDB) in neat benzene, a noncoordinating solvent. In contrast, the replacement of benzene with a 1:1 toluene/thf mixture afforded only unidentified oligomers. However, refluxing $ReCl(CO)_5$ with 4,4′-dipyridylbutadiyne (DPB), a linear linker similar to BPDB, in the same toluene/thf mixture afforded the molecular square $[\{fac\text{-}Re(CO)_3Cl(\mu\text{-DPB})\}_4]$ (**115**) exclusively, and no formation of the corresponding triangle was observed. In addition, only mixtures of unidentified species were obtained when the reaction was performed in neat toluene or benzene. The different behavior observed with structurally similar components was attributed by the authors to the different solubilities and thermodynamic stabilities of the products. In the toluene/thf mixture, the molecular square with DPB edges is scarcely soluble and, thus, precipitates immediately after formation, precluding equilibration with other metallacycles to proceed. Conversely, the BPDB linker imparts higher solubility to the metallacycles in benzene, thus allowing the equilibration process to proceed in solution until the most thermodynamically stable product (i.e., the molecular triangle, for the authors) forms.

Recently, Long and co-workers reported that the reaction of the Ru(II) precursor [Ru(cyclen)Cl(dmso)]Cl (cyclen = 1,4,7,10-tetraazacyclododecane) with 4,4′-bipy in a refluxing ethanol/water mixture afforded the molecular triangle $[\{Ru(cyclen)(\mu\text{-}4,4'\text{-bipy})\}_3]Cl_6$ (**116**).[160] It was found to be stable in aqueous solution at room temperature; no decomposition or isomerization were observed. According to the X-ray structure (Figure 56), in **116** three cyclen-capped Ru(II) fragments are situated at the corners of an equilateral triangle (Ru···Ru distance = 11.264 Å). The strain in the small metallacycle is reflected by the $N_{py}\text{-}Ru\text{-}N_{py}$ angle of 83.7(3)°, which is slightly narrower than the ideal value of 90°, and by the 4,4′-bipy edges that are bowed outward. The resulting warping forces the pyridine rings in each linker to be almost coplanar and nearly perpendicular to the Ru_3 plane. In the crystals, the molecular triangles stack in an eclipsed (prismatic) fashion, forming one-dimensional columns. In contrast, under very similar reaction conditions, the same Ru precursor treated with pyrazine (pyz) afforded the mixed Ru(II)/Ru(III) molecular square $[\{Ru(cyclen)(\mu\text{-pyz})\}_4]Cl_9$ (**117**),[161] whereas reaction of the $Ru(cyclen)(CF_3SO_3)_3$ precursor (apparently a Ru(III) compound) with 4,4′-bipy in methanol yielded the Ru(II) molecular square $[\{Ru(cyclen)(\mu\text{-}4,4'\text{-bipy})\}_4](CF_3SO_3)_8$ (**118**).[160] The X-ray structure of this almost perfect square **118** (even though of low quality) showed several geometrical details significantly different with respect to the corresponding triangle **116** (see above), which reflect the absence of strain: (i) The 4,4′-bipy linkers are linear rather than bowed, and thus, the Ru···Ru distance (11.34 Å) is slightly longer than that in **116**. (ii) The pyridine rings are not perfectly coplanar (twist angle 1.0−5.6°). (iii) The $N_{py}\text{-}Ru\text{-}N_{py}$ angle of 93.(3)° is wider than that in **116** and is closer to the ideal octahedral value of 90°.

7.5.4. Molecular Triangles Formed Exclusively

There are relatively few examples in which the self-assembly of cis-protected metal corners with linear rigid linkers led selectively to molecular triangles. In 2001, Puddephatt and co-workers prepared the molecular triangle $[\{Pt(bu_2bipy)(\mu\text{-L50})\}_3](CF_3SO_3)_6$ (**119**) by self-assembly of

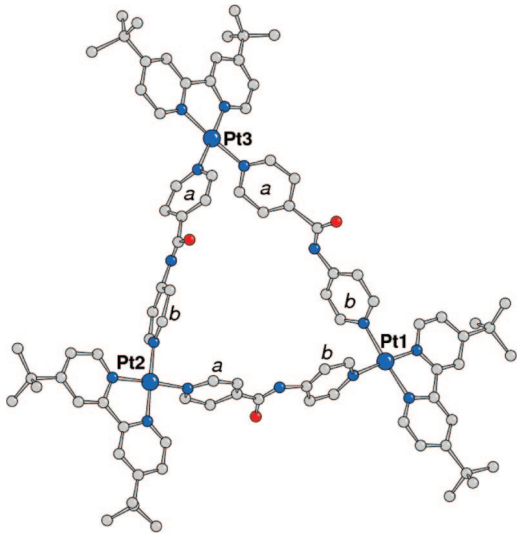

Figure 57. X-ray structure of the cation $[\{Pt(bu_2bipy)(\mu\text{-}L50)\}_3]^{6+}$ (**119**).

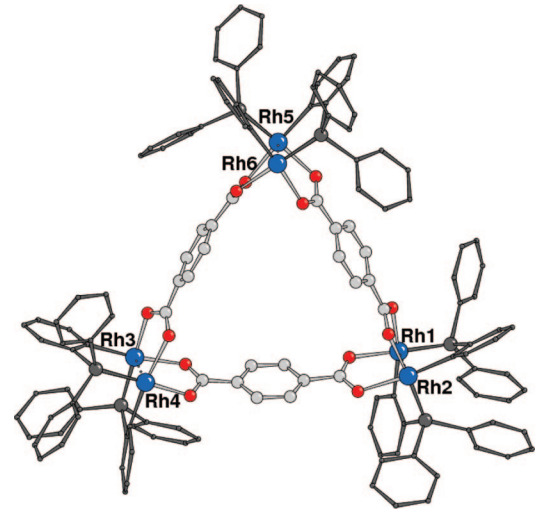

Figure 58. X-ray structure of *S,S,S*-**121** (axial py ligands on Rh atoms not shown for clarity).

the cis-protected precursor $[Pt(bu_2bipy)(O_3SCF_3)_2]$ with the unsymmetrical and roughly linear bis-pyridine linker *N*-(4-pyridinyl)isonicotinamide (L50, Chart 15).[162] The X-ray structural investigation showed that, in **119**, the three Pt atoms form an approximately equilateral triangle with an average Pt···Pt distance of 13.1 Å. The three edges are slightly bowed outward and the pyridyl rings are canted with respect to the Pt_3 plane. Two metallacyclic isomers are possible, depending on the relative orientations of the unsymmetrical linkers. In the solid state, only the less symmetrical isomer was found, in which the three Pt corners have different coordination environments: $Pt(py_a)_2$, $Pt(py_b)_2$, and $Pt(py_a)(py_b)$, respectively (Figure 57). The amide groups along the edges are designed to provide orientation through secondary bonding effects perpendicular to the triangle. In fact, in the crystal, pairs of triangular cations stack on top of each other in antiprismatic fashion, at a distance of 5.1 Å, through pairwise intertriangle NH···OC hydrogen bonds. Interestingly, L50 reacted with the Pd complex $[Pd(bu_2bipy)(thf)_2](BF_4)_2$ to give the corresponding Pd triangle, whereas the reaction with $[Pd(dppp)(O_3SCF_3)_2]$ produced only uncharacterized polymeric species.[162]

The group of Cotton described molecular triangles with dimetallic corners that were formed exclusively. The reaction in organic solvents of racemic *cis*-$[Rh_2(C_6H_4PPh_2)_2(CH_3CN)_6](BF_4)_2$ (a dirhodium paddlewheel complex that has two cisoid nonlabile orthometallated phosphine bridging anions and six labile CH_3CN ligands in equatorial and axial positions), with the tetraethylammonium salts of rigid dicarboxylate (dicarb) linkers, produced crystals of the corresponding neutral triangular compounds $[\{Rh_2(C_6H_4PPh_2)_2(\mu\text{-dicarb})\}_3]$ (dicarb = oxalate (**120**); terephthalate (**121**); 4,4′-biphenyldicarboxylate (**122**)), exclusively.[163] Modification of the reaction conditions provided no evidence for the formation of the corresponding molecular squares. The reason for this well-defined preference was provided by careful analysis of the X-ray structures of the triangles: the *cis*-$Rh_2(C_6H_4PPh_2)_2$ corners have a preferred twist of ca. 23°, which is believed to induce very little strain in the triangular structures compared to the corresponding square structures. Thus, the entropic preference for the smaller ring becomes the controlling thermodynamic factor. In the triangle with oxalate edges, the short dicarboxylate linkers are both bent and twisted about the central C−C bond, with a dihedral angle of 43.8°. The enantiopure molecular triangles were later obtained, and their X-ray structures determined; one example is reported in Figure 58.[164]

7.5.5. Molecular Triangles with Pyrazine Edges

It is now clear that the *directional-bonding approach*,[9] which rationalizes the metal-mediated construction of supramolecular assemblies, allows for several exceptions. As shown above, quite often the combination of 90° metal fragments with linear linkers leads to mixtures of molecular squares and triangles, rather than to the expected molecular squares only. As seen in the previous section, the *exclusive* formation of molecular triangles from this combination of building blocks, in particular with short inflexible linkers, is still a rare event. Unexpectedly, four of these examples concern pyrazine that, being the shortest and most rigid aromatic N-linker, is, *in principle*, the less prone to make molecular triangles when reacted with cis-protected metal corners. We found instead that the reaction between pyrazine and the 90° angular precursor [*trans*-$RuCl_2(dmso\text{-}S)_4$] yields, in a number of different experimental conditions, $[\{trans,cis\text{-}RuCl_2(dmso\text{-}S)_2(\mu\text{-}pyz)\}_3]$ (**123**, Scheme 19), which is the first example of a neutral molecular triangle with pyrazine edges and octahedral metal corners.[21] Quite remarkably, the same metallacycle was obtained also from the reaction between [*trans*-$RuCl_2(dmso\text{-}S)_4$] and the preformed complementary angular fragment [*trans,cis,cis*-$RuCl_2(dmso\text{-}S)_2(pyz)_2$] (Scheme 19).[21]

Two previous examples of molecular triangles with pyrazine edges were known from the literature, and both formed *quantitatively* upon reaction of pyz with 90° angular metal fragments. In each case, the metal corner was a 2+ square-planar fragment, either Rh(I) in $[\{Rh(PPh_3)_2(\mu\text{-}pyz)\}_3](ClO_4)_3$ (**124**)[165] or Pt(II) in $[\{Pt(PEt_3)_2(\mu\text{-}pyz)\}_3](CF_3SO_3)_6$ (**125**).[166] Another strictly related example is the zinc molecular triangle $[\{ZnCl_2(\mu\text{-}bppz)\}_3]$ (**126**, bppz = 2,5-bis(2-pyridyl)pyrazine):[167] in this metallacycle, the edges of the triangle are occupied by pyrazine moieties, and the two pyridyl groups of each linker make additional axial bonds with the two bridged octahedral zinc atoms, one from above and the other from below the Zn_3 plane. The solution NMR spectra of **123**−**126** were found to be consistent with their solid-state X-ray structures (Figures 59 and 60).[21,165−167]

Scheme 19

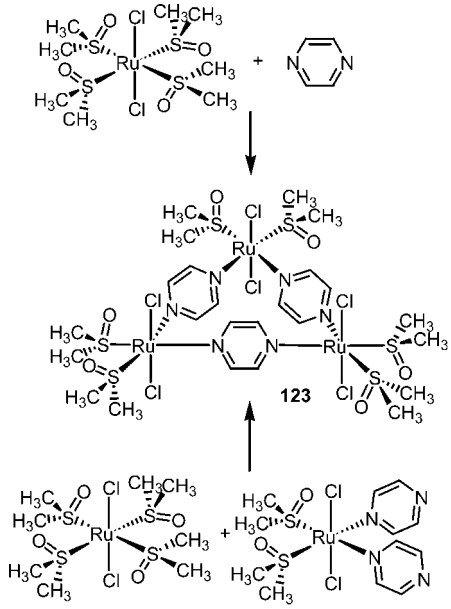

More recently, we isolated and structurally characterized in the solid state by X-ray crystallography a new molecular triangle, $[\{Ru([12]aneS4)(\mu\text{-pyz})\}_3](CF_3SO_3)_6$ (**127**), obtained in low yield upon reaction of [Ru([12]aneS4)(dmso-S)(H_2O)](CF_3SO_3)$_2$ with pyz ([12]aneS4 = 1,4,7,10-tetrathiacyclododecane).[22] The structural data of **127** were unfortunately of low quality, mainly because of the severe disorder in the triflate anions, and did not allow us to get an accurate structural determination. Nevertheless, the formation of the trinuclear cationic metallacycle **127**, featuring *cis*-$[Ru([12]aneS4)]^{2+}$ corners and pyz edges, was clearly confirmed (Figure 61). ^{1}H NMR data suggested that **127** is unstable in solution, also in noncoordinating solvents such as nitromethane.

The main geometrical features of the four metallatriangles with pyz edges **123**−**126** are collected in Table 1. The metal···metal distances in **124** and **125** are closely comparable (6.94−6.99 Å), although slightly shorter than those measured in **123** (7.00−7.18 Å). On the other hand, the metal···metal distances are significantly longer in the Zn metallacycle **126**, most likely in order to allow metal coordination by the axial pyridyl groups of bppz. It is worth noting that, in **124**−**126**, the pyrazine moieties are roughly coplanar and their planes are almost perpendicular to the M_3 plane (range of dihedral angles 84−89°). On the contrary, in the ruthenium molecular triangle **123**, such dihedral angles are much smaller (66−73°), probably because of the octahedral coordination of the Ru corners rather than the packing effects. A similar canting of the pyrazine edges was found in **127** (average = 72°).[22]

In all cases, the $N_{pyz}-M-N_{pyz}$ angles (α, Figure 62) are smaller than the ideal value of 90°, but not to such an extent to account, *alone*, for the formation of a triangle rather than a square. The pyrazine linkers are, as expected, almost perfectly flat, with N−pyz centroid−N angles in the range 176−180°. The largest distortions from the ideal coordination geometry concern, in all cases, the coordination bonds of pyrazine, which are not linear. This feature is clearly evidenced by the centroid(pyrazine)−N−M angles (β, Figure 62), which are always considerably smaller that the ideal value of 180°. Calculations performed on **123** and, above all, on the model corner complex [*trans,cis,cis*-$RuCl_2$(dmso-S)$_2$(pyz)$_2$] (**128**), indicated that the $N_{pyz}-Ru-N_{pyz}$ angle (α) is ca. six times more rigid than the tilt angle of pyrazine (β).[21] The observation that the molecular triangles **123**−**126** are formed exclusively from the components suggests that the enthalpy loss in their formation must be relatively small, so that the reactions are entropy-driven.[168,169]

We note, however, that, in other cases with similar cis-protected metal precursors, even featuring the same metal ions, the reaction with pyrazine afforded molecular squares *exclusively*. If we exclude the case of the tetranuclear pyz metallacycle with $Ti(Cp^*)_2$ corners,[170] in which the geometry of the Ti(II) center can be considered as tetrahedral, in all other examples involving late transition metals, the molecular squares were formed selectively, both with square-planar and octahedral metal corners, when the ancillary ligands on the metal coordination plane have a low steric demand: ethylenediamine in $[\{Pt(en)(\mu\text{-pyz})\}_4](NO_3)_8$,[171] ammonia in $[\{Pt(NH_3)_2(\mu\text{-pyz})\}_4](NO_3)_8$,[172] CO in [*fac*-$ReCl(CO)_3(\mu$-pyz)$\}_4$][173] and [*fac*-$ReBr(CO)_3(\mu$-pyz)$\}_4$],[174] and cyclen in $[\{(cyclen)Ru(\mu\text{-pyz})\}_4]$.[161] We note that the hard or soft nature of the ancillary ligands seems to be less important in influencing the nature of the resulting pyz metallacycle. The relevant role played by the steric demand of the ancillary ligands in determining the outcome of the self-assembly reaction between cis-protected metal fragments and linear linkers, i.e., in influencing the nuclearity of the preferred metallacycle, has been previously evidenced also by other authors.[139,146,147]

On the basis of all these observations, we believe that the preferential formation of the molecular triangles with pyrazine edges, **123**−**126**, instead of the corresponding squares, is determined by at least two concomitant factors: (i) The presence of relatively bulky ancillary ligands in the coordination plane induces a spontaneous contraction of the coordination angle at the metal corner, i.e., the metal fragment is already predisposed to be the corner of a triangle rather than of a square. The average $N_{pyz}-M-N_{pyz}$ angle is still much wider than the 60° required for an equilateral triangle (Table 1), but nevertheless it is narrower than the ideal value of 90° for a square. This is very clear from the X-ray structure of the model corner complex **128** that, in the absence of any metallacycle-related strain, features a $N_{pyz}-Ru-N_{pyz}$ angle of 84.73°, which is not significantly different from those found in **123**.[21] Thus, only a minor energetic contribution is required for narrowing this angle in going from the corner complex to the molecular triangle. On the contrary, a widening of the $N_{pyz}-M-N_{pyz}$ angle for the formation of the molecular square would require a large energy token, as evidenced by our calculations for the $N_{pyz}-Ru-N_{pyz}$ angle. Interestingly, the X-ray structure of $[Pt(NH_3)_2(pyz)_2](NO_3)_2$, the corner complex corresponding to the molecular square $[\{Pt(NH_3)_2(\mu\text{-pyz})\}_4](NO_3)_8$,[172] showed that the $N_{pyz}-Pt-N_{pyz}$ angle is very close to 90° (as in the square), i.e., in this case, the corner complex is geometrically predisposed to give a square rather than a triangle and the formation of the triangle would require a remarkable narrowing of the $N_{pyz}-Pt-N_{pyz}$ angle. (ii) Our calculations (see above) showed that the pyz−Ru coordination bond tolerates a remarkable degree of tilting (β angle) with modest increase of strain.[21] Interestingly, in the X-ray structure of **128**, the centroid(pyrazine)−N−Ru angles (179.2 and 176.6°) are much closer to the ideal value of 180°. In conclusion, the combination of the two relatively small distortions concerning the α and β angles makes

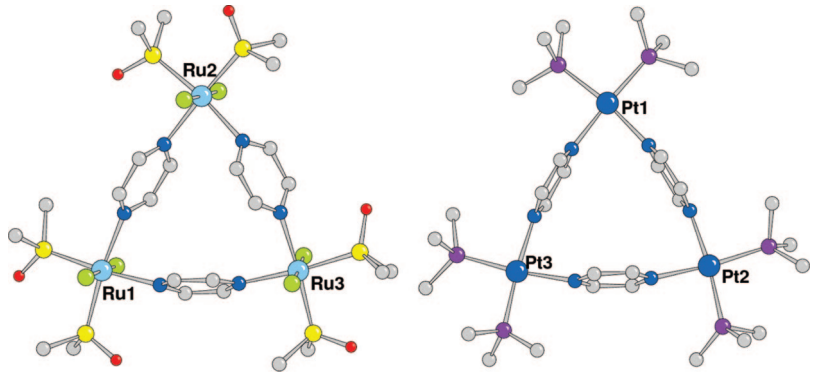

Figure 59. Molecular structures of [{*trans,cis*-$RuCl_2$(dmso-S)$_2$(μ-pyz)}$_3$] (**123**, left) and the cation [{$Pt(PEt_3)_2$(μ-pyz)}$_3$]$^{6+}$ (**125**, right).

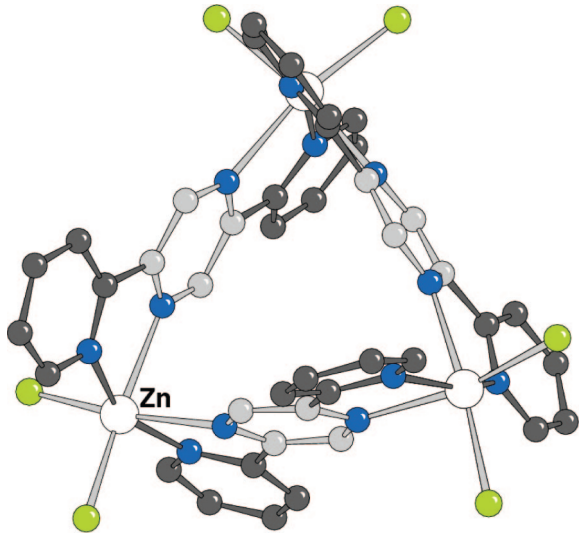

Figure 60. X-ray structure of [{$ZnCl_2$(μ-bppz)}$_3$] (**126**).

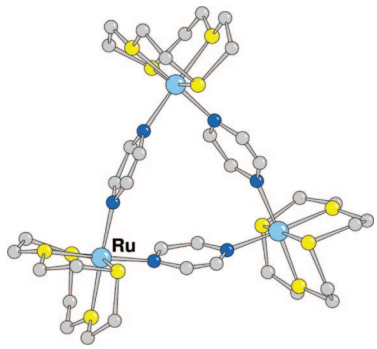

Figure 61. X-ray structure of the cation [{Ru([12]aneS4)(μ-pyz)}$_3$]$^{6+}$ (**127**).

formation of the triangle geometrically possible with moderate enthalpic loss.

7.5.6. Other Short Linkers

The shortest linear linker is the CN^- group. The corresponding trinuclear metallacycles with cyano edges define nine-membered rings. The first example, [{Pd(dppe)(μ-CN)}$_3$](ClO_4)$_3$ (**129**) (dppe = diphenylphosphinoethane), dates back to 1983 and was serendipitously obtained by addition of $AgClO_4$ to a solution of [Pd(dppe)$(CN)_2$].[175] The X-ray structure (Figure 63) showed that the cyano bridges linking two Pd atoms are significantly nonlinear at both ends, with Pd−N−C and N−C−Pd angles of 164(1) and 165(2)°, respectively, and lay slightly above the Pd_3 plane. Actually, it is impossible to distinguish C from N from a crystallographic point of view and thus establish the orientation of the cyano bridges in the solid state (Figure 64). According to ^{31}P NMR studies, in solution the three cyano edges in **129** have a *syn,syn,anti*-orientation.

Other structurally similar cyano-bridged metallacycles were reported later: [{$W(CO)_3$(NO)(μ-CN)}$_3$] (**130**),[176] [{$Sm(Cp)_2(CNC_6H_{11})$(μ-CN)}$_3$] (**131**),[177] and [{$Re(CO)_4$(μ-CN)}$_3$] (**132**).[178] In all cases, the three metals define an approximately equilateral triangle, the nine-membered ring is ca. planar, and the M−C≡N−M links are bowed outward from the M···M vector (W···W distance = 5.34−5.42 Å, Sm···Sm distance = 6.28−6.30 Å). In other words, also in these cases, the main distortion concerns the coordination angles of the linear linker.

The mixed-edge asymmetrical molecular triangles [{Ni(dien)}$_2$(μ,η^4-ox){μ-M$(CN)_4$}] (**133**) (M = Ni, Pd, or Pt; dien = diethylenetriamine; ox = oxalate) (Figure 65) were prepared by reaction of the dinuclear oxalato bridged Ni complex [{Ni(dien)(H_2O)}$_2$(μ-ox)]$(PF_6)_2$ with K_2[M$(CN)_4$].[179]

Similarly, the dianionic cyano/dppa bridged molecular triangle $(NBu_4)_2$[$(C_6F_5)_2$Pt(μ-dppa){(μ-CN)$_2$Pt(C≡C*t*Bu)$_2$}-Pt$(C_6F_5)_2$] (**134**) (dppa = diphenylphosphinoacetylene) was obtained by reaction of the ditopic organometallic acceptor fragment [{*cis*-Pt$(C_6F_5)_2S$}$_2$(μ-dppa)] (S = acetone) with the ditopic dianionic donor fragment $(NBu_4)_2$[*cis*-Pt(C≡C−*t*Bu)$_2$$(CN)_2$] (Scheme 20).[180] In the solid state, the three Pt atoms define a ca. isosceles triangle, with two short (5.160 and 5.143 Å) Pt···Pt distances and one long (7.223 Å) Pt···Pt distance. The three square-planar Pt fragments form dihedral angles with the Pt_3 plane ranging from 8.10 to 36.54°.

8. Concluding Remarks

The first conclusion that spontaneously comes up is that, contrary to what is often stated by authors surprised by unexpected findings, trinuclear metallacycles are not rare at all. Given the right components, with appropriate geometrical and binding complementarities, formation of stable trinuclear metallacycles is a predictable event. This is, for example, the case for the compounds described in sections 4 and 5.2.

According to our motivated classification, metallatriangles are only a fraction of the large family of trinuclear metallacycles. It remains true that, most often, they represent exceptions to the *directional-bonding approach*,[9] in particular when obtained by the combination of cis-protected metal fragments with rigid linear linkers. In this case, they often form as mixtures with the corresponding molecular squares.

Table 1. Selected Geometrical Parameters for the Four Metallatriangles with Pyrazine Edges 123−126

metal (compound)	Ru(II) (**123**)	Rh(I) (**124**)	Pt(II) (**125**)	Zn(II) (**126**)[a,b]
M···M (Å)	7.009, 7.047, 7.184	6.955, 6.993, 6.994	6.937, 6.944, 6.949	7.391
N−M−N (°)	80.7, 82.2, 86.0	80.5, 81.4, 81.8	82.0, 82.1, 83.2	81.6
X−M−X (°)[c]	93.5, 93.7, 94.2	95.5, 97.4, 97.6	93.8, 94.2, 95.3	100.9
M−N−pyz centroid (°)	165.28−171.90	165.56−172.77	167.08−171.62	167.97
pyz mean plane/M_3 (°)	66.0, 68.3, 73.2	84.5, 84.8, 88.1	86.0, 86.8, 88.4	89.2
stacking	antiprismatic	antiprismatic	prismatic	antiprismatic

[a] Linker = bppz. [b] The complex has a crystallographic C_3 symmetry. [c] X is the ligand donor atom located trans to pyrazine (sulfur in **123**, phosphorus in **124** and **125**, and chlorine in **126**).

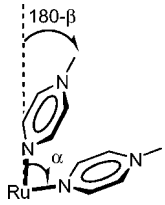

Figure 62. Schematic representation of the distortions that affect the N−Ru−N (α) and the centroid(pyrazine)−N−Ru (β) angles.

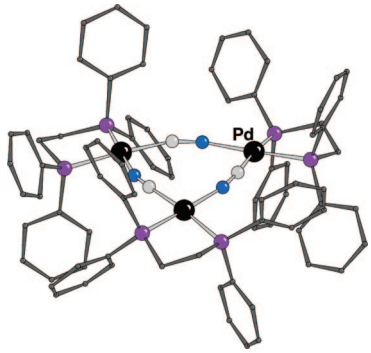

Figure 63. X-ray structure of the cation $[\{Pd(dppe)(\mu\text{-}CN)\}_3]^{3+}$ (**129**).

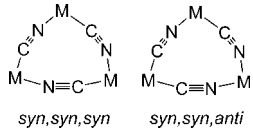

Figure 64. Two possible relative orientations of the cyano-bridges in a generic $[\{M(\mu\text{-}CN)\}_3]$ metallatriangle.

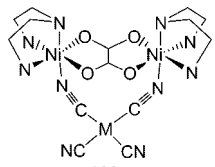

Figure 65. Mixed-edge asymmetrical molecular triangles $[\{Ni(dien)\}_2(\mu,\eta^4\text{-}ox)\{\mu\text{-}M(CN)_4\}]$ (**133**).

In general, as previously noted by Cotton,[164] when the self-assembly process is under thermodynamic control, if the enthalpic token paid to the distortions that occur in the formation of the molecular triangle (i.e., the loss of the directional preferences of the components, distortions in the linkers) is lower than the entropic gain, the smaller metallacycle will prevail. In addition, such distortions, which globally are significative, can be often distributed among $3 \times n$ small contributions, concerning both the linkers and the metal fragments.

It remains to be established if (and how) the formation of such exceptions (i.e., the molecular triangles) can be reasonably anticipated. There is general consensus, derived from a wealth of structural determinations as well as from solution data, that with rigid linear linkers a fundamental role is played by the steric demand of the ancillary ligands in the coordination plane of the metal corner: larger ligands favor molecular triangles, whereas sterically undemanding ligands favor molecular squares.[139,146,147] This is particularly well-illustrated by the case of pyrazine, a rigid linker that allows for no internal deformations. The structural and theoretical findings suggest that the entropically favored molecular triangles are preferred over the expected molecular squares when pyz links cis-protected metal corners that spontaneously favor $N_{pyz}-M-N_{pyz}$ angles narrower than 90° due to the presence of ancillary ligands with significant steric demand on the coordination plane.[21] The rather flexible coordination geometry of pyrazine allows for the closure of the small metallacycle with an inward tilt that requires modest additional strain. On the other hand, formation of the corresponding molecular squares is prevented because of the remarkable energy token required for widening the rigid $N_{pyz}-M-N_{pyz}$ angle to almost 90°.

Thus, in most cases, the flexibility of the coordination geometry of the rigid linker is the major geometrical factor that allows for the formation of a triangular metallacycle from components that are otherwise designed for leading to a molecular square. In other words, it is not (or not only) the flexibility of the organic linker that enables the formation of a metallatriangle, as generally believed: the flexibility of its coordination geometry plays a fundamental role, too.

Scheme 20

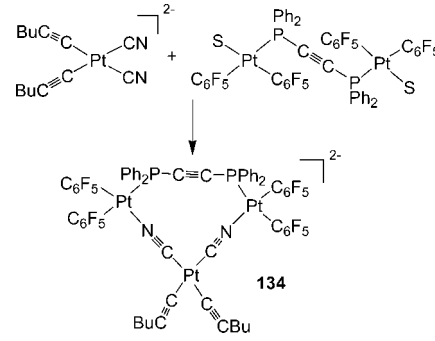

9. Acknowledgments

Acknowledgments are made for financial support of this research to the Italian Ministry for University and Research, Project FIRB-RBNE019H9K. E.A. wishes to thank Prof. Jean-Pierre Sauvage and his team (University of Strasbourg, France) for their kind hospitality and support during the writing of the final draft of this manuscript.

10. Abbreviations

AdoH	adenosine
[9]aneS3	1,4,7-trithiacyclononane
[12]aneS4	1,4,7,10-tetrathiacyclododecane
BINOL	1,1′-bi-2-naphthol
4,4′-bipy	4,4′-bipyridine
bmpze	1,2-bis(3,5-dimethylpyrazol-1-yl)ethane
BPDB	1,4-bis(4-pyridylethynyl)-2,5-dihexyloxybenzene
BPDDB	1,4-bis(4-pyridylethynyl)-2,5-didodecyloxybenzene
BPE	1,2-bis(4-pyridyl)ethylene
bppz	2,5-bis(2-pyridyl)pyrazine
2,2′-bpz	2,2′-bipyrazine
bpzphH	1,3-bis(*N*-pyrazolyl)benzene
bu_2bipy	4,4′-di-*tert*-butyl-2,2′-bipyridine
bzimH	benzimidazole
Cp	η^5-cyclopentadienyl
Cp*	η^5-pentamethylcyclopentadienyl
cyclen	1,4,7,10-tetraazacyclododecane
dach	1,2-diaminocyclohexane
dap	1,3-diaminopropane
DBM	dibenzoylmethanato
DAniF	*N*,*N*′-di-*p*-anisylformamidinate
DArF	*N*,*N*′-diarylformamidinate
depe	1,2-bis(diethylphosphino)ethane
dien	diethylenetriamine
dmpip	*N*,*N*′-dimethylpiperazine
dppa	diphenylphosphinoacetylene
DPB	4,4′-dipyridylbutadiyne
dppbz	1,2-bis(diphenylphosphino)benzene
dppe	diphenylphosphinoethane
dppf	1,1′-bis-(diphenylphosphino)ferrocene
dppm	diphenylphosphinomethane
dppp	diphenylphosphinopropane
9-EtHpxH	9-ethylhypoxanthine
en	ethylenediamine
hpip	homopiperazine
$iptH_2$	isophthalic acid
imH	imidazole
mbzimpH	1,3-bis(1-methyl-benzimidazol-2-yl)benzene
9-MeAdH	9-methyladenine
1-MeCyH	1-methylcytosine
Me_3tacn	1,4,7-trimethyl-1,4,7-triazacyclononane
nctH	nicotine
nptimH	naphthoimidazole
phen	1,10-phenanthroline
4,7-phen	4,7-phenanthroline
pmH	4(3*H*)-pyrimidone
	PPN Bis(triphenylphosphine)iminium
2-pymo	4,6-dimethyl-2-pyrimidinolato
pyz	pyrazine
pzH	pyrazole
$TBPheH_2$	*N*,*N*′-terephthaloyl-bis(*L*-phenylalanine)
teeda	*N*,*N*,*N*′,*N*′-tetraethylethylenediamine
terpy	2,2′:6′,2″-terpyridine
thpyH	2-(2′-thienyl)pyridine
tmeda	*N*,*N*,*N*′,*N*′-tetramethylethylenediamine
Tp^-	hydrotris(3,5-dimethylpyrazol-1-yl)borate
tzH	1,2,4-triazole

11. References

(1) Fujita, M.; Yazaki, J.; Ogura, K. *J. Am. Chem. Soc.* **1990**, *112*, 5645.
(2) Fujita, M. *Chem. Soc. Rev.* **1998**, *27*, 417.
(3) Olenyuk, B.; Fechtenkötter, A.; Stang, P. J. *J. Chem. Soc., Dalton Trans.* **1998**, 1707.
(4) Jones, C. J. *Chem. Soc. Rev.* **1998**, *27*, 289.
(5) Slone, R. V.; Benkstein, K. D.; Bélanger, S.; Hupp, J. T.; Guzei, I. A.; Rheingold, A. L. *Coord. Chem. Rev.* **1998**, *171*, 221.
(6) (a) Caulder, D. L.; Raymond, K. N. *J. Chem. Soc., Dalton Trans.* **1999**, 1185. (b) Caulder, D. L.; Raymond, K. N. *Acc. Chem. Res.* **1999**, *32*, 975.
(7) Leininger, S.; Olenyuk, B.; Stang, P. J. *Chem. Rev.* **2000**, *100*, 853.
(8) Navarro, J. A. R.; Lippert, B. *Coord. Chem. Rev.* **2001**, *222*, 219.
(9) Holliday, B. J.; Mirkin, C. A. *Angew. Chem., Int. Ed.* **2001**, *40*, 2022.
(10) Cotton, F. A.; Lin, C; Murillo, C. A. *Proc. Natl. Acad. Sci. U.S.A.* **2002**, *99*, 4810.
(11) Paul, R. L.; Bell, Z. R.; Jeffrey, J. C.; McCleverty, J. A.; Ward, M. D. *Proc. Natl. Acad. Sci. U.S.A.* **2002**, *99*, 4883.
(12) Würthner, F.; You, C.-C.; Saha-Möller, C. R. *Chem. Soc. Rev.* **2004**, *33*, 133.
(13) Fujita, M.; Tominaga, M.; Hori, A.; Therrien, B. *Acc. Chem. Res.* **2005**, *38*, 371.
(14) Gianneschi, N. C.; Masar, M. S., III; Mirkin, C. A. *Acc. Chem. Res.* **2005**, *38*, 825.
(15) Yu, S.-Y.; Li, S.-H.; Huang, H.-P.; Zhang, Z.-X.; Jiao, Q.; Shen, H.; Hu, X.-X.; Huang, H. *Curr. Org. Chem.* **2005**, *9*, 555.
(16) Nitschke, J. R. *Acc. Chem. Res.* **2007**, *40*, 103.
(17) (a) Yoshizawa, M.; Kusukawa, T.; Fujita, M.; Yamaguchi, K. *J. Am. Chem. Soc.* **2000**, *122*, 6311. (b) Yoshizawa, M.; Kusukawa, T.; Fujita, M.; Sakamoto, S.; Yamagichi, K. *J. Am. Chem. Soc.* **2001**, *123*, 10454.
(18) (a) Brumaghim, J. L.; Michels, M.; Raymond, K. N. *Eur. J. Org. Chem.* **2004**, *22*, 4552. (b) Brumaghim, J. L.; Michels, M.; Pagliero, D.; Raymond, K. N. *Eur. J. Org. Chem.* **2004**, *22*, 5115. (c) Dong, V. M.; Fiedler, D.; Carl, B.; Bergman, R. G.; Raymond, K. N. *J. Am. Chem. Soc.* **2006**, *128*, 14464.
(19) (a) Yoshizawa, M.; Takeyama, Y.; Kusukawa, T.; Fujita, M. *Angew. Chem., Int. Ed.* **2002**, *41*, 1347. (b) Leung, D. H.; Fiedler, D.; Bergman, R. G.; Raymond, K. N. *Angew. Chem., Int. Ed.* **2004**, *43*, 963. (c) Leung, D. H.; Bergman, R. G.; Raymond, K. N. *J. Am. Chem. Soc.* **2006**, *128*, 10240. (d) Nishioka, Y.; Yamaguchi, T.; Yoshizawa, M.; Fujita, M. *J. Am. Chem. Soc.* **2007**, *129*, 7000.
(20) (a) Fiedler, D.; Bergman, R. G.; Raymond, K. N. *Angew. Chem., Int. Ed.* **2004**, *43*, 6748. (b) Fiedler, D.; van Halbeek, H.; Bergman, R. G.; Raymond, K. N. *J. Am. Chem. Soc.* **2006**, *128*, 10240. (c) Yoshizawa, M.; Tamura, M.; Fujita, M. *Science* **2006**, *312*, 251. (d) Pluth, M. D.; Bergman, R. G.; Raymond, K. N. *Science* **2007**, *316*, 85.
(21) Derossi, S.; Casanova, M.; Iengo, E.; Zangrando, E.; Stener, M.; Alessio, E. *Inorg. Chem.* **2007**, *46*, 11243.
(22) Zangrando, E., Kulisic, N., Ravalico, F.; Bratsos, I.; Jedner, S.; Casanova, M.; Alessio, E. *Inorg. Chim. Acta*. **2008**, doi:10.1016/j.ica.2008.02.025.
(23) Indeed, besides M−M bonded dimetal entities, the definition of metal center with structural functions might be extended also to multimetal clustered units. However, since we have not found any example of this type so far, we preferred to give here a more practical definition.
(24) Hall, J. R.; Loeb, S. J.; Shimizu, G.; Yap, G. P. *Angew. Chem., Int. Ed.* **1998**, *37*, 121.
(25) (a) Kryschenko, Y. K.; Seidel, S. R.; Arif, A. M.; Stang, P. J. *J. Am. Chem. Soc.* **2003**, *125*, 5193. (b) Addicott, C.; Das, N.; Stang, P. J. *Inorg. Chem.* **2004**, *43*, 5335. (c) Mukherjee, P. S.; Das, N.; Kryschenko, Y. K.; Arif, A. M.; Stang, P. J. *J. Am. Chem. Soc.* **2004**, *126*, 2464. (d) Das, N.; Ghosh, A.; Arif, A. M.; Stang, P. J. *Inorg. Chem.* **2005**, *44*, 7130. (e) Megyes, T.; Jude, H.; Grósz, T.; Bakó, I.; Radnai, T.; Tárkány, G.; Pálinkás, G.; Stang, P. J. *J. Am. Chem. Soc.* **2005**, *127*, 10731. (f) Jude, H.; Disteldorf, H.; Fischer, S.; Wedge, T.; Hawkridge, A. M.; Arif, A. M.; Hawthorne, M. F.; Muddiman, D. C.; Stang, P. J. *J. Am. Chem. Soc.* **2005**, *127*, 12131. (g) Tárkány, G.; Jude, H.; Pálinkás, G.; Stang, P. J. *Org. Lett.* **2005**, *7*, 4971.
(26) Jude, H.; Sinclair, D. J.; Das, N.; Sherburn, M. S.; Stang, P. J. *J. Org. Chem.* **2006**, *71*, 4155.
(27) Yamamoto, T.; Arif, A. M.; Stang, P. J. *J. Am. Chem. Soc.* **2003**, *125*, 12309.
(28) (a) Cohen, Y.; Avram, L.; Frish, L. *Angew. Chem., Int. Ed.* **2005**, *44*, 520. (b) Macchioni, A.; Ciancaleoni, G.; Zuccaccia, C.; Zuccaccia, D. *Chem. Soc. Rev.* **2008**, *37*, 479.
(29) Schalley, C. A.; Müller, T.; Linnartz, P.; Witt, M.; Schäfer, M; Lützen, A. *Chem.−Eur. J.* **2002**, *8*, 3538.
(30) Graves, C. R.; Merlau, M. L.; Morris, G. A.; Sun, S.-S.; Nguyen, S. T.; Hupp, J. T. *Inorg. Chem.* **2004**, *43*, 2013.
(31) Atom parameters of all structures were retrieved from the Cambridge Structural Database, Allen, F. H. *Acta Crystallogr., Sect. B* **2002**, *58*, 380.
(32) All the ball and stick structures were drawn using the CAMERON program: CAMERON, A Molecular Graphics Package. Watkin, D. M.; Pearce, L.; Prout, C. K. Chemical Crystallography Laboratory, University of Oxford: Oxford, U.K., 1993.
(33) Vaughan, L. G. *J. Am. Chem. Soc.* **1970**, *92*, 730.
(34) Murray, H. H.; Raptis, R. G; Fackler, J. P, Jr *Inorg. Chem.* **1988**, *27*, 26.

(35) (a) Masciocchi, N.; Moret, M.; Cairati, P.; Sironi, A.; Ardizzoia, G. A.; La Monica, G. *J. Am. Chem. Soc.* **1994**, *116*, 7668. (b) Meyer, F.; Jacobi, A.; Zsolnai, L. *Chem. Ber.* **1997**, *130*, 1441.

(36) (a) Dias, H. V. R.; Diyabalanage, H. V. K.; Rawashdeh-Omary, M. A.; Franzman, M. A.; Omary, M. A. *J. Am. Chem. Soc.* **2003**, *125*, 12072. (b) Dias, H. V. R.; Diyabalanage, H. V. K.; Eldabaja, M. G.; Elbjeirami, O.; Rawashdeh-Omary, M. A.; Omary, M. A. *J. Am. Chem. Soc.* **2005**, *127*, 7489. (c) Omary, M. A.; Rawashdeh-Omary, M. A.; Gonser, M. W. A.; Elbjeirami, O.; Grimes, T.; Cundari, T. R.; Diyabalanage, H. V. K.; Gamage, C. S. P.; Dias, H. V. R. *Inorg. Chem.* **2005**, *44*, 8200. (d) Dias, H. V. R.; Gamage, C. S. P.; Keltner, J.; Diyabalanage, H. V. K.; Omari, I.; Eyobo, Y.; Dias, N. R.; Roehr, N.; McKinney, L.; Poth, T. *Inorg. Chem.* **2007**, *46*, 2979. (e) Dias, H. V. R.; Gamage, C. S. P. *Angew. Chem., Int. Ed.* **2007**, *46*, 2192.

(37) (a) Bonati, F.; Minghetti, G.; Banditelli, G. *J. Chem. Soc., Chem. Commun.* **1974**, 88. (b) Minghetti, G.; Banditelli, G.; Bonati, F. *Inorg. Chem.* **1979**, *18*, 658. (c) Bovio, B.; Bonati, F.; Banditelli, G. *Inorg. Chim. Acta* **1984**, *87*, 25.

(38) (a) Raptis, R. G.; Fackler, J. P., Jr *Inorg. Chem.* **1988**, *27*, 4179. (b) Ardizzoia, G. A.; Cenini, S.; La Monica, G.; Masciocchi, N.; Maspero, A.; Moret, M. *Inorg. Chem.* **1998**, *37*, 4284. (c) Ehlert, M. K.; Rettig, S. J.; Storr, A.; Thompson, R. C.; Trotter, J. *Can. J. Chem.* **1990**, *68*, 1444. (d) Ehlert, M. K.; Rettig, S. J.; Storr, A.; Thompson, R. C.; Trotter, J. *Can. J. Chem.* **1992 70**, 2161. (e) Ehlert, M. K.; Storr, A.; Summers, D. A.; Thompson, R. C. *Can. J. Chem.* **1997**, *75*, 491.

(39) (a) Bonati, F.; Minghetti, G. *Angew. Chem., Int. Ed. Engl.* **1972**, *11*, 429. (b) Minghetti, G.; Bonati, F. *Inorg. Chem.* **1974**, *13*, 1600. (c) Minghetti, G.; Bonati, F.; Massobrio, M. *Inorg. Chem.* **1975**, *8*, 1974. (d) Parks, J. E.; Balch, A. L. *J. Organomet. Chem.* **1974**, *71*, 453. (e) Vickery, J. C.; Olmstead, M. M.; Fung, E. Y.; Balch, A. L. *Angew. Chem., Int. Ed. Engl.* **1997**, *36*, 1179. (f) Balch, A. L.; Olmstead, M. M.; Vickery, J. C. *Inorg. Chem.* **1999**, *38*, 3494.

(40) (a) Bovio, B.; Calogero, S.; Wagner, F. E.; Burini, A.; Pietroni, B. R. *J. Organomet. Chem.* **1994**, *470*, 275. (b) Burini, A.; Bravi, R.; Fackler, J. P., Jr.; Galassi, R.; Grant, T. A.; Omary, M. A.; Petroni, B. R.; Staples, R. J. *Inorg. Chem.* **2000**, *39*, 3158.

(41) Dias, H. V. R.; Singh, S.; Campana, C. F. *Inorg. Chem.* **2008**, *47*, 3943.

(42) (a) Balch, A. L.; Doonan, D. I. J. *Organomet. Chem.* **1977**, *131*, 137. (b) Raptis, R. G.; Fackler, J. P., Jr *Inorg. Chem.* **1990**, *29*, 5003. (c) Bonati, F.; Burini, A.; Pietroni, B. R.; Bovio, B. *J. Organomet. Chem.* **1991**, *408*, 271. (d) Vickery, J. C.; Balch, A. L. *Inorg. Chem.* **1997**, *36*, 5978.

(43) Mohamed, A. A.; Burini, A.; Fackler, J. P., Jr *J. Am. Chem. Soc.* **2005**, *127*, 5012.

(44) Burini, A.; Fackler, J. P., Jr.; Galassi, R.; Pietroni, B. R.; Staples, R. J. *J. Chem. Soc., Chem. Commun.* **1998**, 95.

(45) (a) Gade, L. H. *Angew. Chem., Int. Ed. Engl.* **1997**, *36*, 1171. (b) Yang, G.; Raptis, R. G. *Inorg. Chem.* **2003**, *42*, 261.

(46) (a) Barberá, J.; Elduque, A.; Giménez, R.; Oro, L. A.; Serrano, J. L. *Angew. Chem., Int. Ed. Engl.* **1996**, *35*, 2832. (b) Barberá, J.; Elduque, A.; Gimenez, R.; Lahoz, F. J.; Lopez, J. A.; Oro, L. A.; Serrano, J. L. *Inorg. Chem.* **1998**, *37*, 2960. (c) Kim, S. J.; Kang, S. H.; Park, K.-M.; Kim, H.; Zin, W.-C.; Choi, M.-G.; Kim, K. *Chem. Mater.* **1998**, *10*, 1889. (d) Enomoto, M.; Kishimura, A.; Aida, T. *J. Am. Chem. Soc.* **2001**, *123*, 5608.

(47) Brown, D. S.; Massey, A. G.; Wickens, D. A. *Acta Crystallogr., Sect. B* **1978**, *34*, 1695.

(48) Shur, V. B.; Tikhonova, I. A.; Yanovsky, A. I; Struchkov, Yu. T.; Petrovskii, P. V.; Panov, S. Yu.; Furin, G. G.; Vol'pin, M. E. *J. Organomet. Chem.* **1991**, *418*, C29.

(49) Yang, X.; Zheng, Z.; Knobler, C. B.; Hawthorne, M. F. *J. Am. Chem. Soc.* **1993**, *115*, 193.

(50) Schnebeck, R.-D.; Freisinger, E.; Lippert, B. *Chem. Commun.* **1999**, 675.

(51) Espinet, P.; Soulantica, K.; Charmant, J. P. H.; Orpen, A. G. *Chem. Commun.* **2000**, 915.

(52) Jiang, H.; Lin, W. *J. Am. Chem. Soc.* **2003**, *125*, 8084.

(53) Heo, J.; Jeon, Y.-M.; Mirkin, C. A. *J. Am. Chem. Soc.* **2007**, *129*, 7712.

(54) Vicente, J.; Chicote, M.-T.; Alvarez-Falcón, M. M.; Jones, P. G. *Chem. Commun.* **2004**, 2658.

(55) Onitsuka, K.; Yamamoto, S.; Takahashi, S. *Angew. Chem., Int. Ed.* **1999**, *38*, 174.

(56) (a) Skapski, A.; Smart, M. L. *J. Chem. Soc., Chem. Commun.* **1970**, 658. (b) Bancroft, D. P.; Cotton, F. A.; Falvello, L. R.; Schwotzer, W. *Polyhedron* **1988**, *7*, 615. (c) Djalina, N. N.; Dargina, C. V.; Sobolev, A. N.; Buslaeva, T. M.; Romm, I. P. *Koord. Khim.* **1993**, *19*, 57.

(57) (a) Burger, W.; Strähle, J. *Z. Anorg. Allg. Chem.* **1985**, *529*, 111. (b) Baran, P.; Marrero, C. M.; Pérez, S.; Raptis, R. G. *Chem. Commun.* **2002**, 1012. (c) Umakoshi, K.; Yamauchi, Y.; Nakamiya, K.; Kojima, T.; Yamasaki, M.; Kawano, H.; Onishi, M. *Inorg. Chem.* **2003**, *42*, 3907.

(58) Chand, D. K.; Biradha, K.; Kawano, M.; Sakamoto, S.; Yamaguchi, K.; Fujita, M *Chem. Asian. J.* **2006**, *1*−*2*, 82.

(59) Suzuki, K.; Kawano, M.; Fujita, M. *Angew. Chem., Int. Ed.* **2007**, *46*, 2819.

(60) Köhler, R.; Kirmse, R.; Richter, R.; Sieler, J.; Hoyer, E.; Beyer, L. *Z. Anorg. Allg. Chem.* **1986**, *537*, 133.

(61) Saalfrank, R. W; Löw, N.; Demleitner, B.; Stalke, D.; Teichert, M. *Chem.*−*Eur. J.* **1998**, *4*, 1305.

(62) (a) Clegg, J. K.; Lindoy, L. F.; Moubaraki, B.; Murray, K. S.; McMurtrie, J. C. *Dalton Trans.* **2004**, 2417. (b) Clegg, J. K.; Lindoy, L. F.; McMutrie, J. C.; Schilter, D. *Dalton Trans.* **2006**, 3114.

(63) Wisser, B.; Chamayou, A.-C.; Miller, R.; Scherer, W.; Janiak, C. *CrystEngComm* **2008**, *10*, 461.

(64) (a) Soldatov, D. V.; Zanina, A. S.; Enright, G. D.; Ratcliffe, C. I.; Ripmeester, J. A. *Cryst. Growth Des.* **2003**, *3*, 1005. (b) Clegg, J. K.; Bray, D. J.; Gloe, K.; Gloe, K.; Jolliffe, K. A.; Lawrance, G. A.; Lindoy, L. F.; Meehan, G. V.; Wenzel, M. *Dalton Trans.* **2008**, 1331.

(65) (a) Saalfrank, R. W.; Burak, R.; Breit, A.; Stalke, D.; Herbst-Irmer, R.; Daub, J.; Porsch, M.; Bill, E.; Müther, M.; Trautwein, A. X. *Angew. Chem., Int. Ed. Engl.* **1994**, *33*, 1621. (b) Saalfrank, R. W.; Burak, R.; Rehis, S.; Löw, N.; Hampel, F.; Stachel, H.; Lentmaier, J.; Peters, K.; Peter, E.; von Schnering, H. *Angew. Chem., Int. Ed. Engl.* **1995**, *34*, 993.

(66) (a) Beckett, R.; Colton, R.; Hoskins, B. F.; Martin, R. L.; Vince, D. G. *Aust. J. Chem.* **1969**, *22*, 2527. (b) Beckett, R.; Hoskins, B. F. *J. Chem. Soc., Dalton Trans.* **1972**, 291.

(67) (a) Baral, S.; Chakravorty, A. *Inorg. Chim. Acta* **1980**, *39*, 1. (b) Butcher, R. J.; O'Connor, C. J.; Sinn, E. *Inorg. Chem.* **1981**, *20*, 537.

(68) (a) Costes, J.-P.; Dahan, F.; Laurent, J.-P. *Inorg. Chem.* **1986**, *25*, 413. (b) Kwiatkowski, M.; Kwiatkowski, E.; Olechnowicz, A.; Ho, D. M.; Deutsch, E. *Inorg. Chim. Acta* **1988**, *150*, 65. (c) Jiang, Y.-B.; Kou, H.-Z.; Wang, R.-J.; Cui, A.-L.; Ribas, J. *Inorg. Chem.* **2005**, *44*, 709.

(69) (a) Tang, J.; Hewitt, I.; Madhu, N. T.; Chastanet, G.; Wernsdorfer, W.; Anson, C. E.; Benelli, C.; Sessoli, R.; Powell, A. K. *Angew. Chem., Int. Ed.* **2006**, *45*, 1729. (b) Chibotaru, L. F.; Ungur, L.; Soncini, A. *Angew. Chem., Int. Ed.* **2008**, *47*, 4126.

(70) Hulsbergen, F. B.; Ten Hoedt, R. W. M.; Verschoor, G. C.; Reedijk, J.; Spek, A. L. *J. Chem. Soc., Dalton Trans.* **1983**, 539.

(71) (a) Angaroni, M.; Ardizzoia, G. A.; Beringhelli, T.; La Monica, G.; Gatteschi, D.; Masciocchi, N.; Moret, M. *J. Chem. Soc., Dalton Trans.* **1990**, 3305. (b) Angaridis, P. A.; Baran, P.; Boča, R.; Cervantes-Lee, F.; Haase, W.; Mezei, G.; Raptis, R. G.; Werner, R. *Inorg. Chem.* **2002**, *41*, 2219. (c) Boča, R.; Dihan, L.; Mezei, G.; Ortiz-Pérez, T.; Raptis, R. G.; Telser, J. *Inorg. Chem.* **2003**, *42*, 5801. (d) Mezei, G.; McGrady, J. E.; Raptis, R. G. *Inorg. Chem.* **2005**, *44*, 7271. (e) Casarin, M.; Corvaja, C.; Di Nicola, C.; Falconer, D.; Franco, L.; Monari, M.; Pandolfo, L.; Pettinari, C.; Piccinelli, F. *Inorg. Chem.* **2005**, *44*, 6265. (f) Mezei, G.; Raptis, R. G.; Telser, J. *Inorg. Chem.* **2006**, *45*, 8841.

(72) £ukasiewicz, M.; Ciunik, Z.; Mazurek, J.; Sobczak, J.; Staroń, A.; Wołowiec, S.; Ziółkowski, J. *Eur. J. Inorg. Chem.* **2001**, 1575.

(73) (a) Abe, M.; Sasaki, Y.; Yamada, Y.; Tsukahara, K.; Yano, S.; Yamaguchi, T.; Tominaga, M.; Taniguchi, I.; Ito, T. *Inorg. Chem.* **1996**, *35*, 6724. (b) Yamaguchi, T.; Imai, N.; Ito, T.; Kubiak, C. P. *Bull. Chem. Soc. Jpn.* **2000**, *73*, 1205. (c) Seo, J. S.; Whang, D.; Lee, H.; Jun, S. I.; Oh, J.; Jin, Y.; Kim, K. *Nature* **2000**, *404*, 982. (d) Dai, F.-R.; Chen, J.-L.; Ye, H.-Y.; Zhang, L.-Y.; Chen, Z.-N. *Dalton Trans.* **2008**, 1492, and refs therein.

(74) Piñero, D.; Baran, P.; Boca, R.; Herchel, R.; Klein, M.; Raptis, R. G.; Renz, F.; Sanakis, Y. *Inorg. Chem.* **2007**, *46*, 10981, and references therein.

(75) Romero, F. M.; Ziessel, R.; Dupont-Gervais, A.; Van Dorsselaer, A. *Chem. Commun.* **1996**, 551.

(76) Hwang, S.-H.; Moorefield, C. N.; Fronczek, F. R.; Lukoyanova, O.; Echgoyen, L.; Newkome, G. R. *Chem. Commun.* **2005**, 713.

(77) Baker, A. T.; Crass, J. K.; Maniska, M.; Craig, D. C. *Inorg. Chim. Acta* **1995**, *230*, 225.

(78) Garcia-Ruano, J. L.; González, A. M.; López-Solera, I.; Masaguer, J. R.; Navarro-Ranninger, C.; Raithby, P. R.; Rodriguez, J. H. *Angew. Chem., Int. Ed. Engl.* **1995**, *34*, 1351.

(79) Duhme-Klair, A.-K.; Vollmer, G.; Mars, C.; Fröhlich, R. *Angew. Chem., Int. Ed.* **2000**, *39*, 1626.

(80) (a) Wojaczyński, J.; Latos-Grazyński, L. *Inorg. Chem.* **1995**, *34*, 1044. (b) Wojaczyński, J.; Latos-Grazyński, L. *Inorg. Chem.* **1995**, *34*, 1054. (c) Wojaczyński, J.; Latos-Grazyński, L. *Inorg. Chem.* **1996**, *35*, 4812. (d) Wojaczyński, J.; Latos-Grazyński, L.; Olmstead, M. M.; Balch, A. L. *Inorg. Chem.* **1997**, *36*, 4548.

(81) Metselaar, G. A.; Sanders, J. K. M.; de Mendoza, J. *Dalton Trans.* **2008**, 588.
(82) Kamada, T.; Aratani, N.; Ikeda, T.; Shibata, N.; Higuchi, Y.; Wakamiya, A.; Yamaguchi, S.; Kim, K. S.; Yoon, Z. S.; Kim, D.; Osuka, A. *J. Am. Chem. Soc.* **2006**, *128*, 7670.
(83) Dreos, R.; Nardin, G.; Randaccio, L.; Siega, P.; Tauzher, G. *Eur. J. Inorg. Chem.* **2002**, 2885.
(84) Jeong, K. S.; Kim, S. Y.; Oh, Y.; Min, D. W.; Kim, J.; Jeong, N. *CrystEngComm* **2007**, *9*, 273.
(85) (a) Smith, D. P.; Bruce, E.; Morales, B.; Olmstead, M. M.; Maestre, M. F.; Fish, R. H. *J. Am. Chem. Soc.* **1992**, *114*, 10647. (b) Smith, D. P.; Kohen, E.; Maestre, M. F.; Fish, R. H. *Inorg. Chem.* **1993**, *32*, 4119. (c) Chen, H.; Maestre, M. F.; Fish, R. H. *J. Am. Chem. Soc.* **1995**, *117*, 3631. (d) Chen, H.; Olmstead, M. M.; Smith, D. P.; Maestre, M. F.; Fish, R. H. *Angew. Chem., Int. Ed. Engl.* **1995**, *34*, 1514. (e) Chen, H.; Ogo, S.; Fish, R. H. *J. Am. Chem. Soc.* **1996**, *118*, 4993. (f) Fish, R. H. *Coord. Chem. Rev.* **1999**, *185*−*186*, 569.
(86) (a) Korn, S.; Sheldrick, W. S. *J. Chem. Soc., Dalton Trans.* **1997**, 2191. (b) Korn, S.; Sheldrick, W. S. *Inorg. Chim. Acta* **1997**, *254*, 85. (c) Annen, P.; Schildberg, S.; Sheldrick, W. S. *Inorg. Chim. Acta* **2000**, *307*, 115.
(87) Yamanari, K.; Ito, R.; Yamamoto, S.; Fuyuhiro, A. *Chem. Commun.* **2001**, 1414.
(88) (a) Shan, N.; Ingram, J. D.; Easun, T. L.; Vickers, S. J.; Adams, H.; Ward, M. D.; Thomas, J. A. *Dalton Trans.* **2006**, 2900. (b) Shan, N.; Vickers, S. J.; Adams, H.; Ward, M. D.; Thomas, J. A. *Angew. Chem., Int. Ed.* **2004**, *43*, 3938.
(89) Zhu, X.; Rusanov, E.; Kluge, R.; Schmidt, H.; Steinborn, D. *Inorg. Chem.* **2002**, *41*, 2667.
(90) (a) Krämer, R.; Polborn, K.; Robl, C.; Beck, W. *Inorg. Chim. Acta* **1992**, *198*−*200*, 415. (b) Sünkel, K.; Hoffmüller, W.; Beck, W. *Z. Naturforsch.* **1998**, *53b*, 1365.
(91) (a) Carmona, D.; Lahoz, F. J.; Atencio, R.; Oro, L. A.; Lamata, M. P.; Viguri, F.; San Josè, E.; Vega, C.; Reyes, J.; Joó, F.; Kathó, A. *Chem.*−*Eur. J.* **1999**, *5*, 1544. (b) Carmona, D.; Lamata, M. P.; Oro, L. A. *Eur. J. Inorg. Chem.* **2002**, 2239.
(92) (a) Habereder, T.; Warchhold, M.; Nöth, H.; Severin, K. *Angew. Chem., Int. Ed.* **1999**, *38*, 3225. (b) Piotrowski, H.; Polborn, K.; Hilt, G.; Severin, K. *J. Am. Chem. Soc.* **2001**, *123*, 2699. (c) Piotrowski, H.; Hilt, G.; Schulz, A.; Mayer, P.; Polborn, K.; Severin, K. *Chem.*−*Eur. J.* **2001**, *7*, 3197. (d) Severin, K. *Coord. Chem. Rev.* **2003**, *245*, 3.
(93) Lehaire, M.-L.; Scopelliti, R.; Herdeis, L.; Polborn, K.; Mayer, P.; Severin, K. *Inorg. Chem.* **2004**, *43*, 1609.
(94) Mimassi, L.; Guyard-Duhayon, C.; Rager, M. N.; Amouri, H. *Inorg. Chem.* **2004**, *43*, 6644.
(95) Kiplinger, J. L.; Pool, J. A.; Schelter, E. J.; Thompson, J. D.; Scott, B. L.; Morris, D. E. *Angew. Chem., Int. Ed.* **2006**, *45*, 2036.
(96) (a) Rüttimann, S.; Bernardinelli, G.; Williams, A. F. *Angew. Chem., Int. Ed. Engl.* **1993**, *32*, 392. (b) Carina, R. F.; Williams, A. F.; Bernardinelli, G. *Inorg. Chem.* **2001**, *40*, 1826.
(97) Willison, S. A.; Krause, J. A.; Connick, W. B. *Inorg. Chem.* **2008**, *47*, 1258.
(98) Baxter, P. N. W.; Lehn, J.-M.; Rissanen, K. *Chem. Commun.* **1997**, 1323.
(99) Baum, G.; Constable, E. C.; Fenske, D.; Housecroft, C. E.; Kulke, T. *Chem. Commun.* **1999**, 195.
(100) Bonnefous, C.; Bellec, N.; Thummel, R. P. *Chem. Commun.* **1999**, 1243.
(101) Tuna, F.; Hamblin, J.; Jackson, A.; Clarkson, G.; Alcock, N. W.; Hannon, M. J. *Dalton Trans.* **2003**, 2141.
(102) Guo, D.; Duan, C. Y.; Fang, C. J.; Meng, Q. J. *J. Chem. Soc., Dalton Trans.* **2002**, 834.
(103) Thompson, A.; Rettig, S. J.; Dolphin, D. *Chem. Commun.* **1999**, 631.
(104) Wu, Z.; Chen, Q.; Xiong, S.; Xin, B.; Zhao, Z.; Jiang, L.; Ma, J. S. *Angew. Chem., Int. Ed.* **2003**, *42*, 3271.
(105) Schmittel, M.; Mahata, K. *Chem. Commun.* **2008**, 2550.
(106) Since two strands are different, two pseudo 3 × 3 grids are possible, one in which the two equal strands have a cis conformation and the other in which they have opposite conformations (one cis and one trans).
(107) Kraus, T; Buděšínsky, M.; Cvačka, J.; Sauvage, J.-P. *Angew. Chem., Int. Ed.* **2006**, *45*, 258.
(108) Champin, B.; Sartor, V.; Sauvage, J.-P. *New. J. Chem.* **2008**, *32*, 1048.
(109) Provent, C.; Hewage, S.; Brand, G.; Bernardinelli, G.; Charbonnière, L. J.; Williams, A. F. *Angew. Chem., Int. Ed. Engl.* **1997**, *36*, 1287.
(110) Bark, T.; Düggeli, M.; Stoeckli-Evans, H.; von Zelewsky, A. *Angew. Chem., Int. Ed.* **2001**, *40*, 2848.
(111) Lai, S.-W.; Chan, M. C.-W.; Peng, S.-M.; Che, C.-M. *Angew. Chem., Int. Ed.* **1999**, *38*, 669.
(112) Oro, L. A.; Pinillos, M. T.; Tejel, C.; Foces-Foces, C.; Cano, F. H. *J. Chem. Soc., Dalton Trans.* **1986**, 2193.
(113) Chaudhuri, P.; Karpenstein, I.; Winter, M.; Butzlaff, C.; Bill, E.; Trautwein, A. X.; Flörke, U.; Haupt, H.-J. *J. Chem. Soc., Chem. Commun.* **1992**, 321.
(114) *Cisplatin: Chemistry and Biochemistry of a Leading Anticancer Drugs*; Lippert, B., Ed.; VHCA:Zürich, Switzerland, and Wiley-VCH: Weinheim, Germany, 1999.
(115) Schenetti, L.; Bandoli, G.; Dolmella, A.; Trovò, G.; Longato, B. *Inorg. Chem.* **1994**, *33*, 3169.
(116) (a) Longato, B.; Pasquato, L.; Mucci, A.; Schenetti, L.; Zangrando, E. *Inorg. Chem.* **2003**, *42*, 7861. (b) Longato, B.; Montagner, D.; Zangrando, E. *Inorg. Chem.* **2006**, *45*, 8179.
(117) Longato, B.; Pasquato, L.; Mucci, A.; Schenetti, L. *Eur. J. Inorg. Chem.* **2003**, 128.
(118) (a) Rauter, H.; Mutikainen, I.; Blomberg, M.; Lock, C. J. L.; Amo-Ochoa, P.; Freisinger, E.; Randaccio, L.; Zangrando, E.; Chiarparin, E.; Lippert, B. *Angew. Chem., Int. Ed. Engl.* **1997**, *36*, 1296. (b) Barrea, E.; Navarro, J. A. R.; Salas, J. M.; Quirós, M.; Willermann, M.; Lippert, B. *Chem.*−*Eur. J.* **2003**, *9*, 4414. (c) Beck, B.; Schneider, A.; Freisinger, E.; Holthenrich, D.; Erxleben, A.; Albinati, A.; Zangrando, E.; Randaccio, L.; Lippert, B. *Dalton Trans.* **2003**, 2533. (d) Baradjì, E. G.; Freisinger, E.; Costisella, B.; Schalley, C. A.; Brüning, W.; Sabat, M.; Lippert, B. *Chem.*−*Eur. J.* **2007**, *13*, 6019.
(119) Shen, W.-Z.; Gupta, D.; Lippert, B. *Inorg. Chem.* **2005**, *44*, 8249.
(120) Schnebeck, R.-D.; Freisinger, E.; Glahè, F.; Lippert, B. *J. Am. Chem. Soc.* **2000**, *122*, 1381.
(121) Schnebeck, R.-D.; Randaccio, L.; Zangrando, E.; Lippert, B. *Angew. Chem., Int. Ed.* **1998**, *37*, 119.
(122) Schnebeck, R.-D.; Freisinger, E.; Lippert, B. *Angew. Chem., Int. Ed.* **1999**, *38*, 168.
(123) Moriuchi, T.; Miyaishi, M.; Hirao, T. *Angew. Chem., Int. Ed.* **2001**, *40*, 3042.
(124) Qin, Z.; Jennings, M. C.; Puddephatt, R. J. *Inorg. Chem.* **2002**, *41*, 3967.
(125) (a) Yu, S.-Y.; Huang, H.; Liu, H.-B.; Chen, Z.-N.; Zhang, R.; Fujita, M. *Angew. Chem., Int. Ed.* **2003**, *42*, 686. (b) Li, S.-H.; Huang, H.-P.; Yu, S.-Y.; Li, Y.-Z.; Sei, Y.; Yamaguchi, K. *Dalton Trans.* **2005**, 2346.
(126) Liu, L.-X.; Huang, H.-P.; Li, X.; Sun, Q.-F.; Sun, C.-R.; Li, Y.-Z.; Yu, S.-Y. *Dalton Trans.* **2008**, 1544.
(127) Galindo, M. A.; Navarro, J. A. R.; Romero, M. A.; Quirós, M. *Dalton Trans.* **2004**, 1563.
(128) Galindo, M. A.; Galli, S.; Navarro, J. A. R.; Romero, M. A. *Dalton Trans.* **2004**, 2780.
(129) Süss-Fink, G.; Wolfender, J.-L.; Neumann, F.; Stoeckli-Evans, H. *Angew. Chem., Int. Ed. Engl.* **1990**, *29*, 429.
(130) Shiu, K.-B.; Lee, H.-C.; Lee, G.-H.; Ko, B.-T.; Wang, Y.; Lin, C.-C. *Angew. Chem., Int. Ed.* **2003**, *42*, 2999.
(131) (a) Whang, D.; Park, K.-M.; Heo, J.; Ashton, P.; Kim, K. *J. Am. Chem. Soc.* **1998**, *120*, 4899. (b) Park, K.-M.; Kim, S.-Y.; Heo, J.; Whang, D.; Sakamoto, S.; Yamaguchi, K.; Kim, K. *J. Am. Chem. Soc.* **2002**, *124*, 2140.
(132) Cotton, F. A.; Lin, C.; Murillo, C. A. *Proc. Natl. Acad. Sci. U.S.A.* **2002**, *99*, 4810.
(133) Cotton, F. A.; Lin, C.; Murillo, C. A. *Inorg. Chem.* **2001**, *40*, 575.
(134) Fujita, M.; Aoyagi, M.; Ogura, K. *Inorg. Chim. Acta* **1996**, *246*, 53.
(135) Ghosh, S.; Turner, D. R.; Batten, S. R.; Mukherjee, P. S. *Dalton Trans.* **2007**, 1869.
(136) Garcia-Zarracino, R.; Ramos-Quiñones, J.; Höpfl, H. *Inorg. Chem.* **2003**, *42*, 3835.
(137) Baumgartner, T.; Huynh, K.; Schleidt, S.; Lough, A. J.; Manners, I. *Chem.*−*Eur. J.* **2002**, *8*, 4622.
(138) Martin-Redondo, M. P.; Scoles, L.; Sterenberg, B. T.; Udachin, K. A.; Carty, A. J. *J. Am. Chem. Soc.* **2005**, *127*, 5038.
(139) Fujita, M.; Sasaki, O.; Mitsuhashi, T.; Fujita, T.; Yazaki, J.; Yamaguchi, K.; Ogura, K. *Chem. Commun.* **1996**, 1535.
(140) Lee, S. B.; Hwang, S.; Chung, D. S.; Yun, H.; Hong, J.-I. *Tetrahedron Lett.* **1998**, *39*, 873.
(141) Sautter, A.; Schmid, D. G.; Jung, G.; Würthner, F. *J. Am. Chem. Soc.* **2001**, *123*, 5424.
(142) Schweiger, M.; Russell Seidel, S.; Arif, A. M.; Stang, P. J. *Inorg. Chem.* **2002**, *41*, 2556.
(143) Uehara, K.; Kasai, K.; Mizuno, N. *Inorg. Chem.* **2007**, *46*, 2563.
(144) Cotton, F. A.; Murillo, C. A.; Yu, R. *Dalton Trans.* **2006**, 3900.
(145) (a) Ferrer, M.; Rodriguez, L.; Rossell, O. *J. Organomet. Chem.* **2003**, *681*, 158. (b) Ferrer, M.; Mounir, M.; Rossell, O.; Ruiz, E.; Maestro, M. A. *Inorg. Chem.* **2003**, *42*, 5890.
(146) Ferrer, M.; Gutiérrez, A.; Mounir, M.; Rossell, O.; Ruiz, E.; Rang, A.; Engeser, M. *Inorg. Chem.* **2007**, *46*, 3395–3406.
(147) Holló-Sitkei, E.; Tárkányi, G; Párkányi, L.; Megyes, T.; Besenyei, G. *Eur. J. Inorg. Chem.* **2008**, 1573.
(148) Rubin, Y.; Knobler, C. B.; Diederich, F. *J. Am. Chem. Soc.* **1990**, *112*, 4966–4968.

(149) McQuillan, F. S.; Berridge, T. E.; Chen, H.; Hamor, T. A.; Jones, C. J. *Inorg. Chem.* **1998**, *37*, 4959.
(150) (a) McQuillan, F. S.; Jones, C. J. *Polyhedron* **1996**, *15*, 1553. (b) McQuillan, F. S.; Chen, H.; Hamor, T. A.; Jones, C. J. *Polyhedron* **1996**, *15*, 3909.
(151) Zhang, L.; Niu, Y.-H.; Jen, A. K.-Y.; Lin, W. *Chem. Commun.* **2005**, 1002.
(152) Lee, S. J.; Hu, A.; Lin, W. *J. Am. Chem. Soc.* **2002**, *124*, 12948.
(153) Yu, S.-Y.; Huang, H.-P.; Li, S.-H.; Jiao, Q.; Li, Y.-Z.; Wu, B.; Sei, Y.; Yamaguchi, K.; Pan, Y.-J.; Ma, H.-W. *Inorg. Chem.* **2005**, *41*, 9471.
(154) Sun, Q.-F.; Wong, K. M.-C.; Liu, L.-X.; Huang, H.-P.; Yu, S.-Y.; Yam, V. W.-W.; Li, Y.-Z.; Pan, Y.-J.; Yu, K.-C. *Inorg. Chem.* **2008**, *47*, 2142.
(155) Cotton, F. A.; Daniels, L. M.; Lin, C.; Murillo, C. A. *J. Am. Chem. Soc.* **1999**, *121*, 4538.
(156) Even though in the original paper (ref 155) it was unclear whether, upon dissolution of either the molecular triangle **103** or the square **104**, an equilibrium between the two would occur, subsequent articles by the same group (e.g., refs 10 and 144) stated that, in solution, the two rhodium metallacycles are in dynamic equilibrium and are in a ca. 1:1 ratio.
(157) Bera, J. K.; Angaridis, P.; Cotton, F. A.; Petrukhina, M. A.; Fanwick, P. E.; Walton, R. A. *J. Am. Chem. Soc.* **2001**, *123*, 1515.
(158) Cotton, F. A.; Liu, C. Y.; Murillo, C. A.; Wang, X. *Inorg. Chem.* **2006**, *45*, 2619.
(159) (a) Sun, S.-S.; Lees, A. J. *Inorg. Chem.* **1999**, *38*, 4181. (b) Sun, S.-S.; Lees, A. J. *J. Am. Chem. Soc.* **2000**, *122*, 8956.
(160) Berben, L. A.; Faia, M. C.; Crawford, N. R. M.; Long, J. R. *Inorg. Chem.* **2006**, *45*, 6378.
(161) Lau, V. C.; Berben, L. A.; Long, J. R. *J. Am. Chem. Soc.* **2002**, *124*, 9042.
(162) Qin, Z.; Jennings, M. C.; Puddephatt, R. J. *Chem. Commun.* **2001**, 2676.
(163) Cotton, F. A.; Murillo, C. A.; Wang, X.; Yu, R. *Inorg. Chem.* **2004**, *43*, 8394.
(164) Cotton, F. A.; Murillo, C. A.; Stiriba, S.-E.; Wang, X.; Yu, R. *Inorg. Chem.* **2005**, *44*, 8223.
(165) Yu, X.-Y.; Maekawa, M.; Kondo, M.; Kitagawa, S.; Jin, G.-X. *Chem. Lett.* **2001**, 168.
(166) Schweiger, M.; Russell Seidel, S.; Arif, A. M.; Stang, P. J. *Angew. Chem., Int. Ed.* **2001**, *40*, 3467.
(167) Neels, A.; Stoeckli-Evans, H. *Inorg. Chem.* **1999**, *38*, 6164.
(168) Even though most often neglected, we note that solubility might play an important role in the preferential isolation of a certain metallacycle, in particular for ionic species.
(169) For the Zn(II) molecular triangle **126**, we should consider that Zn^{2+} ions have no ligand-field stabilization, and thus, they may tolerate deviations from the ideal octahedral coordination geometry with relatively low enthalpic loss.
(170) (a) Kraft, S.; Beckhaus, R.; Haase, D.; Saak, W. *Angew. Chem., Int. Ed.* **2004**, *43*, 1583. (b) Kraft, S.; Hanuschek, E.; Beckhaus, R.; Haase, D.; Saak, W. *Chem.—Eur. J.* **2005**, *11*, 969.
(171) Kumazawa, K.; Biradha, K.; Kusukawa, T.; Okano, T.; Fujita, M. *Angew. Chem., Int. Ed.* **2003**, *42*, 3909.
(172) Willermann, M.; Mulcahy, C.; Sigel, R. K. O.; Cerdà, M. M.; Freisinger, E.; Miguel, P. J. S.; Roitzsch, M.; Lippert, B. *Inorg. Chem.* **2006**, *45*, 2093.
(173) Slone, R. V.; Hupp, J. T.; Stern, C. L.; Albrecht-Schmitt, T. E. *Inorg. Chem.* **1996**, *35*, 4096.
(174) Rajendran, T.; Manimaran, B.; Lee, F.-Y.; Chen, P.-J.; Lin, S.-C.; Lee, G.-H.; Peng, S.-M.; Chen, Y.-J.; Lu, K.-L. *J. Chem. Soc., Dalton Trans.* **2001**, 3346.
(175) Davies, J. A.; Hartley, F. R.; Murray, S. G.; Pierce-Butler, M. A. *J. Chem. Soc., Dalton Trans.* **1983**, 1305.
(176) Dawes, H. M.; Hursthouse, M. B.; Del Paggio, A. A.; Muetterties, E. L.; Parkins, A. W. *Polyhedron* **1985**, *4*, 379.
(177) Evans, W. J.; Drummond, D. K. *Organometallics* **1988**, *7*, 797.
(178) Calderazzo, F.; Mazzi, U.; Pampaloni, G.; Poli, R.; Tisato, F.; Zanazzi, P. F. *Gazz. Chim. Ital.* **1989**, *119*, 241.
(179) Muga, I.; Gutiérrez; Zorrilla, J. M.; Vitoria, P.; Román, P.; Lloret, F. *Polyhedron* **2002**, *21*, 2631.
(180) Forniés, J; Gómez, J.; Lalinde, E.; Moreno, M. T. *Chem.—Eur. J.* **2004**, *10*, 888.

CR8002449